



Cite this: *Green Chem.*, 2021, **23**, 6223

Metal-free nanostructured catalysts: sustainable driving forces for organic transformations

Behnam Gholipour,^a Salman Shojaei,^a Sadegh Rostamnia,^{*a,b} Mohammad Reza Naimi-Jamal,^c Dokyoon Kim,^d Taras Kavetsky,^{b,e} Nasrin Nouruzi,^a Ho Won Jang,^f Rajender S. Varma^g and Mohammadreza Shokouhimehr^h

Over the past few decades, research on heterogeneous catalysts, especially metal-free catalysts in industrial and research transformations, has intensified. Despite the obvious benefits of heterogeneous transition metal catalysts in quick substrate activation and acceleration of reactions, cost-effectiveness, high activity in harsh process conditions, ensuing pollution and sustainability issues are still some of the significant challenges. In this context, metal-free catalysts have been widely studied over the past few decades. The persistent question in the field of metal-free catalysts is their scalable design and the development with an acceptable economic approach and biocompatibility to achieve green and selective synthesis in the domain of industry and pharmaceuticals, as well as organic transformations. This article portrays recent developments in the exploitation of metal-free catalysts in organic synthesis.

Received 19th April 2021,
Accepted 5th July 2021

DOI: 10.1039/d1gc01366a

rsc.li/greenchem

Introduction

With the advent and extension of green and sustainable chemistry,^{1–5} modern organic synthesis embraces the avoidance of toxic and dangerous reagents and solvents, harsh reaction conditions, and expensive and complex catalysts.^{2,6–9} Over the past decade, there has been a paradigm shift to save energy consumption, atom economy, and use of eco-friendly solvents and alternative activation methods that prevent waste generation by the design of new greener protocols for the organic synthesis of compounds.^{2,10–17} The use of green and clean chemical technologies in the industry, besides being

useful for the production of valuable chemicals, can contribute to the handling of ensuing environmental problems.^{18,19} Given the challenges of the global economy and the need for sustainable chemical proceedings, catalytic reactions play a momentous role in developing newer synthetic procedures for the production of target molecules in fewer steps and with the least amount of chemical waste generation.^{20–25} Catalysts are one of the key pillars for modern chemistry, which is very important in most chemical industrial processes as they provide indispensable chemicals and sustainable fuels to support the global community;^{26–30} they are one of the key components of green chemistry, where benign by design and eco-friendly deployment of catalysts have become recurring themes.^{31–33} Therefore, a green and stable nano-catalyst,^{34–36} especially under continuous flow conditions, must have unique features³⁷ with low cost of production, high stability and activity, efficient recovery, excellent selectivity, and good recyclability. Up to now, various heterogeneous catalysts have been designed and developed to activate important industrial molecules, among which supported noble-metal-based catalysts are more widely used because of their high efficiency.^{38–40} However, the use of noble metal catalysts faces problems such as the scarcity and high price of precious metals.^{41–44} For this reason, it has been suggested that the use of these noble metals be replaced by inexpensive non-noble materials.^{4,43,45} Recently, metal-free catalysts in a friendly reaction medium^{2,13,46,47} have attracted much attention as emerging green catalysts due to benefits such as environmental compatibility, economics, and high efficiency in many industrial cata-

^aOrganic and Nano Group (ONG), Department of Chemistry, Iran University of Science and Technology (IUST), PO BOX 16846-13114, Tehran, Iran.

E-mail: rostamnia@iust.ac.ir

^bDepartment of Surface Engineering, The John Paul II Catholic University of Lublin, Al. Raclawickie 14, 20-950 Lublin, Poland

^cResearch Laboratory of Green Organic Synthesis and Polymers, Chemistry Department, Iran University of Science and Technology (IUST), PO BOX 16846-13114, Tehran, Iran

^dDepartment of Bionano Engineering, Hanyang University, Ansan 15588, Republic of Korea

^eDepartment of Biology and Chemistry, Drohobych Ivan Franko State Pedagogical University, Drohobych, Ukraine

^fDepartment of Materials Science and Engineering, Research Institute of Advanced Materials, Seoul National University, Seoul 08826, Republic of Korea.

E-mail: mrsh2@snu.ac.kr

^gRegional Centre of Advanced Technologies and Materials, Czech Advanced Technology and Research Institute, Palacky University, Šlechtitelů 27, 783 71 Olomouc, Czech Republic. E-mail: varma.rajender@epa.gov

lytic operations; organic metal-free catalysts, such as ionic liquids, dendrimers, small organic molecules with N, P electron-rich centers, *etc.*, have been widely used in a variety of homogeneous organic reactions for rearrangement, condensation, cycloaddition, carbonylation and alkylation reactions.^{48–51} Consequently, the transformation of organic compounds with catalysts, especially the avoidance of transition metals, has become an attractive and important pursuit and several promising catalysts such as functionalized mesoporous silica, graphene, functionalized polymers, and graphitic carbon nitride (g-C₃N₄), among others, have appeared. This review provides an appraisal of recent advances in metal-free catalysts and their application in catalytic organic reactions. Especially, we have explored nanostructured catalysts containing iron oxide nanoparticles (NPs) as their magnetic properties facilitate the separation and isolation of the catalytic moieties to practically achieve the recycling and reusing of catalytic systems.

Concerns for the practical applications

Transition-metal-catalyzed organic reactions have been studied for a century, leading to dramatic transformational achievements and improvements in organic conversions.^{52–60} Many industries utilize homogeneous catalysts comprising precious metals for chemical transformation and processing.^{61–70} However, organic reactions catalyzed by transition-metals are still limited in applications and face challenges due to the instinctive obstacles of catalytic systems.⁷¹ For example, most transition-metal catalysts are generally very expensive and toxic, and their removal in trace amounts from the desired products is very expensive and challenging, especially in the pharmaceutical industry. Another point to consider is that, in many cases, the use of special additives and co-catalysts is imperative to elevate the efficiency and selectivity of the organic reactions besides the sensitivity of transition-metal catalysts to oxygen and moisture. Consequently, the need for strategies based on green metal-free catalysts is obligatory to overcome some of the drawbacks of metal catalysts.⁷¹ Over the last decade, various organocatalysts have been extended for a broad range of organic transformations.^{72–75} Compared with metal-catalyzed organic reactions, organocatalysts have found limited industrial applications, although they are normally stable in air and are not simply poisoned through process impurities, an important feature in developing an efficient procedure for industrial applications.^{73,75} For example, the utilization of a transition-metal-free organocatalytic method is attractive in the pharmaceutical industry due to the elimination of heavy metal residues from the active pharmaceutical ingredients.⁷⁵ From a green chemistry perspective, a metal-free strategy can bring forth benefits such as unique operation, low cost, substrate toleration, selectivity and recyclability.^{71,76,77} Consequently, the fusion of organocatalysis with nanostructured substrates can be a potential complement in newer developments for the chemical and pharmaceutical industries.

A noticeable example in this case is graphitic carbon nitride, which has gained worldwide acceptance due to its numerous advantages such as abundantly available nitrogen-rich raw materials, low cost, fast and easy synthesis, visible light sensitivity and high chemical stability,^{78–87} and for this reason, it can be one of the candidates for deployment as an industrial catalyst and even as a support in the near future.

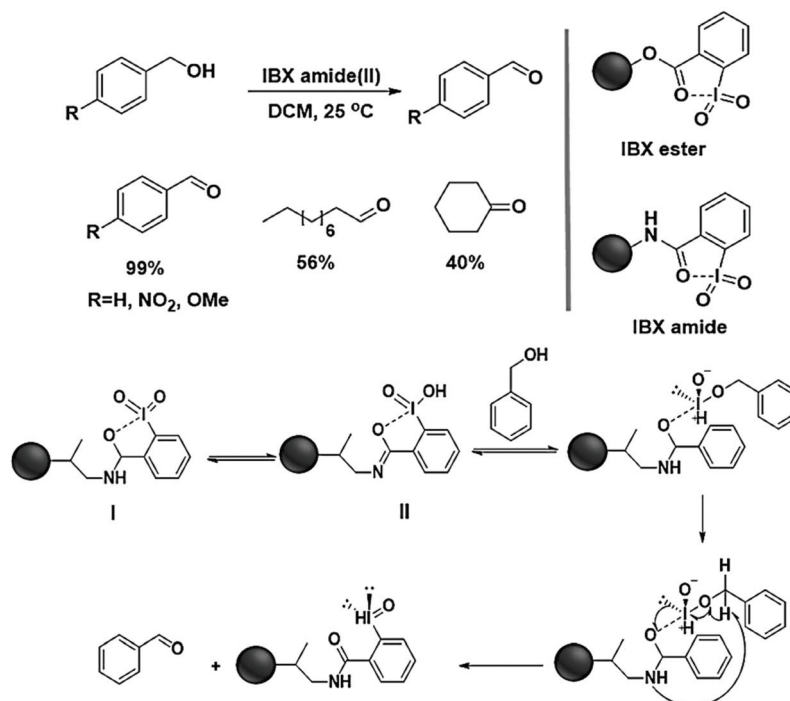
Oxidation of alcohols to aldehydes and ketones

In general, oxidation reactions, especially oxidation of alcohols, are one of the key reactions in the synthesis of organic molecules and chemicals, and therefore the development of green and selective oxidation of alcohols to aldehydes is of great importance.³⁹ Specifically, the oxidation of primary and secondary alcohols to the carbonyl compounds is of particular significance, as these products are widely used as common precursors for many medicines, vitamins and fragrances.⁸⁸ In this context, the oxidation of aromatic and aliphatic alcohols using metal-free catalysts was reported by Lee and co-workers using polymer-supported 2-iodoxybenzoic acid (IBX).⁸⁹ The proposed mechanism entails that the carbonyl oxygen of the IBX amide can enter into a stronger intramolecular nonbonding interaction with iodine, which leads to the formation of a more desirable equilibrium state between (I) and the cyclic IBX derivative (II), and then the interaction of alcohol with the oxygen group IBX and dehydration, and finally the exchange of ligands and disproportionation leads to the formation of aldehydes and the return of IBX to its primary state (Scheme 1). The IBX derivative (I and II) and the same path of alcohol oxidation as that importing the common form of IBX is followed (*i.e.*, ligand exchange and disproportionation), giving an aldehyde and leaving the iodoso compound on the resins (Scheme 1).

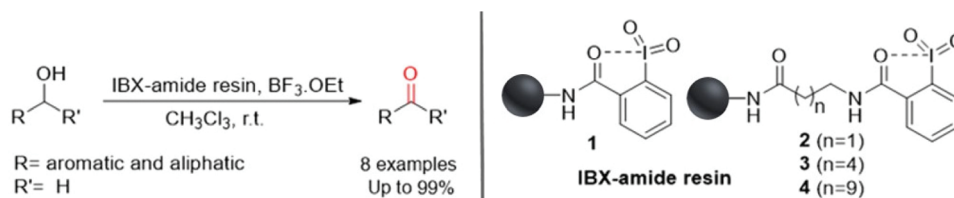
Polymer-supported IBX oxidation of aliphatic and aromatic alcohols showed that the spacer and additive play an important role in the oxidation of alkyl alcohols; extending the chain length of the spacer between the polymer-support and IBX-amide improved the initial conversion rate (Scheme 2).⁹⁰

Polymer-supported IBX amide has been identified as a reusable and effective catalyst for the oxidation of alcohols. IBX synthesis involves two different pathways comprising IBX amide resin A ($n = 0$) and IBX amide resin B ($n = 1$) as shown in Scheme 3; use of IBX amide resin A in the DCM solvent gave the best performance at ambient temperature. A wide variety of alcohols such as benzylic, allylic, aromatic, aliphatic and primary as well as secondary alcohols could be oxidized to the corresponding aldehydes in moderate to good yields (43–99%) with this catalyst that is recoverable and reused in five cycles without loss of activity.⁹¹

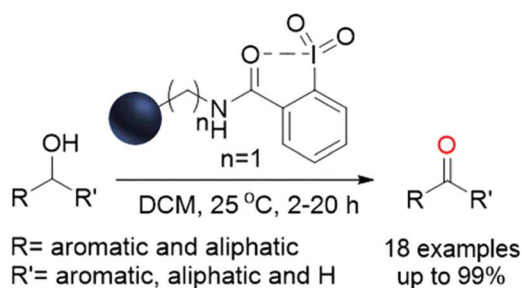
Chemoselective oxidation of primary and secondary alcohols using immobilized 2,2,6,6-tetramethyl-1-piperidinyloxy (TEMPO) on polyethylene glycol (PEG-TEMPO) in the presence of bromide-free NaOCl has been reported (Scheme 4);⁹² excel-



Scheme 1 Oxidation of alcohols catalyzed by IBX amide and mechanism of benzyl alcohol oxidation.



Scheme 2 Oxidation of various alcohols using IBX-amide resin 1–4 with $\text{BF}_3 \cdot \text{OEt}_2$ in CH_2Cl_3 .



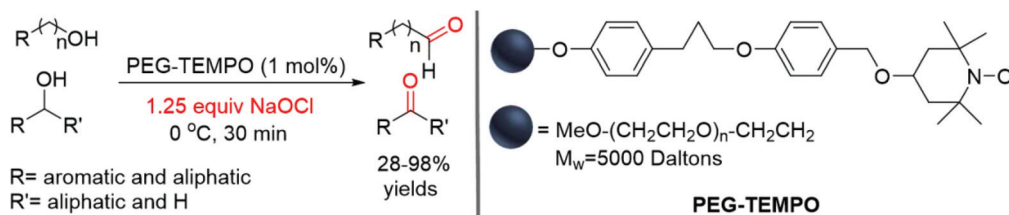
Scheme 3 Oxidation of alcohols using IBX amide resin.

lent yields (93–98%) were obtained for all alcohols except cinnamyl alcohol (28%) and this catalyst could be reused up to six times without losing catalytic activity.

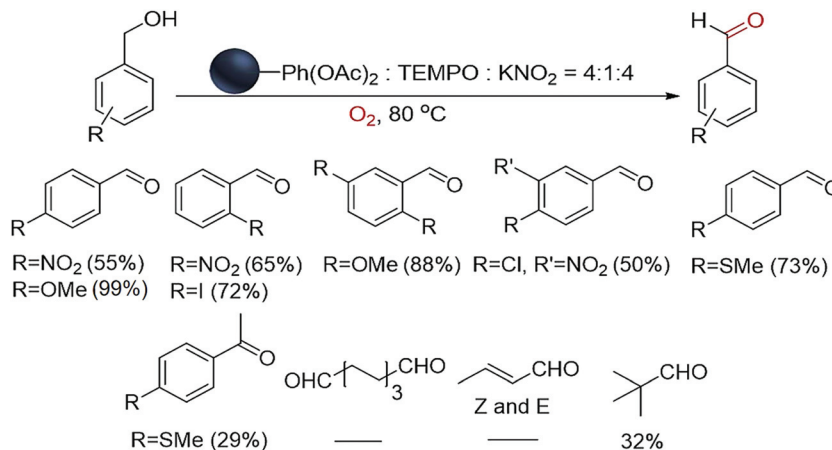
A similar strategy has been described for the oxidation of alcohols to carbonyl compounds using benzyl alcohol as a model reaction and [bis(acetoxy)iodo]-benzene (BAIB) or poly[4

(PBAIS, -[bis(acetoxy)iodo]styrene) PBAIS/TEMPO/ KNO_2 as a catalytic system in water and under an oxygen atmosphere (Scheme 5); reducing the amount of water significantly increased the yield of the product and the ideal result (96%) was discerned in the absence of water. The results also showed that potential chemoselectivity between primary and secondary alcohols, as well as between alkali and aliphatic, is present; the competitive reaction of an equimolar mixture of benzyl alcohol and α -methyl benzyl alcohol afforded a 97% yield of aldehyde while that of ketone was very low. The presence of benzylic and aliphatic alcohols in the same molecule leads to the only benzaldehyde derivative as the exclusive oxidation product.⁹³

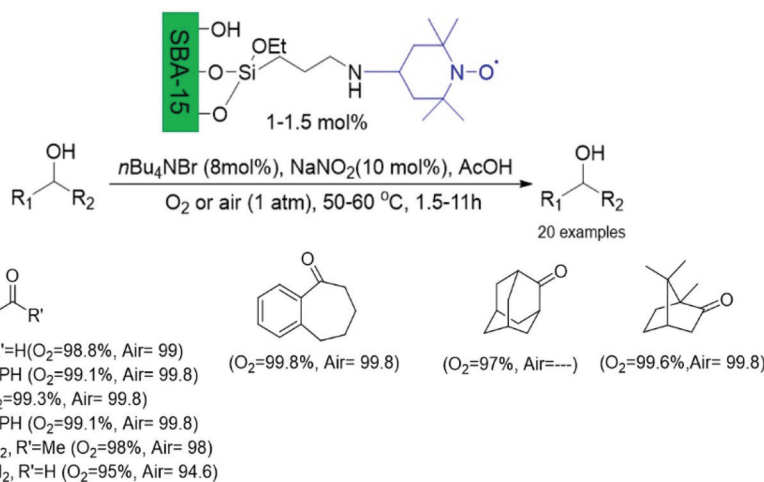
Aerobic alcohol oxidation including (primary, secondary, and highly hindered ones) with TEMPO grafted inside an SBA-15 solid support has been reported as a green and recyclable organocatalyst; the use of O_2 and air gave excellent yields for all alcohols with high selectivities in 1.5–11 h (Scheme 6). The study emphasizes that this heterogeneous catalyst main-



Scheme 4 PEG-TEMPO-catalyzed oxidation of primary and secondary alcohols to carbonyl compounds using NaOCl.



Scheme 5 Oxidation of alcohols using the PBAIS/TEMPO/KNO₂ system.



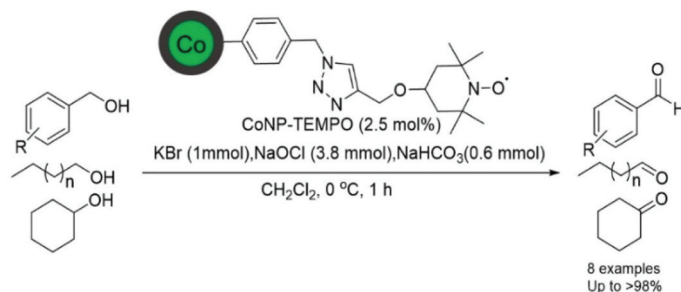
Scheme 6 Aerobic oxidation of various alcohols catalyzed by SBA-15/TEMPO.

tains its sustainability under optimum conditions, and could be retrieved after 14 runs and reused without any change in the morphology and activity.⁹⁴

Reiser *et al.* studied the chemoselective oxidation of benzylic and aliphatic alcohols by using TEMPO grafted on magnetic C/Co-NPs (Co NPs-TEMPO) as a heterogeneous and highly active catalyst; a “click” CuAAC reaction was used to graft TEMPO on C/Co NPs with a magnetic cobalt core and the

ensuing catalyst was reused for the oxidation of 4-methyl benzyl alcohol for up to six runs without loss of catalytic activity (Scheme 7).⁹⁵

The use of graphitic carbon nitride (g-C₃N₄), because of its unique surface and electronic properties, has been expanded to numerous applications, especially as a metal-free photocatalyst. Blechert and Wang *et al.* have developed a green and cost-effective mesoporous graphitic carbon nitride (mpg-C₃N₄)



Scheme 7 Oxidation of various alcohol using Co NPs-TEMPO catalyst.

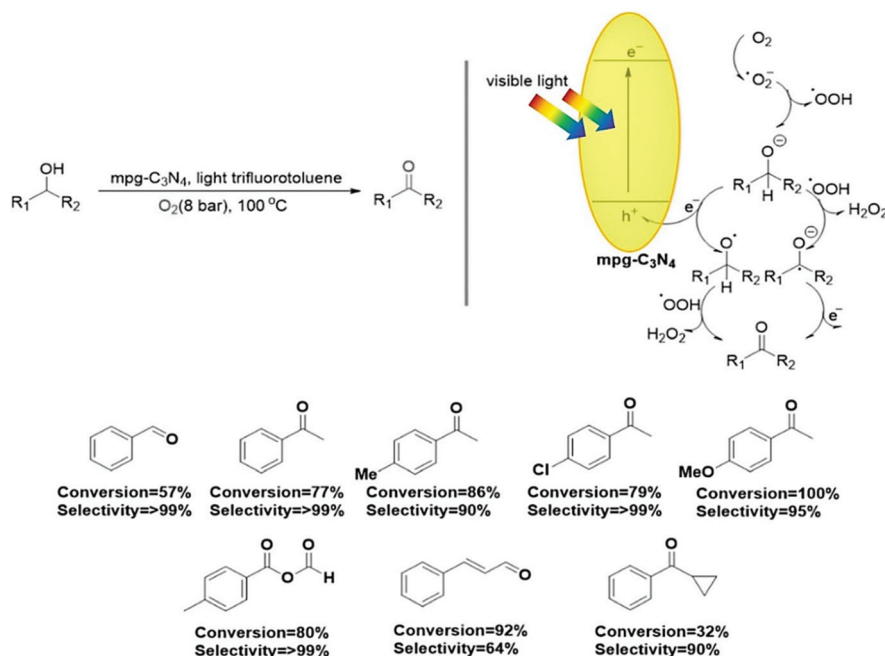
for the selective visible light-assisted photooxidation of alcohols to aldehyde and ketones as it catalyzes the oxidation of alcohols with 32–100% conversion and 64–>99% selectivity under visible-light irradiation for 3 h at 100 °C (Scheme 8).⁹⁶

As shown earlier mpg-C₃N₄ is a prominent metal-free catalyst that could accomplish the oxidation of 2-hydroxy-1,2-diphenylethane at 100 °C under 1 atm O₂ for 10 h along with other derivatives of α -hydroxy ketones, bearing both electron-withdrawing and electron-donating groups, affording moderate yields (49–73%); Scheme 9 illustrates the overall mechanism of the reaction.⁹⁷

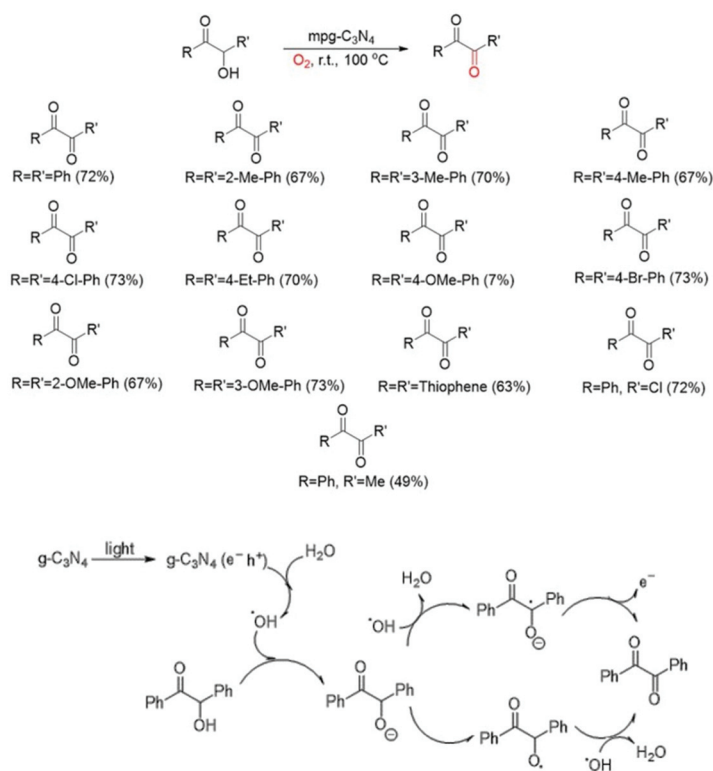
A mesoporous graphitic carbon nitride-based (mpg-C₃N₄) catalytic system has been reported as an active catalyst for enhanced conversion of primary and secondary alcohols in the co-presence of CO₂ and N₂ with O₂. Investigation of O₂/CO₂ and N₂/O₂ ratios revealed that when O₂/CO₂ is used with a ratio of 1/1, the product is predominantly acid (conversion of

90% with selectivity >95%) while with a 1 : 1 ratio of N₂/O₂, the conversion attained was 61% with selectivity for acid being slightly higher than for aldehyde. In a 1 : 7 ratio of O₂/CO₂, the product is dominantly acid (conversion 77% with selectivity >95%) while N₂/O₂ affords 7.1%, wherein the product is predominantly aldehyde with 100% selectivity. Further studies showed that increasing oxygen concentrations in the deployment of O₂/CO₂ increased the conversion of alcohol to the acid, while for the O₂/N₂, aldehyde selectivity is relatively higher (Scheme 10).⁹⁸

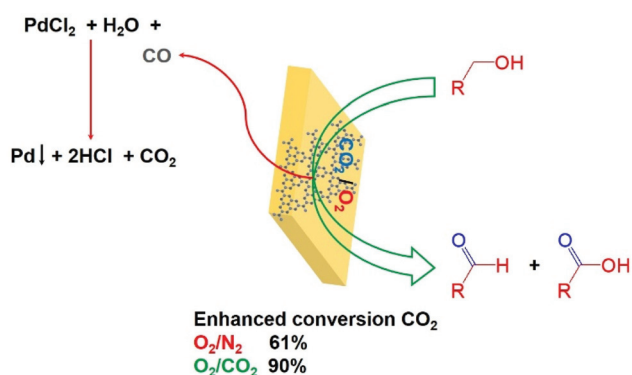
Bielawski *et al.* reported on the oxidation of alcohols by graphene oxide (GO) carbocatalyst under relatively mild conditions where the ideal results were obtained under the conditions 200 wt% GO, at 100 °C, in 24 h. This carbocatalyst, as applied for a variety of primary and secondary benzylic and aliphatic alcohols under optimum conditions, afforded moderate to high conversion (18–>98%) of the corresponding carbonyls (Scheme 11).⁹⁹



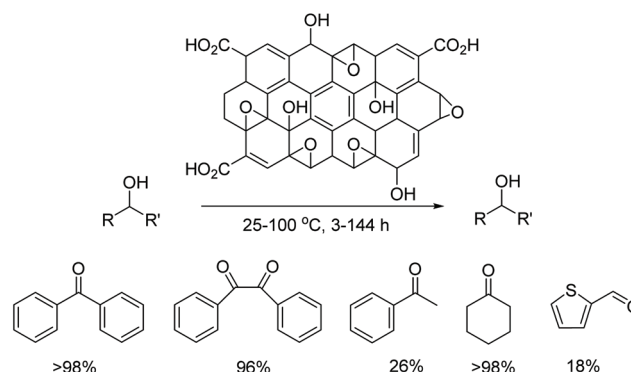
Scheme 8 Selective oxidation of alcohols with mpg-C₃N₄ and proposed mechanism.



Scheme 9 mpg-C₃N₄-catalyzed synthesis of 1,2-diketones with visible light and possible reaction mechanism.



Scheme 10 Benzyl alcohol oxidation with mpg-C₃N₄, promoted by the use of CO₂.



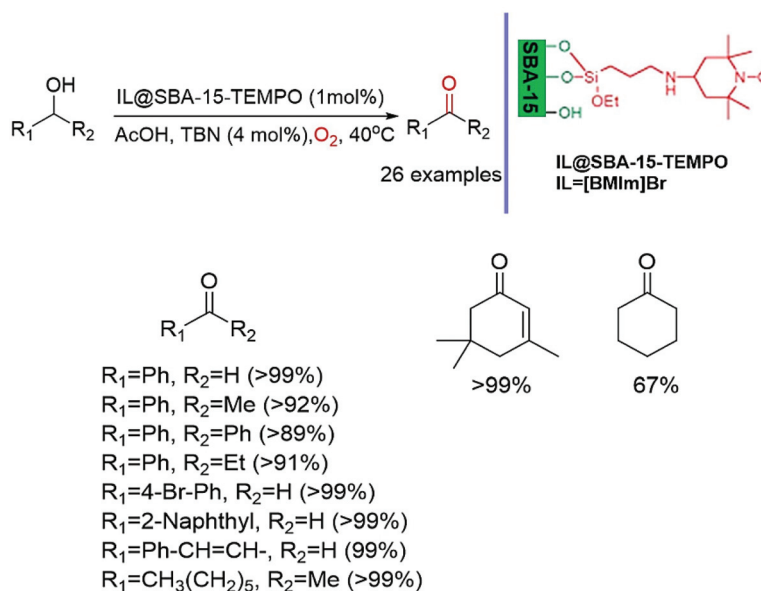
Scheme 11 Oxidation of different alcohols using GO.

Karimi reported an efficient catalytic system *via* the deployment of SBA-15-functionalized TEMPO confined ionic liquid (IL@SBA-15-TEMPO) for the selective aerobic oxidation of alcohols; primary, secondary, allylic and aliphatic alcohols were selectively converted to the respective aldehyde and ketones in excellent yields (>99%) under optimal conditions (Scheme 12). The high stability of IL@SBA-15-TEMPO allowed its recycling for more than 11 times without loss of activity and selectivity.¹⁰⁰

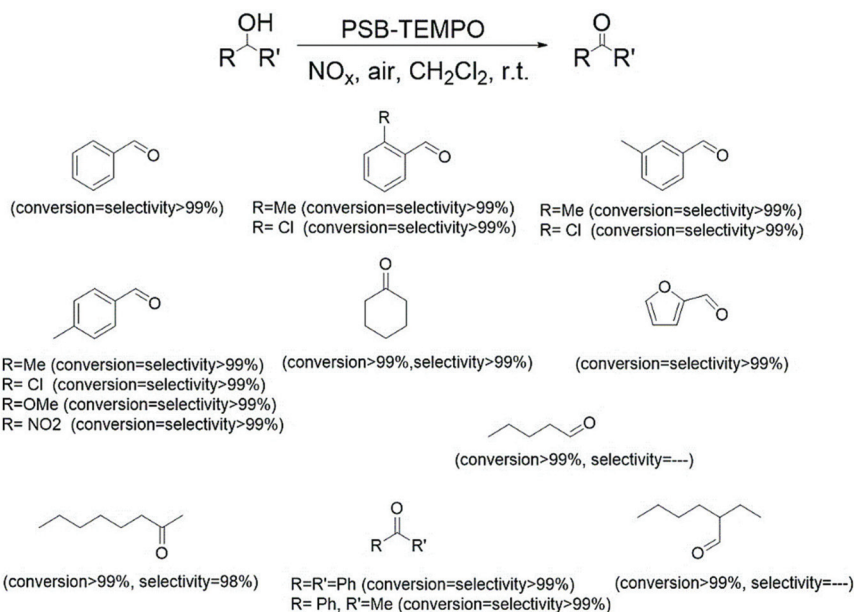
Porous silica bead (PSB)-supported TEMPO with adsorbed NO_x served as a highly efficient and recyclable catalyst for the

oxidation of a wide range of alcohols to their respective aldehydes and ketones with selectivities of >99% under aerobic and room temperature conditions; PSB-TEMPO could be recovered and reused more than 10 times without loss of significant activity and the oxidation proceeds *via* the proposed mechanism illustrated in Scheme 13.¹⁰¹

TEMPO-functionalized Fe₃O₄@SiO₂ MNPs (MNST) have been prepared and applied as an efficient and recyclable metal- and halogen-free catalyst for the aerobic oxidation of a broad range of alcohols in water; 0.2–0.35 mol% of catalyst achieved high conversion for various alcohols including primary, secondary, aliphatic benzylic alcohols, allylic and hindered alcohols to the corresponding aldehyde and ketones of



Scheme 12 Aerobic oxidation of alcohols catalyzed by IL@SBA-15-TEMPO.



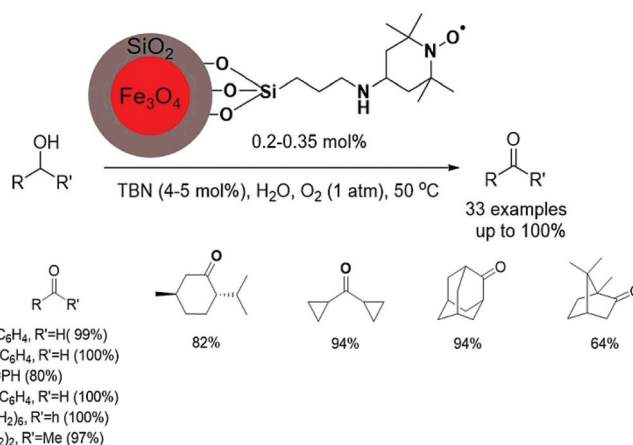
Scheme 13 General protocol and proposed mechanism for the oxidation of alcohols using PSB-TEMPO/NO_x.

up to 100% in 2.5–48 h using 4–5 mol% of ^tBuONO (Scheme 14). MNST was successfully reused for 20 runs without losing activity for the oxidation of benzyl alcohol.¹⁰²

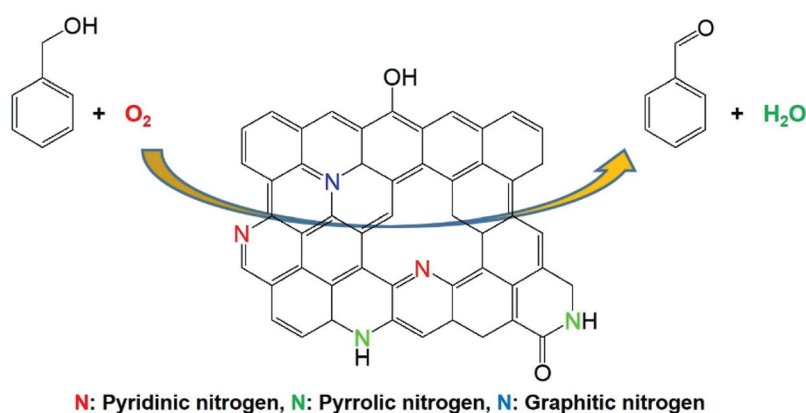
Nitrogen-doped graphene nanosheets have been deployed for the aerobic selective oxidation of various benzylic alcohols to their respective ketones in water. Three samples of N-doped graphene (denoted as NG-T, where T refers to nitriding temperature) were prepared by a postnitridation of GO in an NH₃ atmosphere at temperatures ranging from 800 to 1000 °C; 4%

at 40 °C and 12.8% at 70 °C with 100% selectivity was discerned with NG900 for the conversion of benzyl alcohol to benzaldehyde. Other alcohols such as *p*-nitrobenzyl alcohol, *p*-fluorobenzyl alcohol, *p*-methyl benzyl alcohol, and *p*-methoxybenzyl alcohol could be oxidized at 70 °C with conversion amounts respectively equal to 13.4%, 15.9%, 10.6% and 14.8% with >98% selectivity being obtained (Scheme 15).¹⁰³

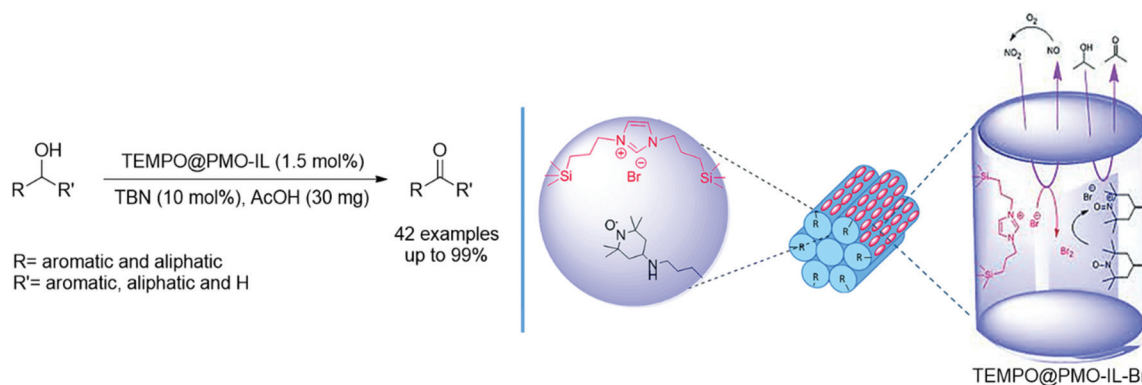
Karimi *et al.* supported TEMPO on ionic liquid (IL)-modified periodic mesoporous organosilica (TEMPO@PMO-IL-Br) and used it for the aerobic oxidation of alcohols in toluene at



Scheme 14 Aerobic oxidation of various alcohols using MNST.



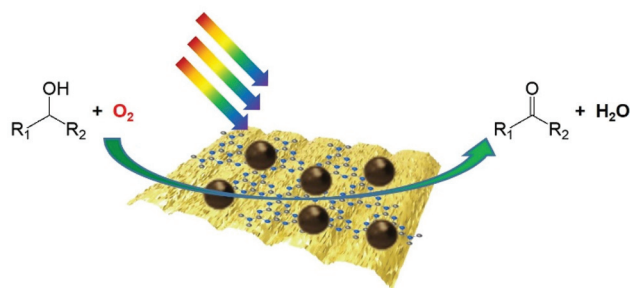
Scheme 15 Aerobic oxidation of alcohols over N-doped graphene nanosheets.



Scheme 16 Aerobic oxidation of various alcohols using TEMPO@PMO-IL-Br. Reproduced from ref. 104 with permission from the Royal Society of Chemistry, copyright 2016.

50 °C in the presence of 1.5 mol% TEMPO@PMO-IL-Br, 10 mol% *tert*-butylnitrite (TBN) and 30 mg AcOH under atmospheric pressure of O₂ (Scheme 16); excellent yields of up to 99% were obtained with demonstrated reusability up to 8 times.¹⁰⁴

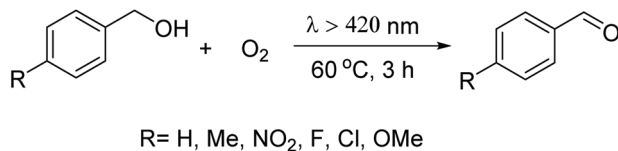
Another example of a metal free-heterogeneous catalyst comprises carbon-nanodot (CD)-doped graphitic carbon nitride (CD-C₃N₄) for visible-light-driven photooxidation of alcohols (Scheme 17); this could be successfully reused at least 5 times without losing activity.¹⁰⁵



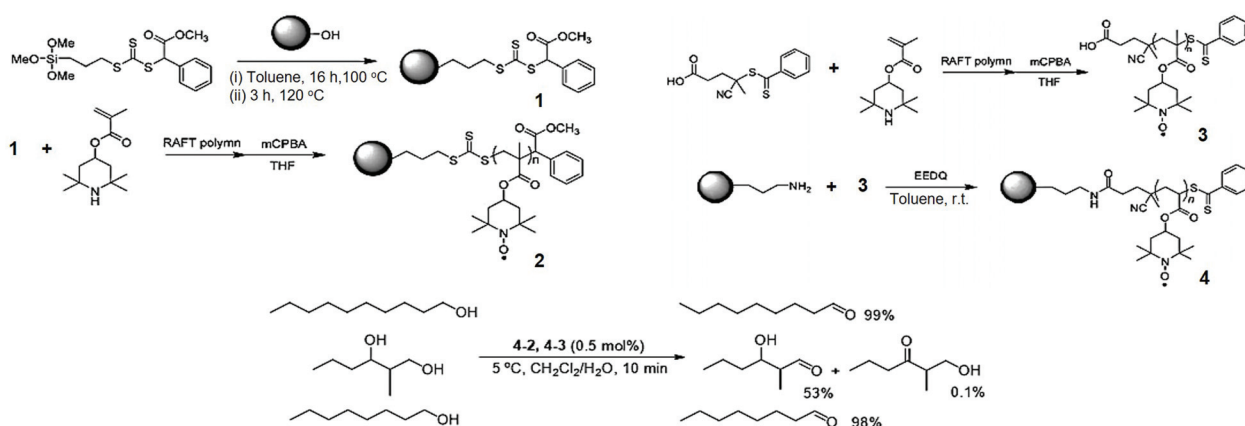
Scheme 17 Photocatalytic aerobic oxidation of alcohols using CD-C₃N₄.

Thiophene motif decorated mesoporous carbon nitride has been prepared *via* copolymerization of 3-aminothiophene-2-carbonitrile (ATCN) and dicyanamide (MCN-ATCN_x, where *x* refers to the weighed-in amount of ATCN) as an efficient and active photocatalyst for the selective oxidation of various *p*-substituted benzyl alcohols. Increasing the quantity of ATCN incorporated in MCN-ATCN_x gradually enhanced the generation of the desired products; MCN-ATCN_{0.05} afforded maximal conversions of 53% with >99% selectivity and apparent quantum efficiency of 8.6% at 420 nm (Scheme 18). ESR spectroscopy showed that the primary alcohol oxidation was a combined action of [•]O₂⁻ and singlet oxygen (¹O₂⁻), instead of a process intermediated by only [•]O₂⁻.¹⁰⁶

An effective heterogeneous catalyst for the oxidation of alcohols has been identified in TEMPO radical polymer that was immobilized onto silica by “grafting from” and “grafting to”



Scheme 18 Selective oxidation of various benzyl alcohols by light irradiation.



Scheme 19 Oxidative conversion of various alcohol poly TEMPO grafted catalysts.

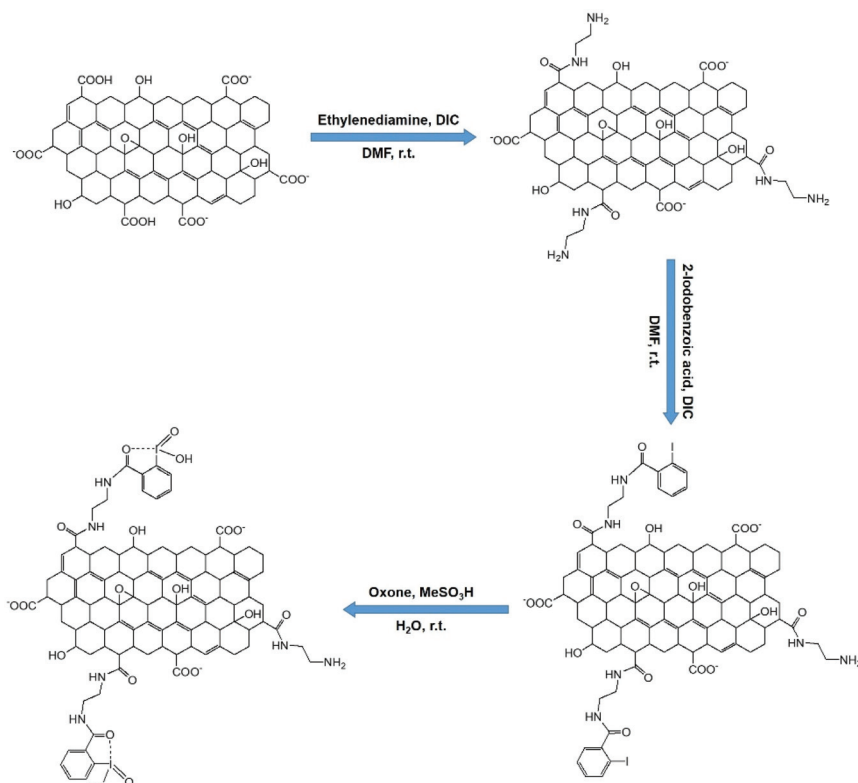
methods using RAFT polymerization; in the “grafting from” method the amount of radical groups was only 44%, while the “grafting to” protocol afforded a radical concentration of 90%. Among various polymers obtained by the “grafting to” method with a different molecular weight (4-1, 4-2, 4-3 and 4-4), 4-2 gave the highest yield for oxidation of benzyl alcohol under optimal conditions, in 10 min, at 5 °C, with 0.5 mol% of catalyst and CH₂Cl₂/water solvent (Scheme 19). For primary alcohols, namely 1-octanol and 1-decanol, the conversion to the corresponding aldehydes was high (*ca.* 98–99%) while for the secondary alcohols, namely 2-octanol and 2-decanol, it was ~4% and 2%, and for unprotected primary alcohol in the presence of secondary alcohol (diol 2-methyl-1,3-hexanediyl), the yield was 54%.¹⁰⁷

The enhanced conversion of alcohols to the corresponding aldehydes and ketones using iodoxybenzoic acid supported on graphene oxide (GO-IBX) as a heterogeneous and compatible catalyst in water was developed by Lee and co-workers; stable and recyclable catalyst showed excellent performance up to 99% of conversion with high selectivity (>99%) for various alcohols under mild conditions (Scheme 20). This catalyst was activated by potassium peroxymonosulfate (oxone) in water and can be recovered and reused for up to 5 runs.¹⁰⁸

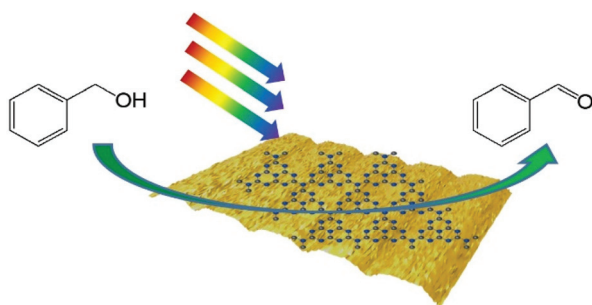
Mu and co-workers have reported a simple and facile method for the modification of g-C₃N₄¹⁰⁹ by refluxing it in sulfuric acid and deploying it as an efficient metal-free photocatalyst for the selective aerobic oxidation of benzyl alcohol to benzaldehyde at 100 °C for 4 h using trifluorotoluene as a solvent with 23% yield and 98% selectivity (Scheme 21).

Various nitrogen-doped activated carbon catalysts have been prepared *via* treatment of activated carbon (AC) with NH₃ and H₂O₂; NH₃ stream was deployed for 1 h and then H₂O₂ (in an autoclave at 100 or 130 °C for 5 h) to synthesize nitrogen-doped activated carbon (AC) catalyst. The ensuing efficient catalyst afforded aerobic oxidation of several benzylic alcohols (Scheme 22).¹¹⁰

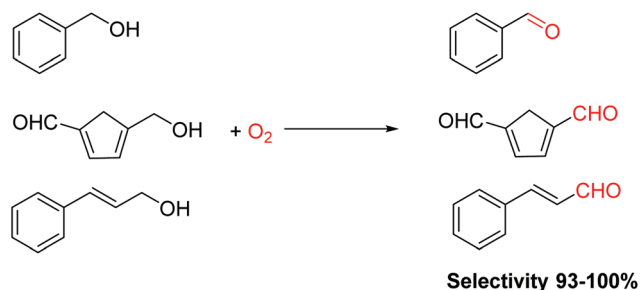
Phosphorus-doped graphitic carbon nitride-based (PGC) material with controlled P-bond configuration has been introduced for the selective and aerobic oxidation of primary, alicyc-



Scheme 20 Oxidation of alcohols by GO-supported IBX in water.



Scheme 21 Photocatalytic oxidation of benzyl alcohol under visible light ($\lambda > 420$ nm) using g-C₃N₄.

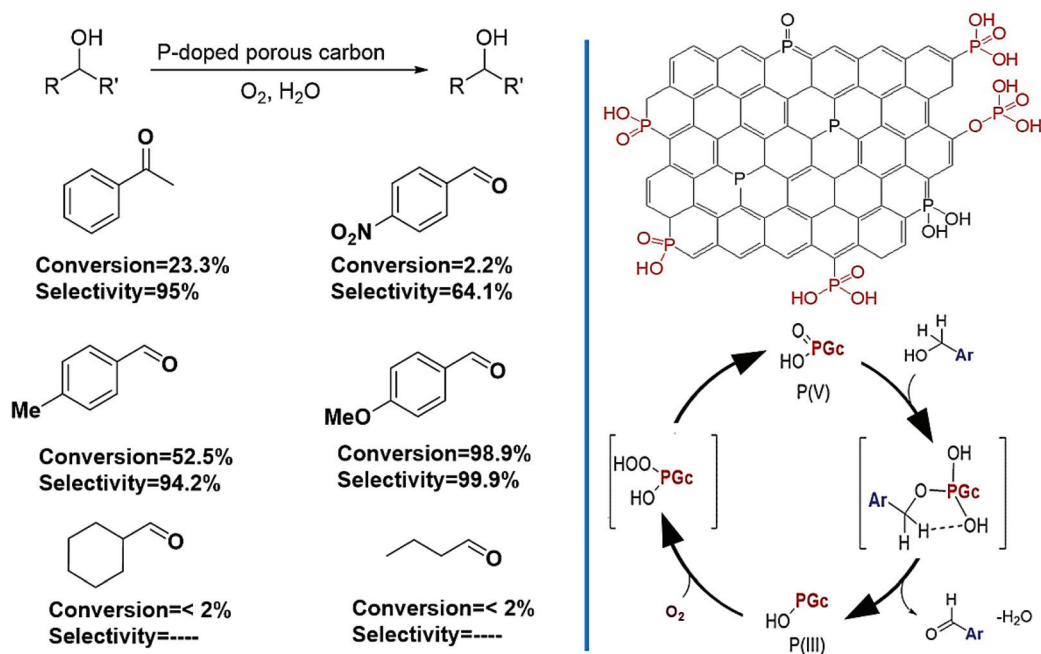


Scheme 22 Aerobic oxidation of alcohols with N-doped AC.

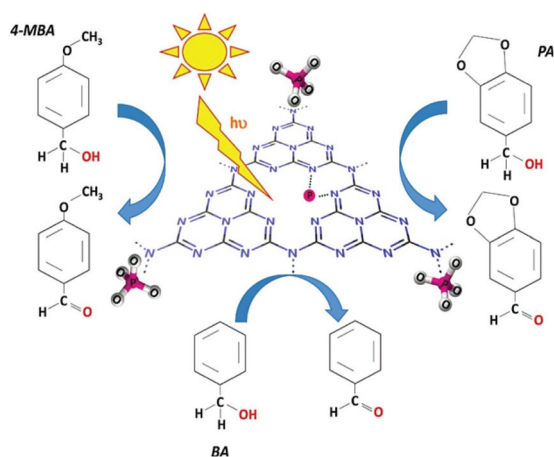
lic, linear and secondary benzylic alcohols in water and under solvent-free conditions; P-doped carbon nitride and its connectivity to the P bond configuration and its relationship to catalytic efficiency was compared with rGO and GO. The results showed that 50 wt% of PGc-30 (conversion of 14.9% with selectivity of 97%) performed better than 50 wt% PGc-180 (conversion of 8.4% with selectivity of 94%) and 50 wt% GO (conversion of 13% with selectivity of 95%), where 30 and 180 refer to the time of irradiation. In terms of the reaction mechanism, condensation between the alcohol and the P=O moieties on PGc occurs followed by the interaction of the alcohol with the PGc surface *via* π - π interactions with the graphitic domains and hydrogen bonding with the polar groups such as P-OH (Scheme 23).¹¹¹

P-Doped g-C₃N₄ as a photocatalyst was deployed for the selective oxidation of aromatic alcohols in water. A set of P-doped C₃N₄ and g-C₃N₄ photocatalysts was prepared by thermal condensation of melamine, thiourea and urea in the presence of NH₄(H₂PO₄). For comparison purposes, a g-C₃N₄ sample was made by using thermally exfoliated C₃N₄ powders and cyanuric acid; all the g-C₃N₄ catalysts accomplished the selective conversion of alcohols to the corresponding aldehydes. In general, the selectivity relative to aldehyde under UV and visible irradiation improved with P-g-C₃N₄, while the alcohol conversion slightly decreased (Scheme 24).¹¹²

The utility of electrochemically synthesized metal-free carbon quantum dots (CQDs) has been explored for the selective liquid phase oxidation of alcohols to aldehydes; among



Scheme 23 Proposed mechanism for aerobic oxidation of alcohols catalyzed by PGc.



Scheme 24 Conversion of alcohols to the corresponding aldehydes in the presence of $g\text{-C}_3\text{N}_4$ -based materials. Reproduced from ref. 112 with permission of Elsevier, copyright 2017.

various oxidants examined, namely O_2 , H_2O_2 , and $NaClO$, at $70^\circ C$ for the oxidation of benzyl alcohol, it was shown that $NaClO$ provided the highest yield with 75% conversion and 99.9% selectivity, and recycling of the catalyst for 5 runs. Other alcohols such as cyclohexanol, cinnamic alcohol and n -octanol were converted in 68%, 36%, and 100% amounts with selectivity of >99%, respectively (Scheme 25). It was found that CQD catalyst had superior activity and selectivity for the oxidation of alcohols compared with other C-based transition metal-free catalysts such as carbon nanotubes and graphene.¹¹³

More recently, the effect of pH and salt using $g\text{-C}_3\text{N}_4$ as a base catalyst for the oxidation of benzyl alcohol under visible light was investigated; maximum conversion achieved was

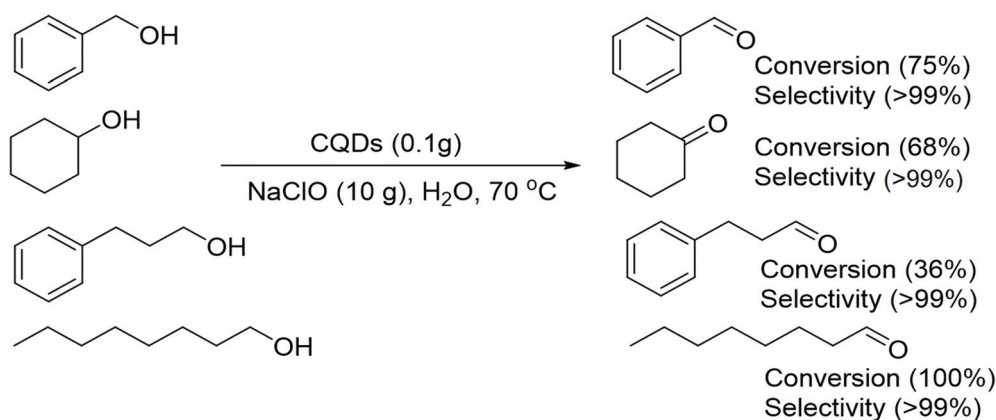
21% with 10% selectivity at pH 8.66 with a concentration of K_2HPO_4 of 0.6 mmol while 98% selectivity was attained at pH 11.87 (Scheme 26). Consequently, a suitable pH and salt concentration were significant factors for boosting of protons on the surface and the electronic conductivity to separate electrons during photocatalysis.¹¹⁴

TEMPO-functionalized with hyperbranched polyimide (HBPI) has been explored as a heterogeneous catalyst for the aerobic oxidation of benzyl alcohol in the presence of a catalytic amount of HNO_3 and atmospheric oxygen pressure at $90^\circ C$ (Scheme 27); selectivity for benzaldehyde was 100%.¹¹⁵

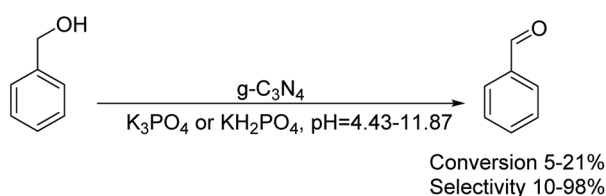
The application of ordered nanoporous TEMPO-based polymer resin, prepared *via* self-assembled lyotropic liquid crystal, has been extended for the selective aerobic oxidation of various alcohols with substrate size selectivity; 99% selectivity and 100% conversion were discerned for 5 consecutive runs over a period of 3 h to obtain benzaldehyde.¹¹⁶ This resin was prepared by the radical crosslinking of a mixture comprising two new TEMPO-based LLC monomers (1a $[BF_4]$ + 1b $[BF_4]$), and monomer LLC (2), in the presence of a small amount of H_2O ; a reversed hexagonal (HII) mesosphere ensued (Scheme 28).

Reduction of substituted nitrobenzene derivatives

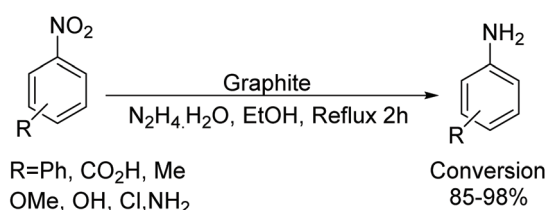
Aniline and its derivatives form the substructures of a multitude of pharmaceutical compositions. The reduction of nitroarenes is the most common shortest and effective route for the manufacture of anilines, and new and effective catalysts are sought for greener transformation.¹¹⁷ In 1985, Han and colleagues reported the reduction of various nitroarenes to the



Scheme 25 Selective liquid-phase oxidation of alcohols using CQDs.



Scheme 26 The effect of pH and salt on the photocatalytic activity of $g\text{-C}_3\text{N}_4$ in the oxidation of benzyl alcohol.



Scheme 29 Graphite-catalyzed reduction of nitrocompounds with N_2H_4 .



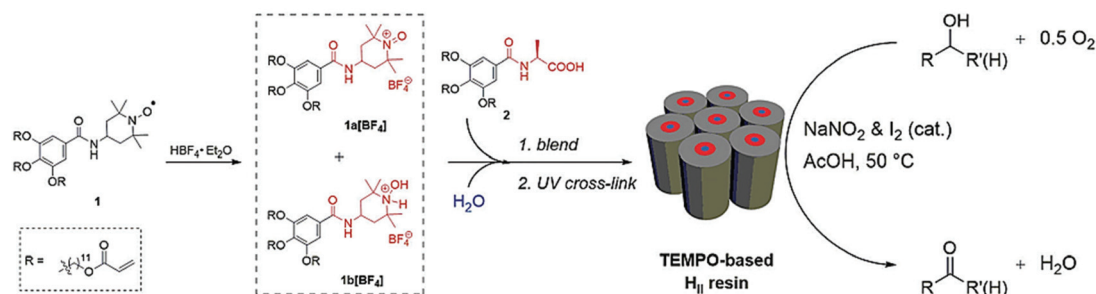
Scheme 27 Aerobic oxidation of benzyl alcohol using TEMPO functionalized with hyperbranched polyimide.

respective anilines in the presence of hydrazine hydrate as a reducing agent using graphite, with a high conversion of 85–98% (Scheme 29).¹¹⁸

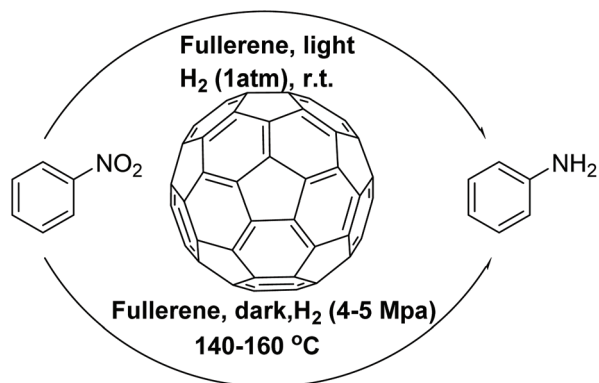
The results of Li and Xu's research indicated that there is a cooperative effect between C_{60} and C_{60}^- that activates H_2 , and with their deployment in a ratio of 2 : 1, quantitative conversion with 100% selectivity was achieved from nitrobenzene to

aniline at 160 °C and 4–5 MPa H_2 , in the dark (Scheme 30). In the case of C_{60} under light irradiation, 1 atmosphere H_2 and ambient temperature, conversion was 100% with a 92.4% selectivity, while for C_{60}^- under the same conditions, conversion of 98.2% with a 72.5% selectivity was attained. For C_{70} and C_{70}^- , the conversion and selectivity were less than C_{60} .¹¹⁹

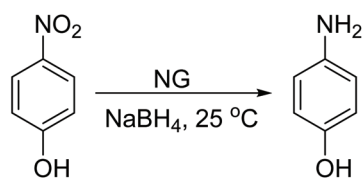
In another protocol, nitrogen-doped graphene (NG) has been studied for the reduction of 4-nitrophenol; the reaction in the presence of NaBH_4 was completed (4-nitrophenol and NaBH_4 ratio 1 : 100) in 21 minutes (Scheme 31) *via* kinetics following the quasi-zero-like reaction. The data from FTIR and the analysis of the results from theoretical studies showed that nitrophenol ions from the oxygen hydroxyl communicate with the nitrogen of graphene. The theoretical studies indicated that only carbon atoms beside nitrogen are active, which interact with nitro phenol ions due to poor fusion and a higher positive charge density.¹²⁰



Scheme 28 TEMPO-based nanoporous polymer resin in the aerobic oxidation of alcohols. Reproduced from ref. 116 with permission from the Royal Society of Chemistry, copyright 2018.



Scheme 30 Hydrogenation of nitrobenzene to aniline by C_{60} under varying conditions. Reproduced from ref. 119 with permission from the American Chemical Society, copyright 2009.



Scheme 31 The reduction of 4-nitrophenol to 4-aminophenol using NG.



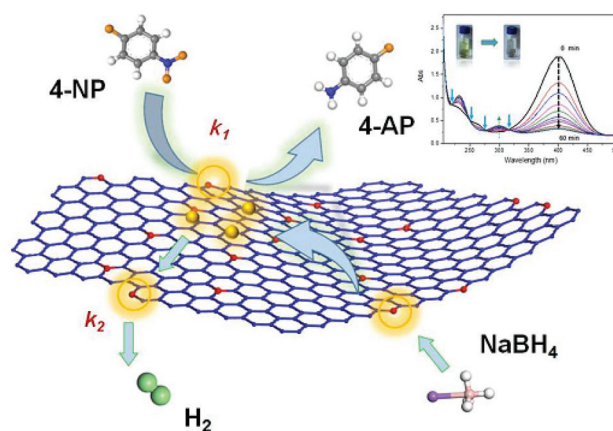
Scheme 32 3D-NGF-assisted reduction of *p*-NP in the presence of $NaBH_4$.

In a strategy to deploy graphene as a non-metal catalyst, Liu's research team reported a three-dimensional nitrogen-doped graphene (3D-NGF) for the reduction of *p*-nitrophenol (*p*-NP) wherein the creation of synergistic effects exhibited good performance in addition to its high stability, up to 8 runs. The large surface of graphene and synergistic effects increased the electron absorption of *p*-NP molecules culminating in elevated electron transfer efficiency; the reduction reaction could be completed in 18 minutes (Scheme 32).¹²¹

According to experimental and thermodynamic studies, the catalyst, graphene doped with sulfur (SG), displayed excellent performance for the reduction of *p*-NP to *p*-aminophenol (*p*-AP) via first-order kinetics (Scheme 33).¹²² Scheme 34 presents the proposed mechanism route for the metal-free catalytic reduction of 4-NP to 4-AP using $NaBH_4$ as the reductant.

Cleavage of ethers

Graphite served as a metal-free catalyst in the cleavage of alkyl ethers using tetrahydropyran and acyl halides; tetrahydropyran in the presence of various acyl halides afforded a 36–85% yield



Scheme 33 Catalytic reduction 4-NP to 4-AP with SG. Reproduced from ref. 122 with permission from the American Chemical Society, copyright 2017.

while benzoyl bromide gave a 67–97% yield (Scheme 35). Interestingly, *tert*-alkyl ethers were selectively cleaved in the presence of secondary ethers in excellent yields; in contrast, primary and secondary alkyl ethers were inert under the reaction conditions. Apparently, the mechanism is similar to that proposed for the iron(III) chloride-acetic anhydride system, which included *O*-acylation of ether via C–O cleavage to create the stable carbonium ion; the acylium cation and the cationic intermediate are presumably stabilized through graphite in a cation– π interaction.¹²³

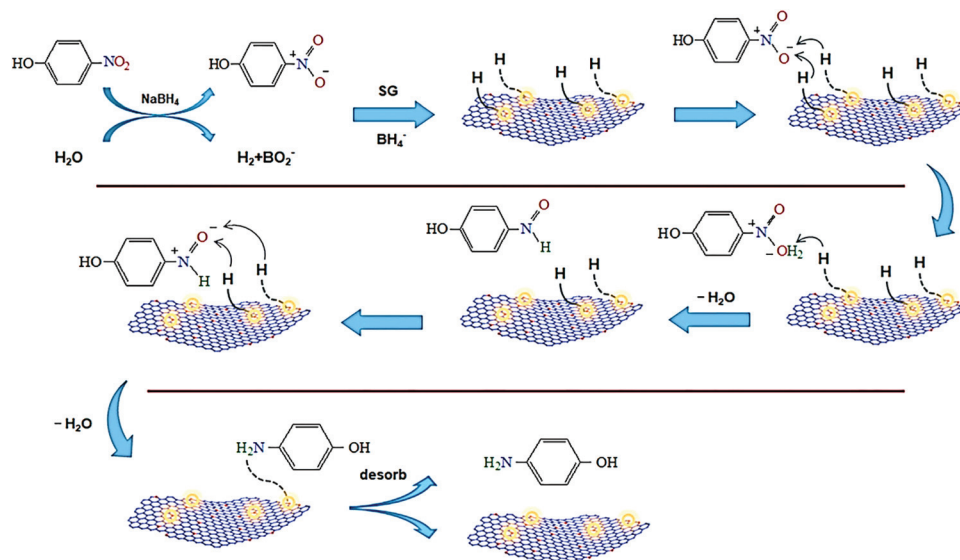
Friedel–Crafts-type substitutions

An efficient Friedel–Crafts reaction without the addition of Lewis acids has been reported between a broad range of ArH and $PhCOBr$ with graphite; within 3–24 h, products were obtained in 60–97% yields (Scheme 36).¹²⁴

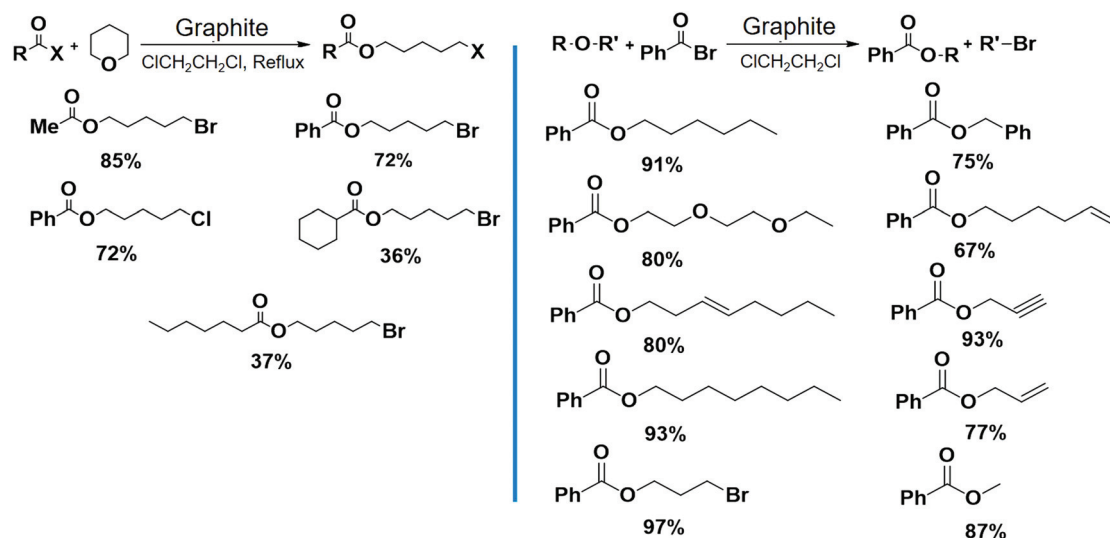
One of the main challenges in organic chemistry is the use of carboxylic acids or alcohols as electrophiles for a sustained Friedel–Crafts reaction that is usually difficult to perform. In this context, Thomas *et al.* reported the direct activation of benzene using $mpg-C_3N_4$ to accomplish Friedel–Crafts reactions with a range of electrophilic groups, specifically for OH and NH_2 groups; formic acid and tetramethyl ammonium bromide gave a nearly quantitative yield (Scheme 37).¹²⁵

The alkylation of aromatic compounds and primary alcohols deploying various acid halides or alkyl halides (1 without using strong Lewis acid) has been accomplished using graphite; the products were attained within 1–24 h in 29–100% yields (Scheme 38).¹²⁶

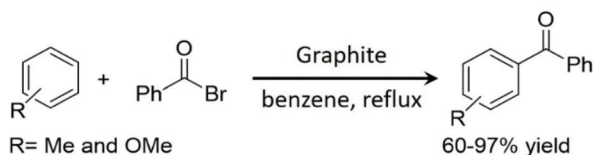
A hydrothermal method was used to create a magnetic carbon-based solid acid core–shell catalyst ($Fe_3O_4@C-SO_3H$) by the functionalization of 2-hydroxyethylsulfonic acid, wherein the catalyst displayed excellent activity for the alkylation of benzene and dodecene under solvent-free conditions (Scheme 39); under the optimized conditions at 80 °C for



Scheme 34 Proposed mechanism route for the reduction of 4-NP to 4-AP using NaBH₄. Reproduced from ref. 122 with permission from the American Chemical Society, copyright 2017.



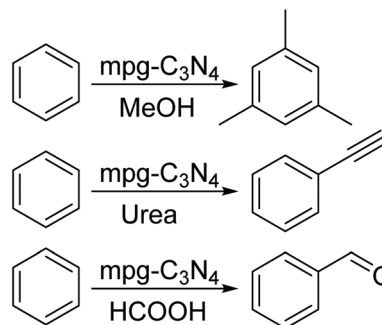
Scheme 35 Graphite-catalyzed acylative cleavage of ethers with benzoyl bromide and cleavage of tetrahydropyran with acyl halide.



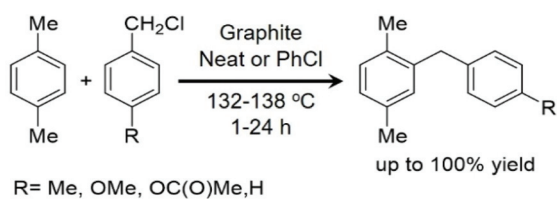
Scheme 36 Graphite-catalyzed Friedel-Crafts acylation.

60 minutes, 100% conversion was attained with 74.4% selectivity and the catalyst could be easily separated and reused for six runs without a significant loss of activity.¹²⁷

Efficient and stable PS-SO₃H@phenylenesilica with a double-shell (DSNs) and yolk-double-shell (YDSNs) structure



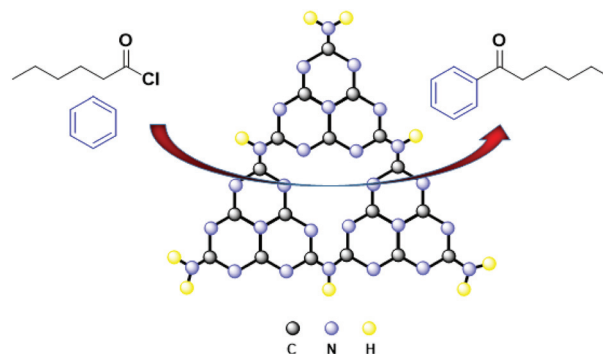
Scheme 37 Friedel-Crafts-type reactions of benzene with various electrophiles catalyzed by mpg-C₃N₄.



Scheme 38 Graphite-catalyzed alkylation of *p*-xylene.

has been synthesized *via* the sulfonation of polystyrene (PS) and it could accomplish the Friedel–Crafts alkylation of toluene with 1-hexene; usage of 0.65 g TEOS afforded PS@phenylenesilica DSNs while 0.4 g of TEOS gave PS-SO₃H@phenylenesilica YDSNs. Among these two acid catalysts, the PS-SO₃H@phenylenesilica YDSNs afforded a conversion of 94.9% after 6 h, while for PS-SO₃H@phenylenesilica DSNs the conversion was 31.3% (Scheme 40), presumably because the YDSN nanostructure exhibited resistance to swelling of PS-SO₃H during the catalytic process.¹²⁸

The use of silica as a template for the synthesis of mpg-C₃N₄ deploying precursors, namely, guanidine hydrochloride, dicyandiamide, and urea, has been demonstrated in the Friedel–Crafts reaction for activating benzene (Scheme 41). The conversion yield for mpg-C₃N₄-G (>90%) is greater than

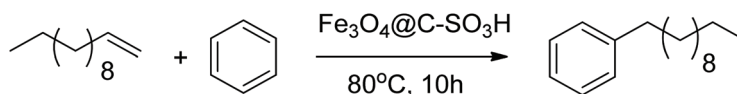


Scheme 41 mpg-C₃N₄-catalyzed Friedel–Crafts reaction by activation of benzene.

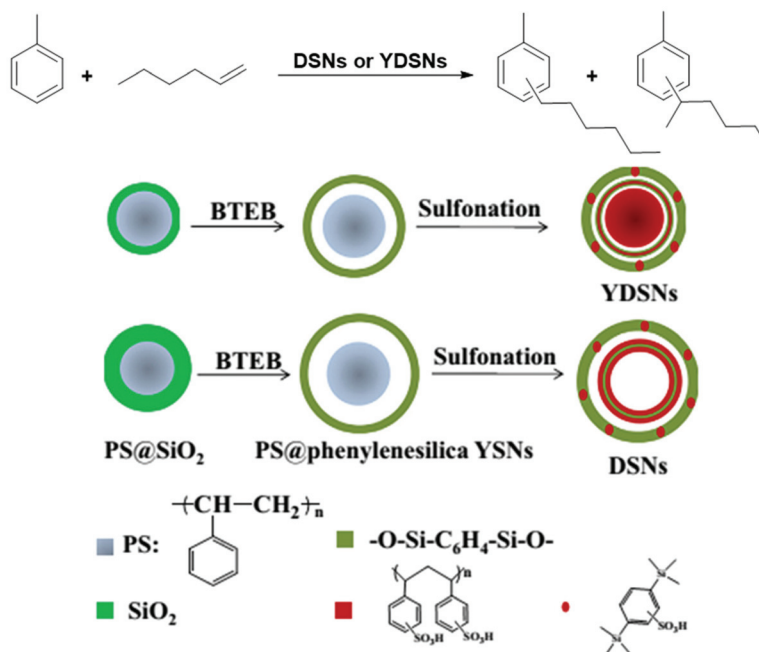
that of mpg-C₃N₄-D (83%) and mpg-C₃N₄-U (80%) over a 2 h period, although at low temperature, mpg-C₃N₄-G displayed good performance (82% yield) at an ambient temperature while at 70 °C the yield was more than 90%.¹²⁹

[4 + 2] cycloadditions

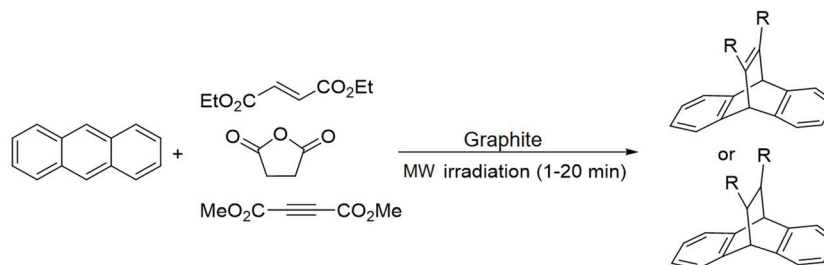
The study of Diels–Alder and carbonyl–ene reactions has been shown using graphite under microwave (MW) heating at high



Scheme 39 Alkylation of benzene and dodecene using Fe₃O₄@C-SO₃H.



Scheme 40 Friedel–Crafts alkylation reaction using YDSNs and DSNs. Reproduced from ref. 128 with permission of Elsevier, copyright 2014.



Scheme 42 [4 + 2] cycloadditions between anthracene and various electron-deficient dienophiles using graphite.

temperatures and ambient pressure in an open reactor wherein a [4 + 2] reaction of anthracene with various electron-deficient dienophiles such as dimethyl fumarate, maleic anhydride and DMAD could be facilitated in the presence of graphite under MW heating (Scheme 42).¹³⁰

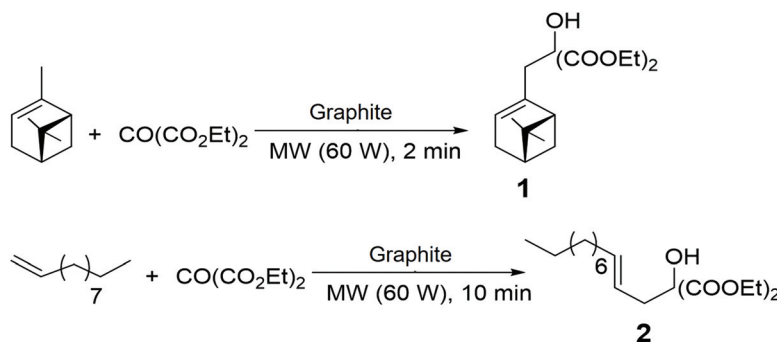
Similar reactivity was discerned in the carbonyl-ene cyclization of $\text{CO}(\text{CO}_2\text{Et})_2$ with β -pinene in the presence of graphite under MW irradiation in 2 minutes, which led to product (1) with a yield of 67%, and in a reaction of 1-decene in 10 minutes affording product (2) (cis/trans with a ratio 30 : 70) with a yield of 50% (Scheme 43).¹³¹ Interestingly, the cyclization of (+)-citronellal to (–)-isopulegol (1a) and (+)-neoisopulegol (1b) (1a/1b in the ratio 68 : 30 and other isomers 2%) at 4 min afforded 80% conversion (Scheme 44).

Oxidation of *n*-butane to 1-butene

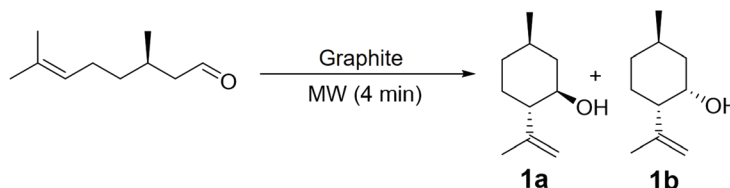
To comprehend the mechanism of oxidative dehydrogenation of ethylbenzene to styrene, Figueiredo *et al.* performed a

detailed kinetic study by examining parameters such as the partial pressures of ethylbenzene (EB) and oxygen, temperature and time using activated carbon. Matching the experimental results with the kinetic model showed that the main reaction occurred *via* a redox mechanism involving quinone/hydroquinone groups on the carbon catalyst surface (Mars-van Krevelen mechanism). Initially, the chemical adsorption of EB molecules occurs first *via* the ketonic carbonyl groups on the nanocarbon catalysts, and subsequently hydrogen accumulation and styrene desorption leads to the reduction of the nanocarbon catalysts. The molecular oxygen eventually re-oxidizes the catalysts and ends up with water excretion of the catalytic cycle (Scheme 45).¹³²

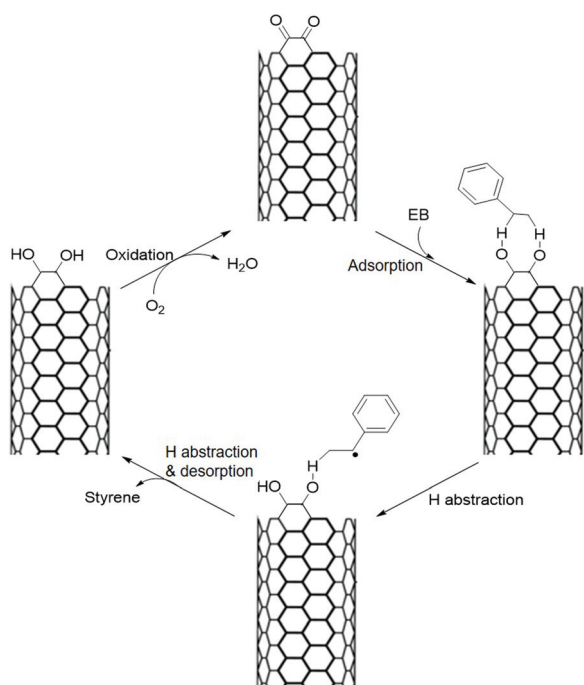
The direct production of styrene through the dissolution of ethyl benzene is of great importance in the industry where well-touted iron oxide is often used in the temperature range of 560–650 °C. To prevent the formation of coke and to maintain a high level of activity, steam is used for a long time, which reduces the energy efficiency. In this regard, Figueiredo *et al.* demonstrated that the oxidative dehydrogenation of ethyl



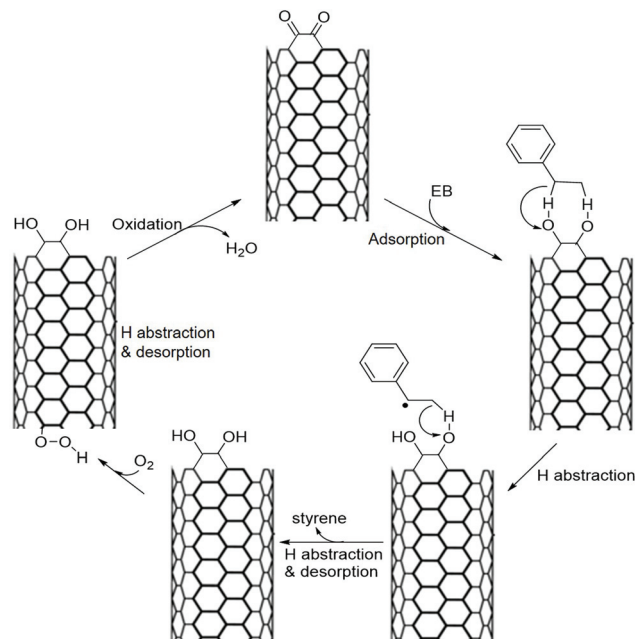
Scheme 43 Carbonyl-ene cyclization of $\text{CO}(\text{CO}_2\text{Et})_2$ with β -pinene and 1-decene using graphite.



Scheme 44 Ene cyclization of (+)-citronellal to (±)-isopulegol using graphite.



Scheme 45 Activated carbon-catalyzed EB to styrene.



Scheme 47 Mechanistic study for the oxidative dehydrogenation of ethylbenzene.

benzene using a carbon nanostructure offers a comparable and much higher activity than a metal catalyst; nanostructured carbon could lead to a stable performance in a scale-up reactor over a long time. Extensive catalytic tests at higher temperatures showed that coke deposition deactivated the activated carbon catalysts in the oxidative dehydrogenation (ODE) of ethylbenzene. Under these conditions the majority of micropores are blocked and the amount of oxygen and hydrogen in the catalyst composition increases over a period of time, leading to enhanced oxidation; all catalysts are lost during longer reaction times. Working under milder conditions (lower temperature (330–350 °C) and partial pressure of oxygen) delays this effect but leads to reduced catalytic activity (Scheme 46).¹³³

Subsequently, the mechanism provided by Figueiredo was questioned by Su's research team as it did not fully describe the oxidative dehydrogenation process of ethylbenzene; a mechanistic study revealed that the catalytic process follows a Langmuir–Hinshelwood mechanism. The isotopic effect also confirmed the kinetic step of hydrogen abstraction associated with the EB oxidative dehydrogenation reaction under CNT catalysis. The main difference between the Mars–van Krevelen

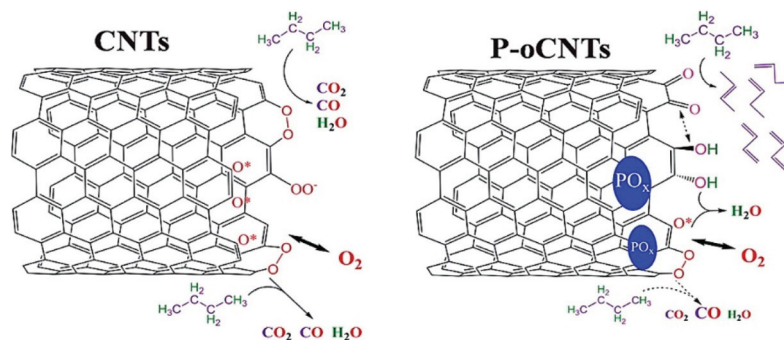


Scheme 46 Oxidative dehydrogenation of ethylbenzene with activated carbon.

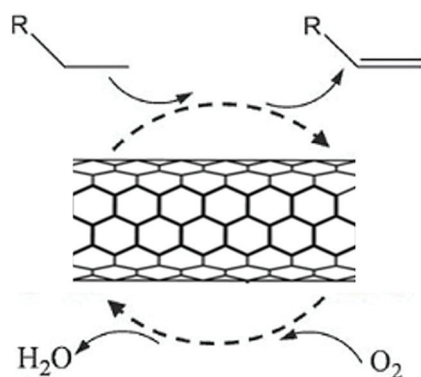
mechanism and Langmuir–Hinshelwood mechanism is related to the oxygen activation and re-oxidation steps, so that the oxygen molecules are activated at sites with defective carbon catalysts. In contrast, the reactive atomic oxygen that forms constituents diffuses into the sp^2 carbon base plate, which finally reaches the active sites under the reduced state and causes oxidation (Scheme 47).¹³⁴

In 2008, Su and coworkers demonstrated that the oxidized CNT-based metal-free catalyst could catalyze the oxidative dehydrogenation of *n*-butane to 1-butene. Investigation of reactions at temperatures of 400–450 °C in the presence of O_2 indicated that, in the absence of catalyst, mostly by-products such as 1-butene, 2-butene, butadiene, CO_2 , and CO were produced and the alkene yield was only 0.9%. Due to the higher stability of CNTs in O_2 , it was found that, during the reaction, CO_2 was produced mainly from the oxidation of hydrocarbon feedstock materials. Continued activation of CNTs with oxygen and phosphorus groups resulted in increased yields of 6.7% and 13.8%, respectively (Scheme 48).¹³⁵

Nucleophilic oxygen species, such as O^{2-} , are a prerequisite for the selective synthesis of higher alkynes. Then again, in the activation of O_2 , other nucleophilic intermediates such as O_2^{2-} , O_2^- , and O^- are formed, which results in the total oxidation of the produced alkene. In a continuation of their research, Su's group revealed that the modification of CNTs with 0.003 wt % B_2O_3 improved the production of propane by up to 18% by 0.01% loading (Scheme 49).¹³⁶ In another study, modified MCNTs with B_2O_3 (B-oCNTs) and P_2O_5 (P-oCNTs) displayed a completely similar behavior, corroborating the previous results for C_3H_8 .¹³⁷



Scheme 48 CNT-catalyzed oxidative dehydrogenation of *n*-butane to 1-butene. Reproduced from ref. 135 with permission of Science, copyright 2008.



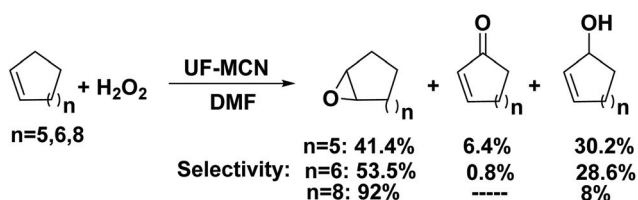
Scheme 49 The oxidative dehydrogenation of alkanes over functionalized CNTs.

Oxidation of olefins

Metal-free mesoporous carbon nitride, synthesized by nanocasting with urea/formaldehyde (UF-MCN), provides a cost-effective oxidation of cyclic olefins such as cyclopentene, cyclohexene and *cis*-cyclooctene in good yields (65–80%) with selectivity of 40–90% to the corresponding epoxide in the presence of hydrogen peroxide at 75 °C for 10 h (Scheme 50). The best result was obtained in DMF solvent and the conversion and selectivity of the products increased with an increase in the size of the ring.¹³⁸

Hydration of alkynes

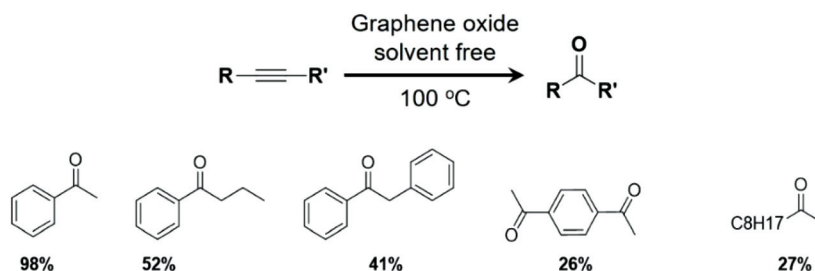
Compared with the conventional hydration of alkynes under acidic conditions at elevated temperatures (200 °C), Bielawski *et al.*⁹⁹ reported a graphene-facilitated method for hydrating various alkynes such as terminal and internal alkynes (Scheme 51); reaction with 200 wt% graphene at 100 °C for 24 h resulted in the generation of the desired product with good to excellent yields (26–98%).



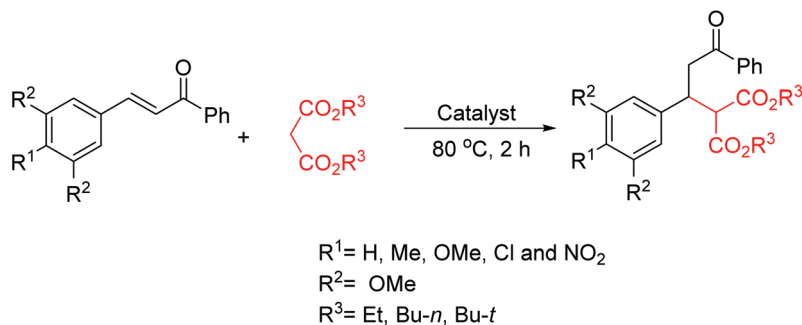
Scheme 50 Oxidation of cyclic olefins with UF-MCN.

Michael reaction using solid base catalyst

Kubota and co-workers introduced two types of organic-functionalized molecular sieves (OFMSs) and silicate–organic com-



Scheme 51 Hydration of various alkynes using graphene oxide.



Scheme 52 The SOCM and OFMS catalyzed Michael reaction using chalcone derivatives and malonic esters.

posite materials (SOCMs) mesostructure as catalysts for a Michael's reaction of chalcone derivatives with malonic esters (Scheme 52).¹³⁹ Their results at 80 °C for 2 h under a nitrogen atmosphere showed that OFMSs with a high pore volume or surface area in polar solvents (EtOH and DMF) gave a better yield (43–87%) than in a non-polar solvent such as benzene (3–4% yield). In contrast, SOCMs are significantly active in polar solvents and benzene (58–99% yield).

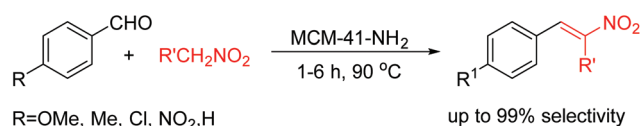
The preparation of solid magnetic sulfonic acid ($\text{Fe}_3\text{O}_4@\text{SiO}_2@\text{Me}\&\text{Et-PhSO}_3\text{H}$) modified with hydrophobic regulators served as an efficient and recyclable catalyst for one-pot aza-Michael and Mannich-type reactions; various aldehydes, ketones and amines afforded the corresponding products in high to excellent yield (aza-Michael: 85–99%, Mannich: 86–99%). The high reactivity of the $\text{Fe}_3\text{O}_4@\text{SiO}_2@\text{Me}\&\text{Et-PhSO}_3\text{H}$ was ascribed to the synergistic effects between the adequate hydrophobicity and the acidity of the silicon networks (Scheme 53).¹⁴⁰

Nitroaldol condensation by solid base catalyst

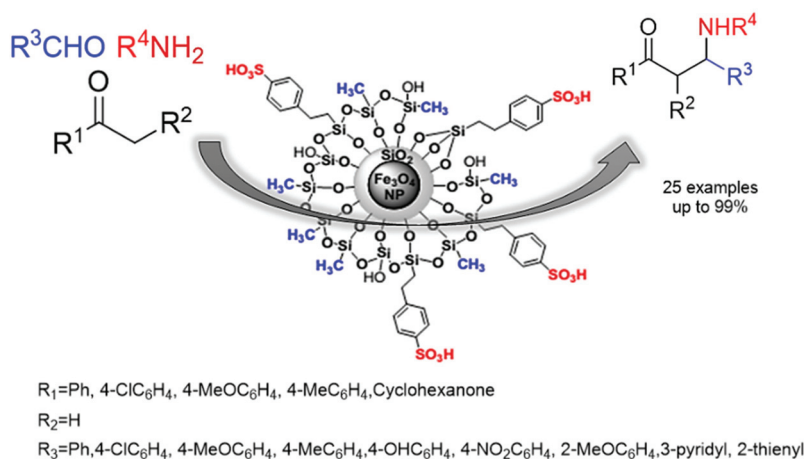
In 2001, Sartori's group offered a propylamine-modified MCM-41 silica for the synthesis of (*E*)-nitrostyrenes *via* nitroal-

dol condensation between nitroalkanes and various aromatic aldehydes, with excellent yields (88–98%) and high selectivity (97–99%) (Scheme 54).¹⁴¹

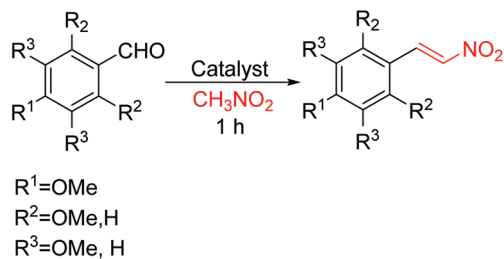
Amine-functionalized monodisperse mesoporous silica spheres (MMSSs) have been prepared using quaternary ammonium salts with various alkyl-chains such as $\text{C}_{10}\text{TMABr}$, $\text{C}_{14}\text{TMACl}$, $\text{C}_{16}\text{TMACl}$, $\text{C}_{18}\text{TMACl}$ in methanol solvent. The average diameter of MMSSs is directly related to the methanol, so that by accurately controlling the methanol, a proportion of MMSSs with a size of 560–600 nm and a pore size of 0–2.66 nm could be synthesized. The synthesized MMSSs were found to be suitable for a nitroaldol reaction of benzaldehyde derivatives and nitromethane; an excellent conversion for $\text{C}_{16}\text{-MS-AP}$ with a yield of 86–100% and a TON of 48–56% was attained (Scheme 55).¹⁴² The diameter of the particles influ-



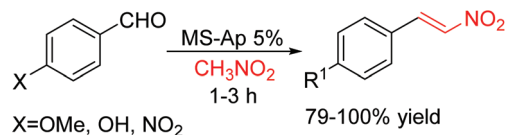
Scheme 54 Condensation between nitroalkanes and aromatic aldehydes catalyzed by MCM-41-NH₂.



Scheme 53 $\text{Fe}_3\text{O}_4@\text{SiO}_2@\text{Me}\&\text{Et-PhSO}_3\text{H}$ -catalyzed one-pot aza-Michael and Mannich reactions. Reproduced from ref. 140 with permission of Elsevier, copyright 2015.



Scheme 55 Reaction of substituted aldehydes with nitromethane for nitroalkene preparation.



Scheme 56 Nitroaldol condensation using MS-AP5%.

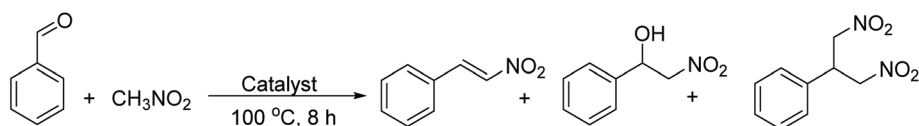
enced the yield of the products, so that at 90 °C in 1 h for 4-hydroxybenzaldehyde, an 86% yield was observed (Scheme 56).¹⁴³

Iwasawa *et al.* introduced an organo-functionalization of double-amine catalyst on silica-alumina (SA-NH₂-NEt₂) for the synthesis of 1,3-dinitroalkanes wherein the hybrid system catalyst was prepared by varying the percentages of primary and tertiary amines; SA-NH₂-NEt₂ (60/40 NH₂/NEt₂) afforded the best catalytic performance in terms of 100% conversion and 48–93% selectivity for various aldehydes. The use of an amine group in the functionalized amine groups SA-NH₂-NEt₂ (60/40 NH₂/NEt₂) led to a 1,3-dinitroalkane product with a yield of 93% while SA-NH₂ and SA-NEt₂ offered a nitro styrene product with a yield of 71% and 68%, respectively (Scheme 57).¹⁴⁴

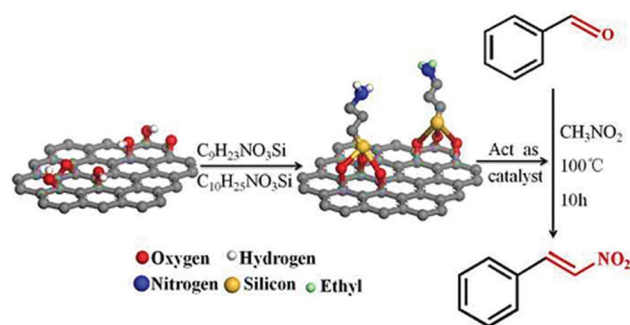
Similarly, the synthesis of *trans*-β-nitrostyrene has been reported using primary and tertiary amine bifunctional graphene oxide (GO-NH₂-NEt₂) where it showed the highest activity with NH₂:NEt₂ in 1:1 ratio with a 99.5% yield and a 100% selectivity; however, for GO-NH₂ and GO-NEt₂, the selectivity was 100% but the conversion was less than that of GO-NH₂-NEt₂ (39.9 and 30.9%, respectively), thus indicating a cooperative catalysis between the primary amines (NH₂) and tertiary amines (NEt₂) in GO-NH₂-NEt₂ (Scheme 58).¹⁴⁵

Knoevenagel condensation

A selective and water-stable metal-free catalytic exchange-system has been introduced for Knoevenagel condensation



Scheme 57 Reaction of benzaldehyde and nitromethane with SA-NH₂-NEt₂.



Scheme 58 Bifunctional graphene-oxide-catalyzed synthesis of β-nitrostyrene. Reproduced from ref. 145 with permission from the Royal Society of Chemistry, copyright 2013.

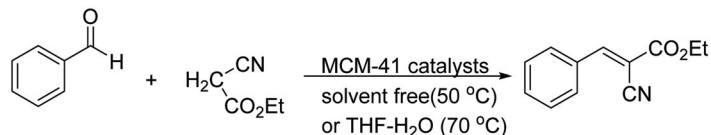
deploying assorted Mobil Composition of Matters (MCMs) for the reaction between benzaldehyde and ethyl cyanoacetate under solvent-free conditions at 150 °C; 81% conversion was observed with 75% selectivity for Na-MCM-41 and 67% conversion with 60% selectivity for Cs-MCM-41A (Scheme 59). The use of solvent and temperature were found to increase the selectivity where THF-H₂O solvent for Na-MCM-41 delivered 99% selectivity while Cs-MCM-41 afforded 98% selectivity.¹⁴⁶

Nitrogen-doped carbon materials, obtained *via* ammoxidation of carbon black and activated carbon with NH₃, served as base catalysts for Knoevenagel condensation wherein nitrogen doping boosted the coexistence of O₂ with NH₃ and the higher reactivity of carbon to oxygen. The ratio of surface N/O species was also significant as the maximum activity was achieved at a ratio of 0.8–1 (Scheme 60).¹⁴⁷

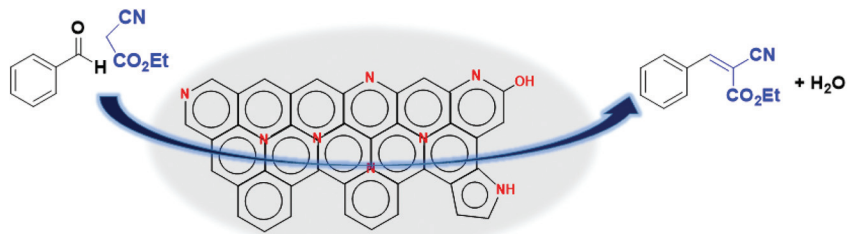
Deprotonated polymeric mesoporous graphitic carbon nitride (mpg-C₃N₄), as a heterogeneous catalyst, has been deployed in Knoevenagel condensation reactions (Scheme 61); various aldehydes and nitriles afforded the corresponding products in conversions of up to 99% with selectivity up to 100% by using acetonitrile as the solvent and tBuOK as the base at 70 °C.¹⁴⁸

A metal-free protocol has been reported for the synthesis of 2-oxoindolin-3-ylidene malononitrile/cyanoacetates in good yield (85–95%) from substituted isatins and malononitrile or ethyl cyanoacetate in the presence of sulfonic-acid-functionalized SBA-15 (SBA-Pr-SO₃H) in H₂O under reflux conditions for 5–15 min (Scheme 62).¹⁴⁹

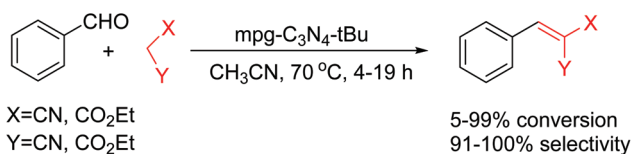
A nano-Fe₃O₄-encapsulated silica (Fe₃O₄@SiO₂-SO₃H) for the synthesis of tetraketone derivatives was shown *via* the Knoevenagel condensation and Michael addition reactions of various aromatic aldehydes with dimedone, 1,3-indanedione, and 1,3-dimethyl barbituric acid in H₂O at room temperature;



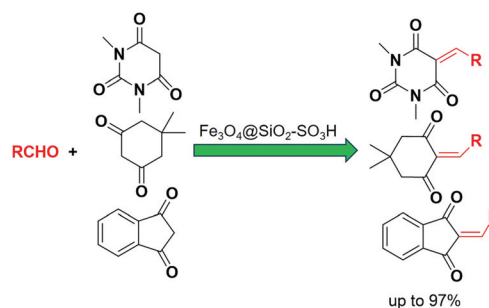
Scheme 59 Knoevenagel condensation of benzaldehyde and ethyl cyanoacetate with different MCM-41 catalysts.



Scheme 60 Nitrogen-doped carbon catalyst used for Knoevenagel and transesterification reactions.

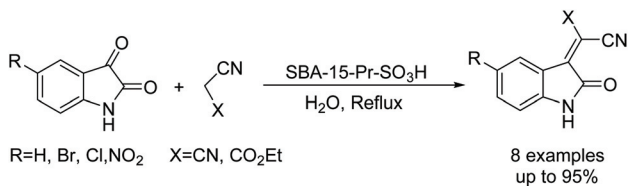


Scheme 61 Various Knoevenagel condensations catalyzed by mpgC₃N₄-tBu.



R=Ph, 4-Br-C₆H₄, 3-Br-C₆H₄, 2-Cl-C₆H₄, 4-Cl-C₆H₄, 2-MeO-C₆H₄, 4-MeO-C₆H₄, 4-Me-C₆H₄, 2-NO₂-C₆H₄, 3-NO₂-C₆H₄, 4-NO₂-C₆H₄, 2,4-Cl₂-C₆H₃, 2-OH-C₆H₄, 3,4-(MeO)₂-C₆H₃, 4-(Me₂N)-C₆H₄, Naphthalene-2-carbaldehyde, 4-F-C₆H₄, 2-Thiophene, C₆H₅CH=CH

Scheme 63 Knoevenagel condensation catalyzed by Fe₃O₄@SiO₂-SO₃H.

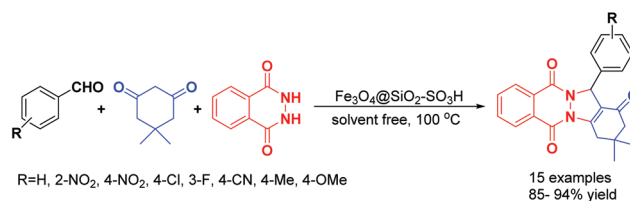


Scheme 62 SBA-Pr-SO₃H-catalyzed synthesis of 2-oxoindolin-3-ylidene.

and good to excellent yields (44–97%) were obtained (Scheme 63).¹⁵⁰

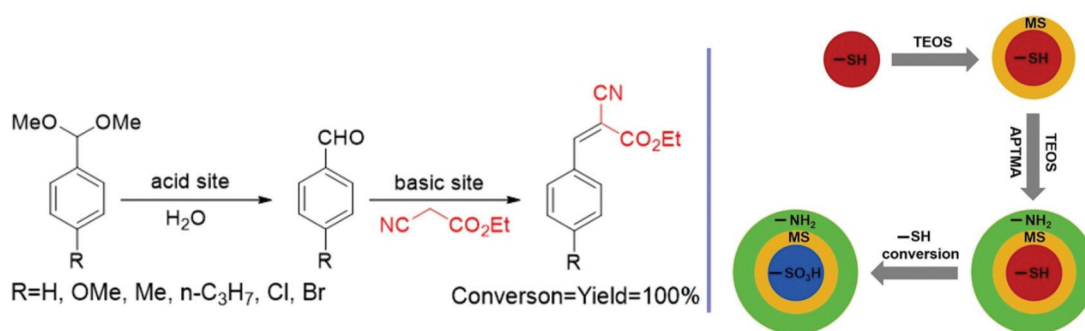
Sulfuric acid grafting onto silica-coated Fe₃O₄ NPs has been evaluated in a domino Knoevenagel condensation/Michael addition/intramolecular cyclodehydration sequence for the synthesis of indazolo[2,1-*b*]phthalazine-triones and pyrazolo[1,2-*b*]phthalazine-diones under solvent-free conditions at 100 °C. Fe₃O₄@SiO₂-SO₃H afforded the corresponding products in excellent yields (85–94%) in the presence of 0.075 gr of catalyst at 100 °C within 30–45 min (Scheme 64) and the catalyst could be recovered and reused for up to 6 cycles without a significant decrease in activity.¹⁵¹

Bifunctional mesoporous silica nanoreactors, with dual activity emanating from both the acid and base, were successfully prepared by using a co-condensation method and it successfully catalyzed one-pot deacetalization–Knoevenagel condensation reaction. The acid–base bifunctional core–shell-



Scheme 64 Solvent-free synthesis of indazolo[2,1-*b*] phthalazine-triones and pyrazolo[1,2-*b*] phthalazine-diones catalyzed by Fe₃O₄@SiO₂-SO₃H.

shell consisted of a core made of SO₃H and shells comprising MS (mesoporous silica) and NH₂, respectively. The reaction consisted of two separate steps in which hydrolysis of the acetal was carried out by the acidic sites followed by Knoevenagel condensation *via* the base sites leading to the desired product; nearly quantitative yield and conversion was attained by the deployment of MS-SO₃H@MS@MS-NH₂ at 80 °C (Scheme 65).¹⁵²

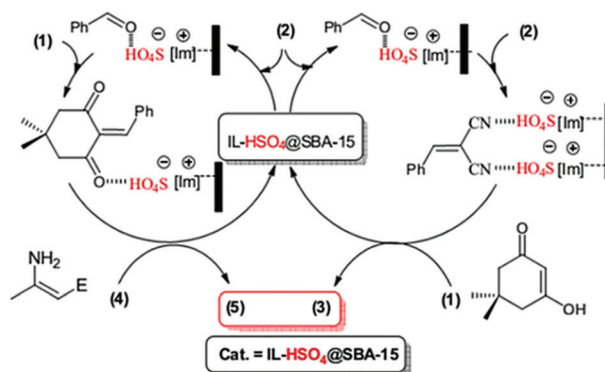
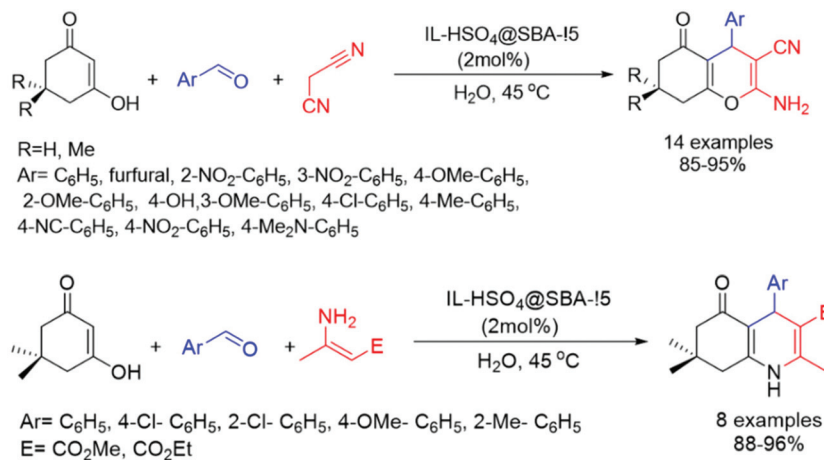


Scheme 65 Acid–base bifunctional core–shell–shell-structured MS-SO₃H@MS@MS-NH₂-catalyzed one-pot deacetalization–Knoevenagel condensation.

In another study, [MPlm][HSO₄]*@*SBA-15 was used as an environmentally friendly, metal- and halogen-free recyclable catalyst for the synthesis of tetrahydrochromenes from aldehyde, malononitrile and -CH nucleophile and for the preparation of polyhydroquinolines from aldehyde, dimedone, enaminone and NH₄OAc *via* Knoevenagel–Michael–cyclization under mild and greener conditions. The active sites in the pores of SBA-15, due to the hydrophobic nature of the ionic

liquid and efficient mass transfer, leads to the enhanced efficiency for the desired products; the catalyst maintained its catalytic performance up to 76% during 11 test runs in the recycling study. The mechanism of the reaction is depicted in Scheme 66.⁴⁷

Fan *et al.* developed the use of SBA-15 as a template for the preparation of two-dimensional mesoporous carbon nitride under varying carbonization temperatures with a tunable



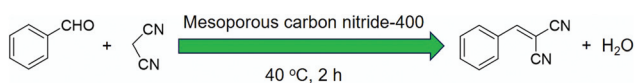
Scheme 66 The synthesis of tetrahydro-4*H*-chromenes and polyhydroquinolines using IL-HSO₄@SBA-15 and the plausible mechanism. Reproduced from ref. 47 with permission from Elsevier, copyright 2014.

surface area for the Knoevenagel condensation. Carbonization in the range 300–800 °C revealed that mesoporous carbon nitride-400 (400 refers to the temperature of carbonization) showed the best result with the highest catalytic activity in the Knoevenagel condensation of benzaldehyde and acetone with malononitrile under mild conditions; excellent yields with 100% selectivity in 2 h were discerned (Scheme 67).¹⁵³

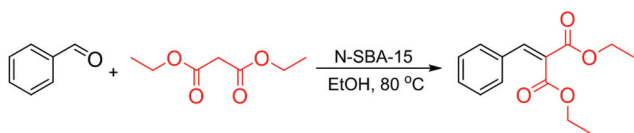
In 2015, Polshettiwar and co-workers reported that by adjusting the temperature of the nitridation, the catalytic activity of SBA-15 could be enhanced. The results indicated that although the increase in nitridation temperature leads to an increase in N content, the catalytic activity does not increase, presumably due to two important factors: (1) the concentration of silanol groups and (2) the reaction of siloxane with NH₃ molecules, which have a common role in the degree of nitridation of SBA-15 at assorted temperatures. The ideal results were obtained for the Knoevenagel condensation reaction between benzaldehyde and diethyl malonate under reflux in ethanol for 24 h, using SBA-15 with a TON of 3150 (Scheme 68).¹⁵⁴

Giambastiani and co-workers utilized aziridine-decorated multi-walled carbon nanotubes (MW@NAz) for the Knoevenagel condensation using benzaldehyde as an electrophile and ethyl cyanoacetate and dimethyl malonate as two nucleophiles in EtOH (Scheme 69); a high yield (>99%) was achieved using 10 mg of catalyst at 78 °C.¹⁵⁵

Graphitic carbon nitride (g-C₃N₄) served as a solid base catalyst for the Knoevenagel condensation at ambient tempera-



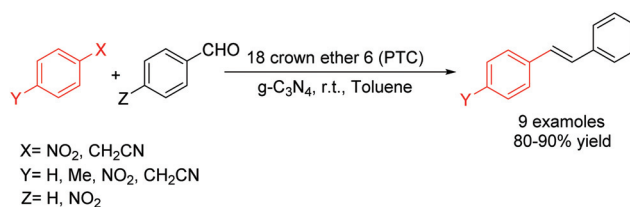
Scheme 67 Catalytic activity of mesoporous carbon nitride-400 in Knoevenagel condensation.



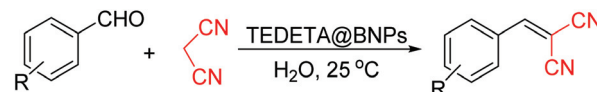
Scheme 68 Catalytic activity of N-SBA-15 in the Knoevenagel condensation reaction.



Scheme 69 Catalytic activity of MW@N^{Az} for Knoevenagel condensation.



Scheme 70 g-C₃N₄-catalyzed Knoevenagel condensation with 18 Crown ether.

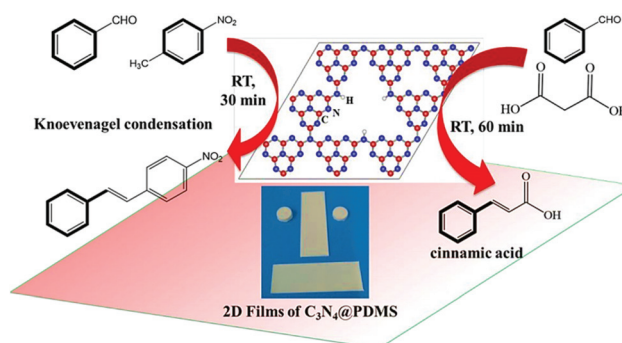


Scheme 71 TEDETA@BNPs-catalyzed Knoevenagel condensation.

ture for the synthesis of substituted stilbene in the presence of 18 Crown ether 6 (PTC), among several others, as a phase transfer catalyst; assorted substrates afforded a yield of 80–99% at ambient temperature and with a short reaction time (30 min) in toluene (Scheme 70).¹⁵⁶

N,N,N',N'-Tetraethyldiethylenetriamin (TEDETA) supported on boehmite NPs (BNPs) as a reusable, metal-free organo-catalyst for the Knoevenagel condensation reaction has been reported; the reaction of numerous aldehydes, bearing both donor and acceptor groups, with malononitrile afforded excellent (89–98%) yields in water at ambient temperature (Scheme 71).¹⁵⁷

Organic-inorganic hybrid, namely polydimethylsiloxane (PDMS), as a strong support has been used for immobilizing g-C₃N₄ to obtain a 2D film of g-C₃N₄@PDMS heterogeneous catalyst with high mechanical strength for the Knoevenagel condensation under PTC. The deployment of g-C₃N₄@PDMS in the presence of 18 Crown ether 6 (PTC) catalysts generated cinnamic acids using various aldehydes and malonic acid at 25 °C in toluene solvent (80–99% yields) including substituted stilbenes; PDMS had no catalytic role and served only as a support for the g-C₃N₄ (Scheme 72).¹⁵⁸



Scheme 72 Knoevenagel condensations using a 2D film of g-C₃N₄@PDMS. Reproduced from ref. 158 with permission from the American Chemical Society, copyright 2020.

Tandem reactions

Magnetic mesoporous silica adorned with sulfonic acid and diamine groups was synthesized by Jun and his colleagues and used as an excellent hybrid and recyclable catalyst for the conversion of benzaldehyde dimethyl acetal to benzaldehyde through acid-catalyzed deacetalization, followed by the conversion of benzaldehyde to 1-nitro-2-phenylethylene *via* the base-catalyzed Henry reaction. The recovery and reusability of MMAB (magnetic mesoporous acid–base) catalyst for a one-pot tandem reaction was shown for 5 consecutive runs, affording a yield of over 90% (Scheme 73).¹⁵⁹

Sequential dehydration–hydrothiolation

In 2016, Basu *et al.* developed the first catalytic metal-free protocol for a one-pot sequential dehydration–hydrothiolation reaction starting from two groups of secondary aryl alcohols with various thiols (Scheme 74); good yields (67–81%) were obtained for all unsymmetrical thioether products under optimum conditions comprising graphene oxide carboxylate (10 mg) in toluene at 65 °C under a N₂ atmosphere, and this carboxylate could be reused 5 times without any loss of catalytic activity.¹⁶⁰

Oxidation of thiols and sulfides

Among organic transformations, the oxidation of sulfides to sulfoxides has wide-ranging applications and is of notable importance.¹⁶¹ Historically, sulfoxides have been significant structural units in view of their broad utility as intermediates or products in the synthesis of pharmaceuticals, agrochemicals and other good chemicals.^{162,163} Among various catalytic

methods, the use of metal-free catalysts stands out, as exemplified by silica sulfuric acid (SSA) for the selective oxidation of various sulfides to sulfoxides and sulfones deploying aqueous H₂O₂ alone as an oxidant at room temperature in CH₃CN (Scheme 75). With 1 eq. of H₂O₂ and 0.1 g of SSA, in 15–360 min, sulfoxide (55–96%) was obtained as the main product, while using 3 eq. H₂O₂ and 0.2 g SSA in 45–140 min afforded sulfone (43–100%).¹⁶⁴

Immobilized propylsulfonic acid on mesoporous SBA-15 (SBA-15-Pr-SO₃H) served as an efficient and recyclable nanoreactor for the chemoselective oxidation of various sulfides to the corresponding sulfoxides in the presence of H₂O₂ at 40 °C (Scheme 76); increasing the H₂O₂ from 1 eq. to 3 eq. increased the formation of sulfone. In terms of recovery and reuse, this catalyst showed an average of 8 cycles with an efficiency of 98–96%.¹⁶⁵

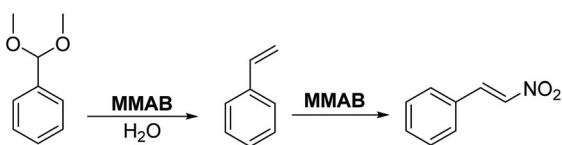
Graphite oxide carbocatalyst has been successfully applied for the selective oxidation of thiols to disulfides and sulfides to sulfoxides; a broad range of sulfides (aromatic and aliphatic) could be successfully converted to their corresponding sulfoxides using graphite oxide (300 wt%) at 100 °C in 24 h, with good yields (51–92%) (Scheme 77).¹⁶⁶

Zhang and co-workers found that mesoporous graphitic carbon nitride (mpg-C₃N₄) could increase the selective photo-oxidation rate of sulfides to sulfoxides *via* coupling with isobutyraldehyde (IBA) in the presence of O₂ (1 atm) at ambient temperature in CH₃CN; the use of IBA and mpg-C₃N₄ themselves indicated minor activity for the oxidation of methylphenylsulfide (MPS) while much improved conversion (97%) and selectively (98%) for the MPSO was obtained in 4 h, in the presence of mpg-C₃N₄ and IBA. The general protocol with the proposed mechanism is illustrated in Scheme 78.¹⁶⁷

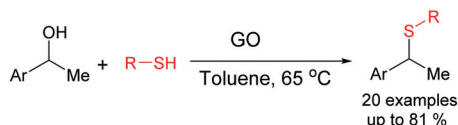
Shen *et al.* prepared silica-supported taurine and homotaurine non-metal catalysts by immobilizing them on the surface of SiO₂ and demonstrated their use as heterogeneous catalysts for the chemoselective oxidation of sulfides to sulfoxides (Scheme 79). Excellent yields for the oxidation of aromatic and aliphatic sulfides with 30% H₂O₂, up to 99.9% conversion and 99.2% selectivity, were obtained at room temperature in 24 h.¹⁶⁸

Rostamnia and co-workers introduced a metal- and halogen-free hydrogensulfate ionic liquid/SBA-15 system (IL-HSO₄@SBA-15) for a green and competent oxidation of aromatic and aliphatic organic sulfides with high selectivity towards sulfoxides using aqueous hydrogen peroxide. After elaborate screening of temperature, amount of catalyst, and several solvents, the best conditions for the chemoselective oxidation of thioanisole with 1.5 mol% IL-HSO₄@SBA-15 were found to be water as the solvent at room temperature, and 30% H₂O₂ as an oxidant; various types of primary and secondary aliphatics could be converted in high yield to sulfoxides (up to 100%). IL-HSO₄@SBA-15 could be reused up to 14 times with a slight decrease in activity. The reaction mechanism and catalytic oxidized derivatives are shown in Scheme 80.²²

In another study, the same research team developed the use of single-site supported *N*-sulfonic acid and *N*-sulfamate on SBA-15 for a greener and sustainable oxidation of sulfides. This solid acid catalyst with a sulfamic acid content and ionic

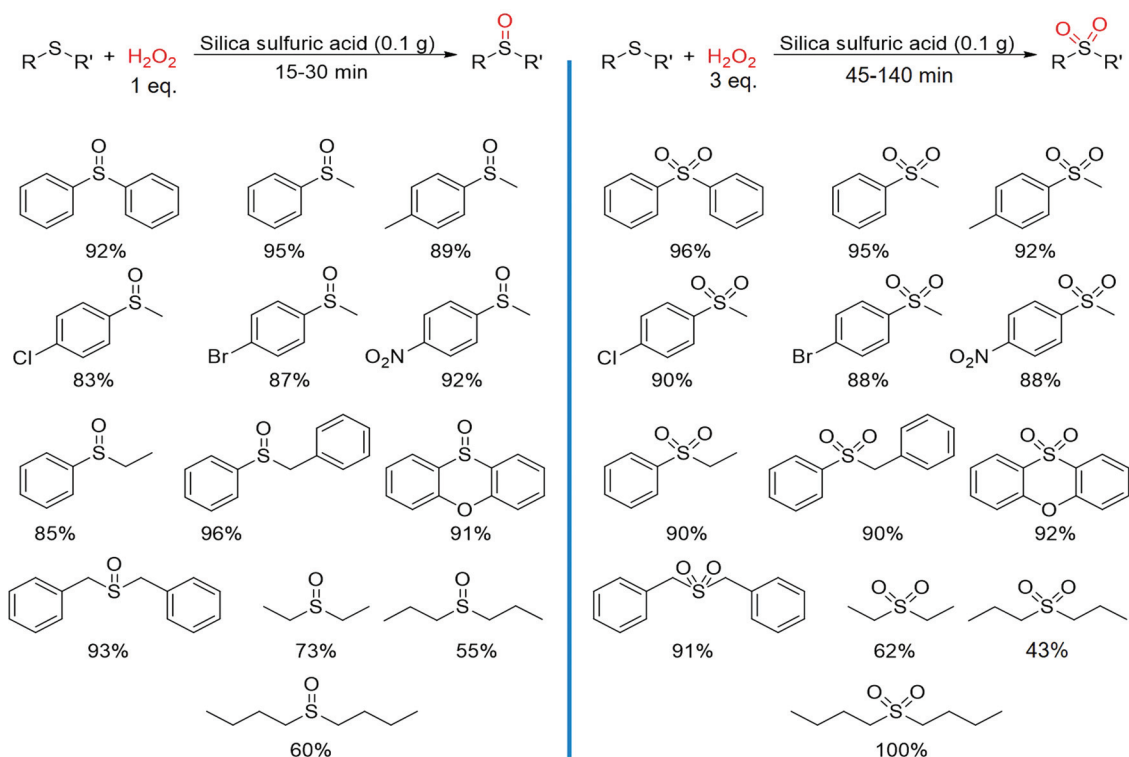


Scheme 73 Catalytic deacetalization and Henry reaction using MMAB catalyst.

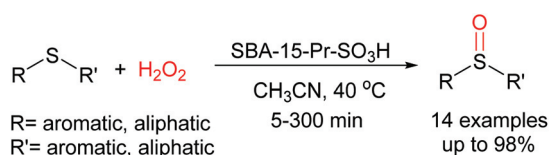


Ar = 2-C₁₀H₇, C₆H₅, 3,4-(OCH₃)₂C₆H₃, 3-NO₂C₆H₄, 4-CH₃C₆H₄, C₆H₅, C₆H₅
 R = C₆H₅, 4-ClC₆H₄, 4-CH₃C₆H₄, 2,6-(CH₃)₂C₆H₃, 4-FC₆H₄, 4-NH₂C₆H₄, CH₃(CH₂)₄,
 Cy, CH₃(CH₂)₆, CH₃(CH₂)₄.

Scheme 74 GO catalyzed one-pot sequential dehydration–hydrothiolation.



Scheme 75 Oxidation of sulfides to sulfoxides and sulfones by H_2O_2 in the presence of SSA.



Scheme 76 Selective oxidation of sulfides into sulfoxides using SBA-15-Pr-SO₃H.

liquid characteristics, due to its zwitterionic feature of sulfamic acid motifs, afforded enhanced recyclability options and lower production of VOCs in the oxidation of aromatic sulfides using hydrogen peroxide under aqueous conditions in 15–45 minutes. The catalytic power of SBA-15/En-NHSO₃H did not diminish during the 11 recovery and reuse steps (Scheme 81).¹⁶⁹

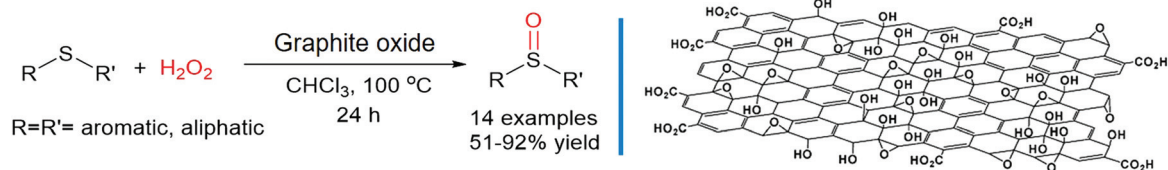
The chemoselective oxidation of sulfides to the corresponding sulfones using carboxyl-decorated graphene oxide sheets as an efficient metal-free heterogeneous catalyst has

been reported under mild conditions, which is influenced by various factors such as the amount of catalyst, temperature and hydrogen peroxide concentration (Scheme 82).¹⁷⁰

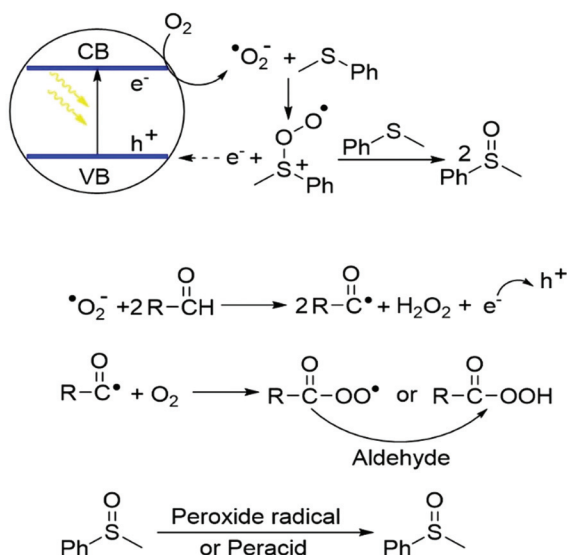
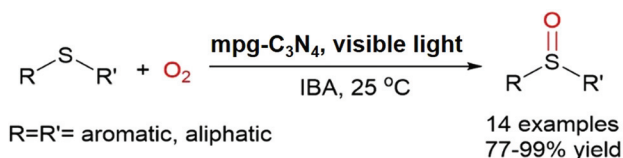
Recently, a selective and mild photo-oxidation of sulfides to sulfoxides has been reported wherein C₆₀/g-C₃N₄ was applied as an electron source for the formation of superoxide (O₂^{•-}). The photocatalytic reactions were performed under optimal conditions using 4 wt% C₆₀/g-C₃N₄, CH₃OH as solvent and 1 atm O₂ at room temperature; a synergistic effect between C₆₀ and g-C₃N₄ afforded more than 95% selectivity and 71% conversion in the oxidation of sulfides into sulfoxides. The general protocol with the proposed mechanism is illustrated in Scheme 83.¹⁷¹

Cyclotrimerisation

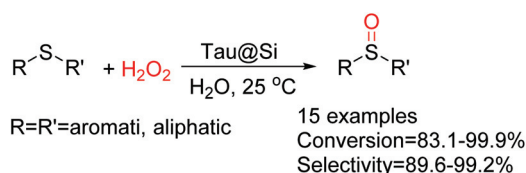
A cyclisation of diverse functionalized nitriles and alkynes has been reported which is catalyzed by mesoporous graphitic



Scheme 77 Oxidation of various sulfides by using graphite oxide. Reproduced from ref. 166 with permission from the Royal Society of Chemistry, copyright 2011.



Scheme 78 Oxidation of various sulfides by an mpg-C₃N₄-IBA system and the possible reaction mechanism.



Scheme 79 Tau@Si-catalyzed oxidation of various sulfides.

carbon nitride (mpg-C₃N₄) at 140 °C; 20% conversion was attained for acetonitrile in 80 h with TOF = 55 day⁻¹, and 75% for phenylacetylene in 24 h with TOF = 126 day⁻¹. According to DFT results, the activation of the nitriles presumably occurred through the H-bond, while the activation of the alkenes proceeded *via* π -stacking (Scheme 84).¹⁷²

Oxidation of ethyl- and methylbenzene

The selective and solvent-free oxidation of toluene and various derivatives to the corresponding aldehydes has been developed using metal-free mesoporous graphitic carbon nitride (mpg-C₃N₄) catalyst in the presence of O₂ as an oxidant. The g-C₃N₄ nanostructure was developed by tuning the homogeneous oxidation to heterogeneous oxidation; capturing all free $\text{O}_2^{\bullet-}$ radicals at 160 °C resulted in a high selectivity (>99%) in the conversion of different derivatives to aldehydes (Scheme 85).¹⁷³

Similar to doped-carbocatalysts, N-doped graphene materials have been developed from both inorganic and organic nitrogen sources and pyrolytic graphene oxide as the carbon substrate. The detailed growth mechanism for the N sites in these N-doped graphene materials and their corresponding catalytic activity in the selective oxidation of ethylbenzene was investigated; different precursors and binding energy of the N sites resulted in diverse trends with annealing temperature. Thus, the contents and compositions of nitrogen sites could be changed by the nitrogen precursor, at low and high binding energies and annealing temperatures. These N-doped carbon materials displayed excellent activity in the selective oxidation of ethylbenzene; the yield of acetophenone did not depend on the total nitrogen amount whereas the type of graphitic nitrogen sites was responsible for the reaction to acetophenone (Scheme 86).¹⁷⁴

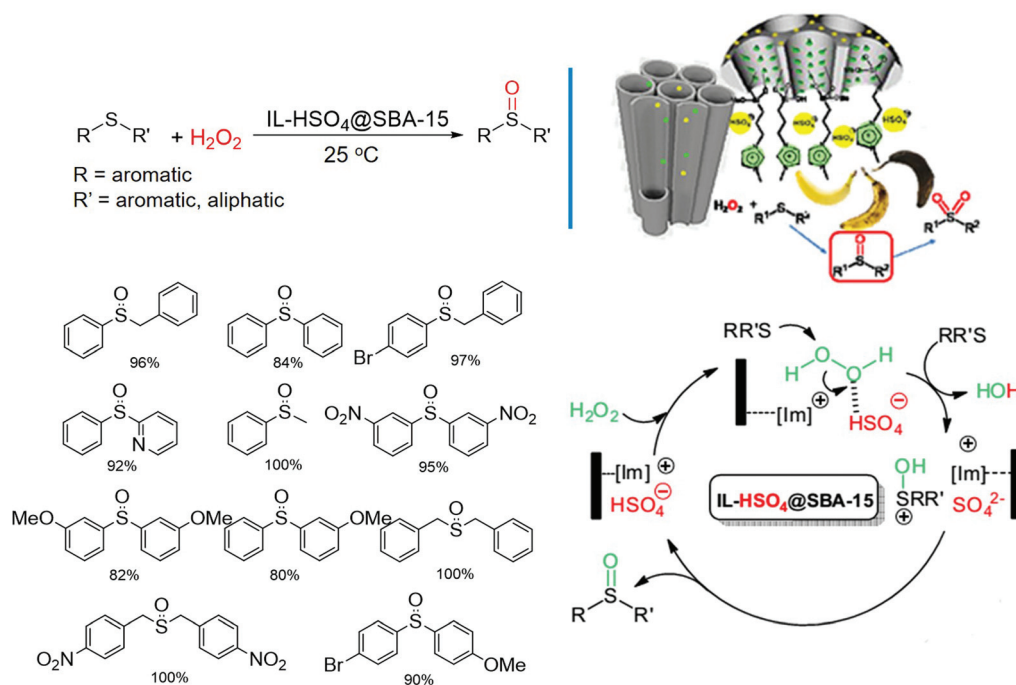
In 2014, Sicilia *et al.* developed the oxidation of ethylbenzene to acetophenone with N-doped graphene in view of theoretical studies that were used to characterize the active sites on the surface of N-doped graphene, in terms of the charge and spin density induced by doping of graphene with N atoms in the graphitic configuration. Studies asserted that the identified mechanism, in view of thermodynamics and kinetics, are favorable due to the overall high exothermicity and low activation energies, respectively, wherein OOH radicals are active peroxide species that promote the reaction. On the other hand, kinetically the formation of the OOH and its decomposition to other active oxygen species are affiliated with low activation energies (Scheme 87).¹⁷⁵

Li and coworkers directly incorporated boron atoms into polymeric g-C₃N₄ using BH₃NH₃ as the boron source, and prepared boron-doped polymeric carbon nitride solids (CNBs). The combination of CNBs with H₂O₂ afforded a higher conversion of toluene and ethylbenzene in comparison with g-C₃N₄, with uniformly high selectivity (>99%) of benzaldehyde and acetophenone. Increasing the oxidation potential was accomplished by incorporation of boron, which lowered the highest occupied molecular orbital position of the resulting material (Scheme 88).¹⁷⁶

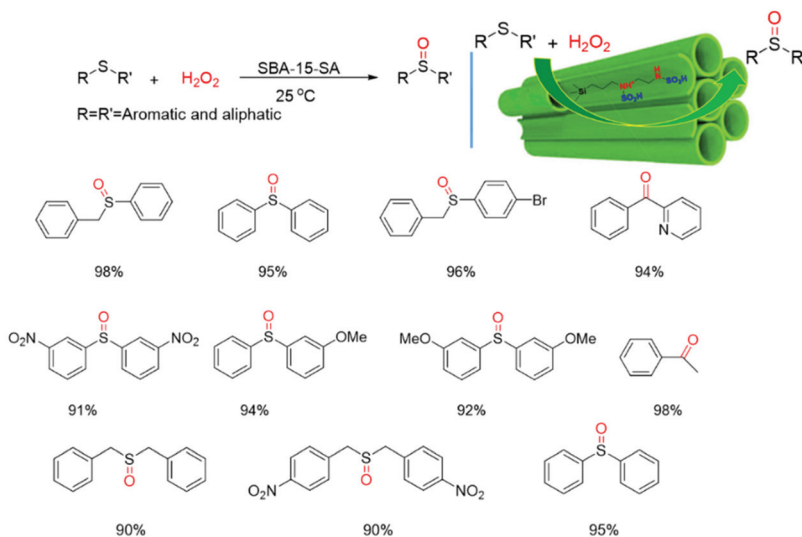
Graphene doped as a metal-free carbocatalyst afforded 90% selectivity in the ketone–alcohol mixture. A logical mechanism was confirmed using 2,6-di-*tert*-butyl-4-methylphenol as a carbon-centered free-radical quencher. Based on these results, it was proposed that the doped N or B atom did not participate in the activation of the reactants, but instead influenced the electronic structure of the adjacent carbon atoms, which promoted their catalytic activities (Scheme 89).¹⁷⁷

Transesterification of alcohols

Mesoporous graphitic carbon nitride (mpg-C₃N₄) has been used as a heterogeneous and metal-free catalyst for the solvent-free transesterification of ethylacetoacetate with various alcohols with good to excellent conversion in 6 h at a –110 °C reaction temperature. The best results were obtained



Scheme 80 IL-HSO₄@SBA-15 for green oxidation of sulfides and possible mechanisms. Reproduced from ref. 22 with permission from Elsevier, copyright 2015.



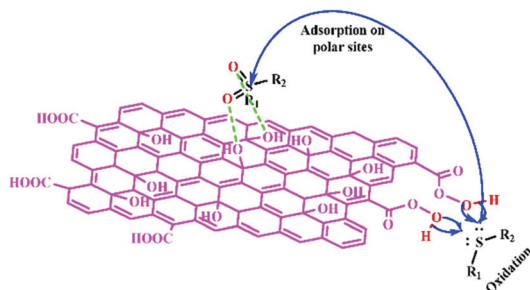
Scheme 81 Oxidation of sulfides by using SBA-15-SA. Reproduced from ref. 169 with permission of Elsevier, copyright 2016.

for 1-butanol with 69% conversion and 100% selectivity (Scheme 90).¹⁷⁸

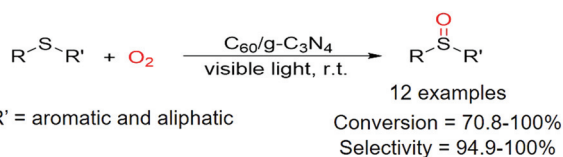
Aerobic oxidation of xanthene

Fujita and coworkers reported the development of a first metal-free aerobic oxidation of xanthene to xanthone (XO) based on a N-doped carbon catalyst where the activity was

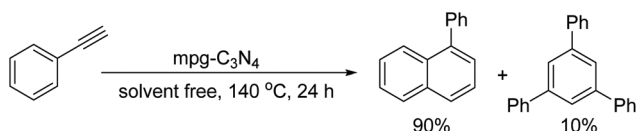
completely dependent on the N source gases. For N-doping at 800 °C, the total amount of doped N atoms was in the order NH₃-air > NH₃ > NO, respectively. The X-ray photoelectron spectroscopy (XPS) data indicated the existence of pyridine and pyrrole/pyridone-type N species with two types of N, N (1) and N (2) species on N-carbons. The dispersion for N (2) was much larger than for N (1), indicating that N (1) species are involved in the active sites for the reaction. The exact relationship between the catalyst activity and species N (1) was con-



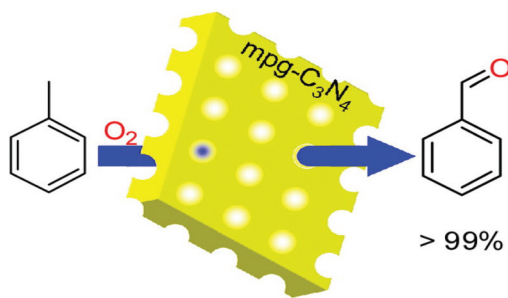
Scheme 82 Acidic graphene-oxide-catalyzed oxidation of sulfide. Reproduced from ref. 170 with permission of Elsevier, copyright 2017.



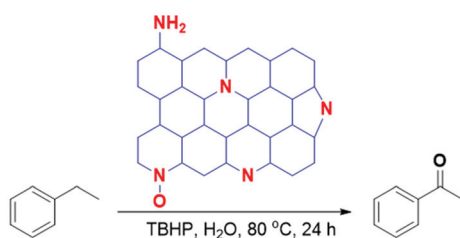
Scheme 83 Oxidation of various sulfides by C₆₀/g-C₃N₄ and possible reaction mechanism.



Scheme 84 Cyclotrimerization of phenylacetylene catalyzed by mpg-C₃N₄.



Scheme 85 Catalytic oxidation of toluene using mpg-C₃N₄. Reproduced from ref. 173 with permission from the American Chemical Society, copyright 2012.



Scheme 86 Catalytic activity of N-doped graphene in the selective oxidation of ethylbenzene.

sidered with O (1) and O (2). It was found that there is a better correlation between XO yield and N (1) than O (2) species (Scheme 91).¹⁷⁹

N-Formylation

An environmentally friendly and chemoselective synthesis of biologically and industrially active formamides has been achieved through the reaction of various amines and ethyl formate at 50 °C under solvent conditions catalyzed by covalently bonded zwitterionic sulfamic acid onto SBA-15 (SBA-15/PrEn-NHSO₃H) (Scheme 92). Rostamnia and group showed that double-sulfonation of ethylenediamine in SBA-15 leads to the formation of a cooperative system to catalyze the reaction in terms of simple handling, easy recovery and high recyclability, with a low-amount catalyst; assorted derivatives, using 1 mol% of the catalyst, afforded yields of 56–98%.¹⁸⁰

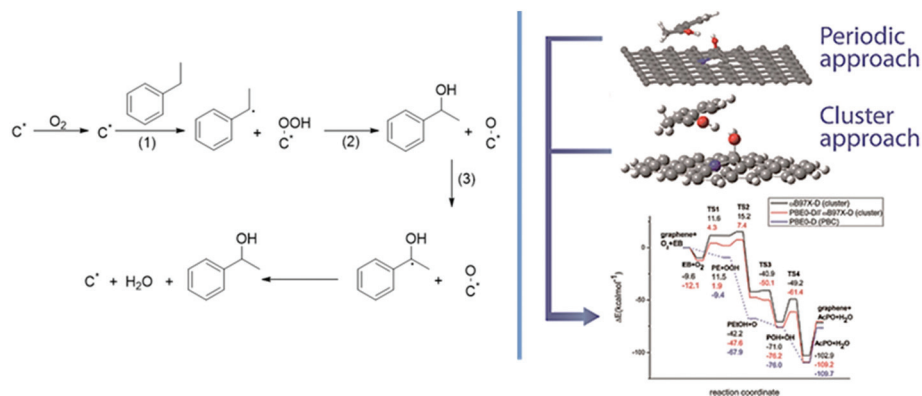
Esterification of O-alkyl alkylphosphonic and carboxylic acids

In 2015, Wilson *et al.* exploited a mesoporous sulfonic acid silica where propylsulfonic-acid-functionalized SBA-15 (PrSO₃H/SBA-15) was as an effective catalyst for the upgrading of a pyrolysis bio-oil *via* esterification of acetic acid with benzyl alcohol; enhanced sulfonic acid site densities and the loss of surface silanols are responsible for the increase in acid strength due to the surface crowding of sulfonate groups and the rate of benzyl acetate production (Scheme 93).¹⁸¹

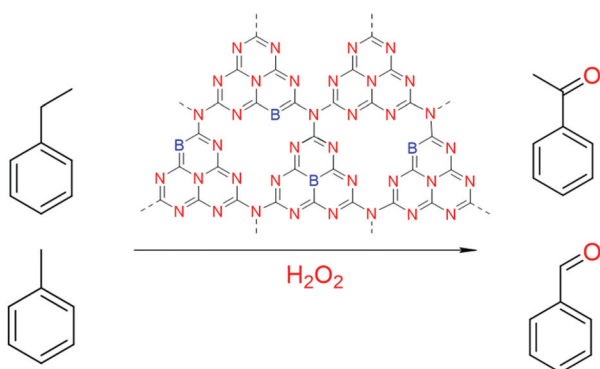
The surface hydrophobicity of organosulfonic-acid-functionalized silica-coated magnetic catalysts (1: Fe₃O₄@SiO₂@Et-PhSO₃H) and (2: Fe₃O₄@SiO₂@Me&Et-PhSO₃H) was assessed in water-generating reactions, especially the esterification reaction of fatty alcohols, hydrophobicity, water-toleration by the catalysts' surface and the mass transfer of reaction partners being the key properties. Methyl groups on the surface of bifunctional catalyst 2 attributed to its hydrophobic character, resulting in better mass transfer, while the shielding effects of methyl groups on catalyst 2 prevented the deactivation of sulfonic active sites by ensuing water as by-product, culminating in enhanced water-toleration and water extrusion from the surface of the catalyst (Scheme 94).¹⁸²

Polymerization of divinylbenzene with 4-vinylpyridine monomers can also be utilized to produce mesoporous materials for catalytic applications as illustrated by Kara *et al.* to prepare a porous magnetic sulfonic-acid-functionalized polymeric material *m*-poly (DVB-4VP-SO₃H) for the conversion of propionic acid to methyl ester with negligible loss of activity after four repetitive cycles (Scheme 95).¹⁸³

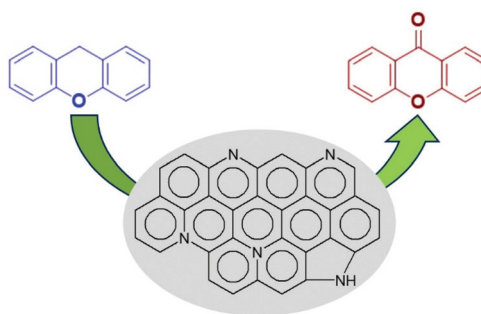
Similarly, esterification of O-alkyl alkylphosphonic and carboxylic acids to obtain organophosphorus and carboxylic esters has been investigated deploying polymer-supported sulfonated magnetic resins (PSMRs) in high yields under mild reaction conditions (Scheme 96).¹⁸⁴



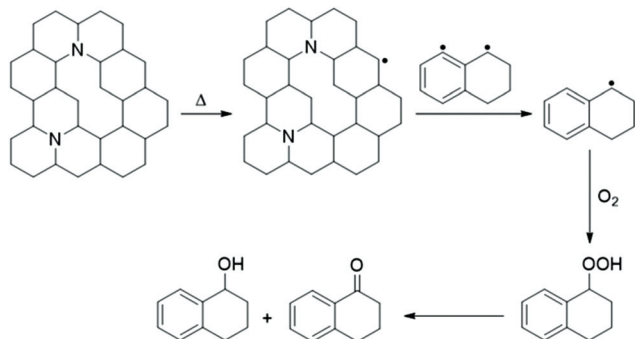
Scheme 87 Possible reaction mechanism for the oxidation of ethylbenzene to acetophenone over nitrogen-doped graphene. Reproduced from ref. 175 with permission from the American Chemical Society, copyright 2014.



Scheme 88 Boron-doped polymeric carbon-nitride-catalyzed oxidation of ethylbenzene to acetophenone in the presence of H_2O_2 .

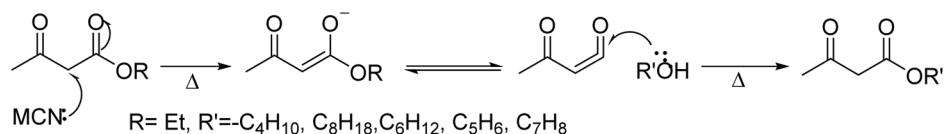


Scheme 91 Oxidation of xanthene to xanthone using nitrogen-doped carbon.

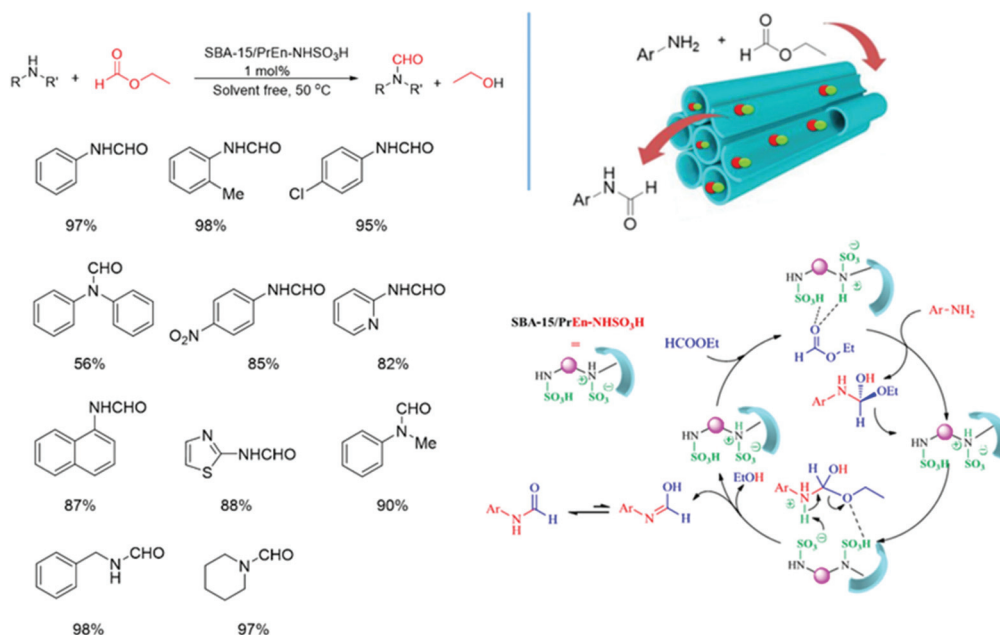


Scheme 89 Proposed mechanism for aerobic oxidation using (N)G as a catalyst.

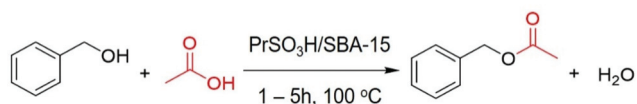
In an extension of the esterification protocol, the preparation of a solid acid catalyst with sulfonated polystyrene (PS) encapsulated within the hollow interiors of silica-based hollow nanostructures have been reported by Yang *et al.* They uncovered that two types of PS- SO_3H @phenylenesilica nanostructure with double-shell (DSNs) and yolk-double-shell nanostructure (YDSNs) result in larger and smaller inner void spaces, respectively. Furthermore, the swelling and aggregation of PS- SO_3H in a confined nanospace can be directly related to the acid strength of the solid acid as DSNs with PS- SO_3H in a more aggregated state show higher acid strength than YDSNs with PS- SO_3H in a less aggregated condition. Both of these acidic nanostructures display comparable activity and are more active than Amberlyst-15 in the esterification reaction of fatty acids (Scheme 97).¹²⁸



Scheme 90 General reaction mechanism involved in the transesterification reaction with mpg- C_3N_4 .



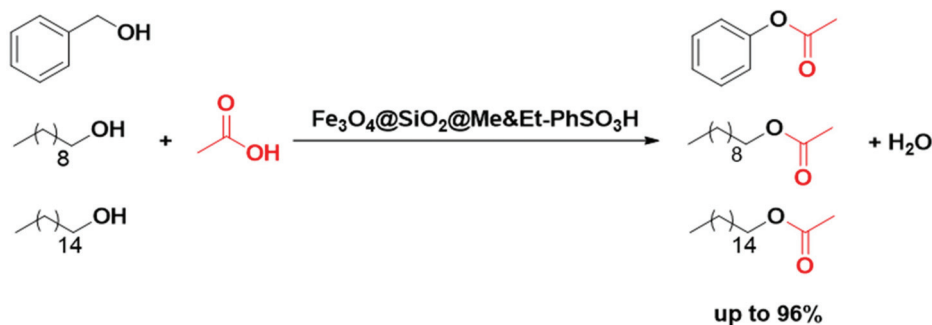
Scheme 92 Chemoselective synthesis of formamides catalyzed by SBA-15/PrEn-NHSO₃H. Reproduced from ref. 180 with permission of Elsevier, copyright 2016.



Scheme 93 Acetic acid esterification with benzyl alcohol catalyzed with PrSO₃H/SBA-15.

Hydrogenation of aldehydes and ketones

Potassium phosphate is an amazing basic active catalyst for the catalytic transfer hydrogenation of carbonyl compounds to the corresponding alcohols. For this purpose, a pretreatment at 600 °C is vital to obtain the active sites by desorption of CO₂ and creating sites of lower basicity after heat treatment for 5 h.

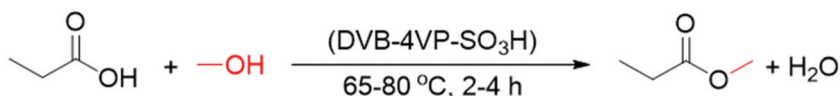


Scheme 94 Esterification reaction of fatty alcohols catalyzed with Fe₃O₄@SiO₂@Me&Et-PhSO₃H.

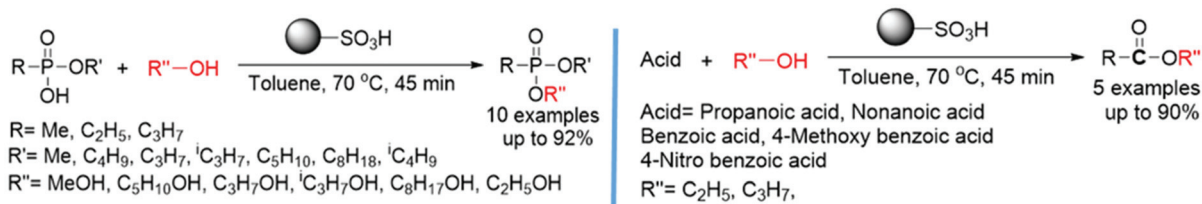
Deploying 2-propanol as a hydride source, substituted benzaldehydes with electron-withdrawing have a higher rate of reaction than benzaldehyde or alkyl-substituted benzaldehydes while the ketones were reduced at a lower rate than aldehydes (Scheme 98).¹⁸⁵

Oxidation of 5-hydroxymethylfurfural to 2,5-diformylfuran

The conversion of biomass into of commercial chemical materials has garnered tremendous attention lately, the preparation of 5-hydroxymethylfurfural (HMF) as a biofuels resource *via* the acid-catalyzed dehydration of fructose being a prominent example. A magnetic solid acid catalyst (Fe₃O₄@Si/Ph-SO₃H) comprising a sulfonic-acid-functionalized silica shell has been prepared and utilized successfully with higher



Scheme 95 Esterification of propionic acid with methanol catalyzed by (DVB-4VP-SO₃H).



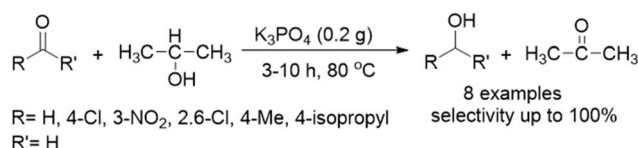
Scheme 96 Sulfonated magnetic resin catalyzed esterification of *O*-alkyl alkylphosphonic and carboxylic acids.

activity comparable to conventional solid sulfonic acid and other homogeneous acid catalysts for the dehydration of fructose to HMF with a fructose conversion of 99% and HMF yield of 82% (Scheme 99).¹⁸⁶

The application of polymer-supported IBX amide reagent has been described for the highly-selective oxidation of HMF to 2,5-diformylfuran (DFF) under mild conditions including the dehydration of fructose to HMF followed by oxidation of HMF to DFF. In general, readily-accessible solid acid catalyst with polymer-supported IBX amide reagent is highly suitable for the direct conversion of fructose to DFF (Scheme 100).¹⁸⁷

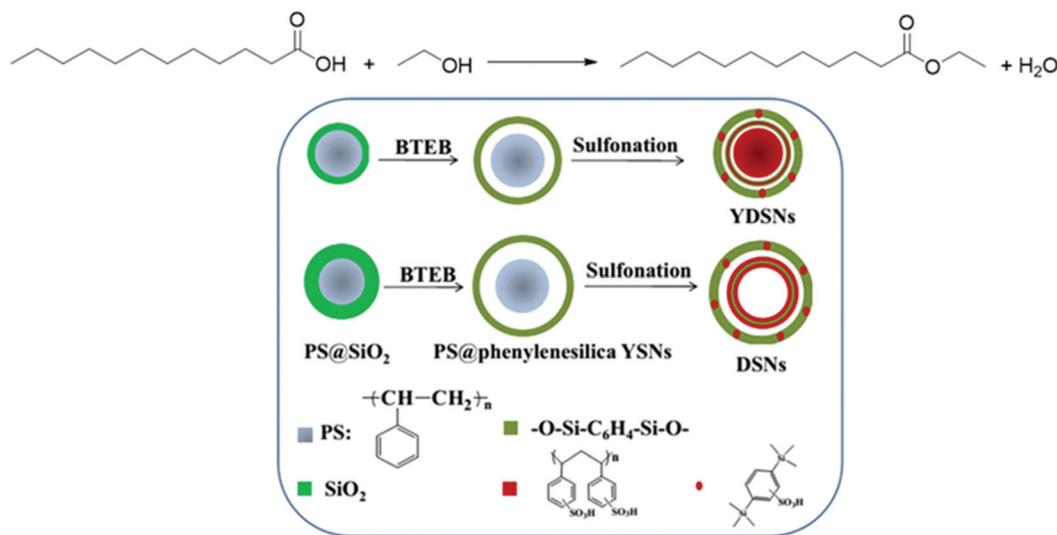
Protection and deprotection of alcohols

The protection/deprotection reaction successions form a full part of organic operations such as the procurement of

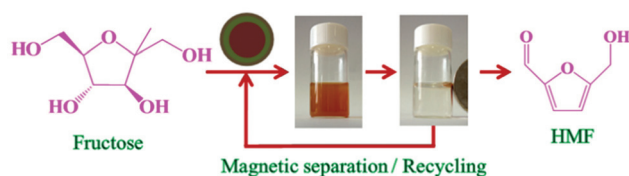


Scheme 98 Catalytic transfer hydrogenation of carbonyl compounds using K₃PO₄.

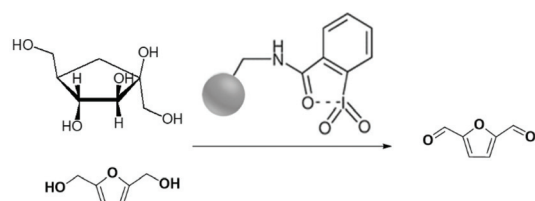
monomer building blocks, fine chemicals and forerunners for pharmaceuticals and these reactions frequently include the utilization of acidic, basic, or perilous and corrosive reagents and toxic metal salts. In this regard, the use of metal-free solid base catalysts to protect/protect functional groups, performed under mild conditions, has been considered.² In 1998, Varma and co-workers exploited the catalytic activities of mineral oxides based on K 10 montmorillonite clay which in the trans-



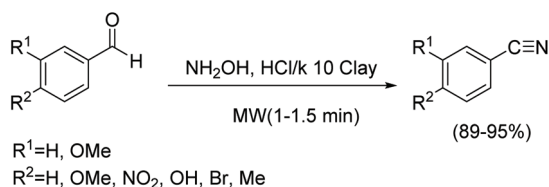
Scheme 97 Catalytic performance of yolk-double-shell (PS-SO₃H@phenylenesilica) in the esterification reaction. Reproduced from ref. 128 with permission from Elsevier, copyright 2014.



Scheme 99 Conversion of fructose to 5-hydroxymethylfurfural using $\text{Fe}_3\text{O}_4@\text{Si}/\text{Ph-SO}_3\text{H}$ as an acid catalyst. Reproduced from ref. 186 with permission of Elsevier, copyright 2014.



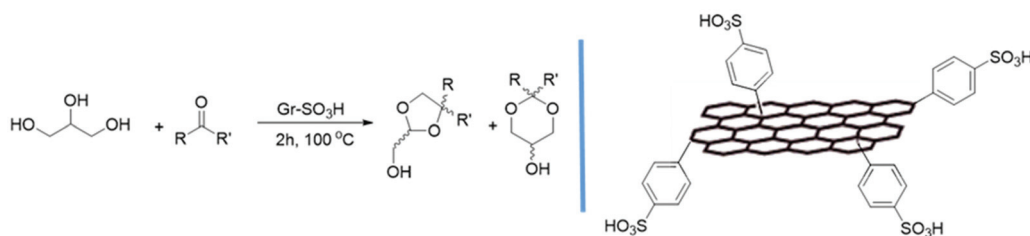
Scheme 100 Selective oxidation of fructose and 5-hydroxymethyl-2-furfural to DFF with IBX amide.



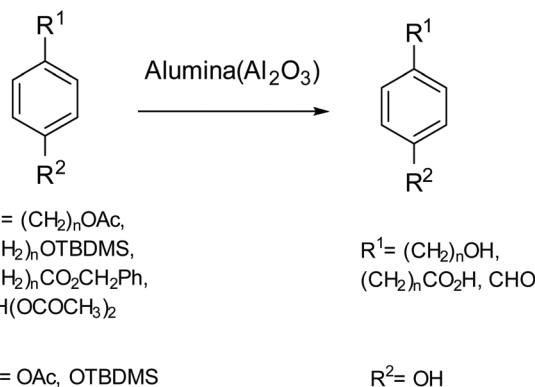
Scheme 101 Transformation of arylaldehydes to nitriles with clay-supported hydroxylamine hydrochloride.

formation of arylhalides to nitriles are accelerated by microwave irradiation under solvent-free conditions (Scheme 101).¹⁸⁸

Solid metal-free catalysts have been widely deployed during the past decades for the protection and deprotection of organic functional groups. Felpin *et al.* discovered new properties of the honeycomb-structure of graphene sheets for the successful acetalization of glycerol with both aldehydes and ketones under neutral and acid-free conditions. Mechanistic studies have revealed that the unique electronic properties of graphene are responsible for this uncovered reactivity as the



Scheme 102 Acetalisation of glycerol with carbonyl compounds by using $\text{GR-SO}_3\text{H}$. Reproduced from ref. 189 with permission from the Royal Society of Chemistry, copyright 2016.



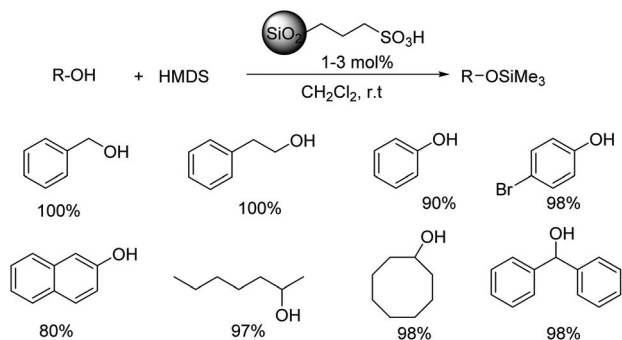
Scheme 103 Deprotection of acetylated varieties of substrate by using alumina.

intervention of metallic cations or residual acidic species ($-\text{COOH}$) at the surface of graphene were ruled out (Scheme 102).¹⁸⁹

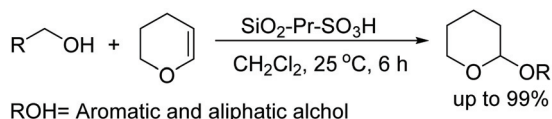
In the past two decades, many research groups have used solid metal-free catalysts for the protection and deprotection of organic functional groups. Varma and his group developed a simple high-yielding and economical method for the deprotection of acetylated phenols and alcohols, benzyl esters and the cleavage of *t*-butyldimethylsilyl ethers *via* an activated alumina surface (Scheme 103). The products were obtained under mild and solvent-free conditions on the alumina surface using microwave irradiation without the generation of any chemical waste.^{190–192}

An example of the deprotection of *tert*-butyldimethylsilyl (TBDMS) ethers by using sulfonic-acid-functionalized nanoporous silica has appeared where TBDMS ethers in the presence of $\text{SiO}_2\text{-Pr-SO}_3\text{H}$ were deprotected to the corresponding alcohols in methanol at 35 °C with discernible recovery and reuse without considerable loss of reactivity. The protection of alcohols was also carried out by the same group using hexamethyldisilazane (HMDS) and dihydropyran (DHP); the alcohols were converted to the corresponding silyl ethers and tetrahydropyranyl (THP) ethers in good yields (Scheme 104).¹⁹³

Similarly, $\text{SiO}_2\text{-Pr-SO}_3\text{H}$ has been deployed in this protection process using tetrahydropyran at room temperature to deliver the corresponding protected products in good to high yields; double bond isomerization in *d*-citronal during acetal



Scheme 104 Synthesis of trimethylsilyl ethers using nanoporous solid silica sulfonic acid.



Scheme 105 SiO₂-Pr-SO₃H for protection reactions using tetrahydropyran.

formation was possible because of the mild and low acidic reaction conditions to prevent side-reactions (Scheme 105).¹⁹⁴

Protection of amino functional groups

The *tert*-butoxycarbonyl (Boc) is one of the most important and efficient functional groups for the protection of amines. Chemoselective Boc protection of amines has been conducted by treatment with (Boc)₂O in the presence of SiO₂-Pr-SO₃H in CH₂Cl₂, CH₂Cl₂-MeCN or MeOH-MeCN at room temperature; *N*-Boc derivatives of aliphatic (acyclic and cyclic), aromatic, and heteroaromatic amines; primary and secondary amines; aminols, amino-esters; and sulfonamides have been prepared (Scheme 106).¹⁹⁵

In 2007, our group reported a simple and chemoselective-benzyloxycarbonylation of amines using silica sulfuric acid (SSA) as an eco-friendly synthetic protocol under solvent-free conditions at ambient temperature. For a wide variety of primary (aliphatic and cyclic) secondary amines, amino alco-



Scheme 107 SSA catalyzed benzyloxycarbonyl (Cbz) protection of amines.

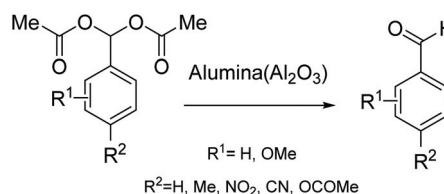
hols, and heterocyclic amines, significant yields (87–96%) were obtained (Scheme 107).¹⁹⁶

Protection of carbonyl functional groups

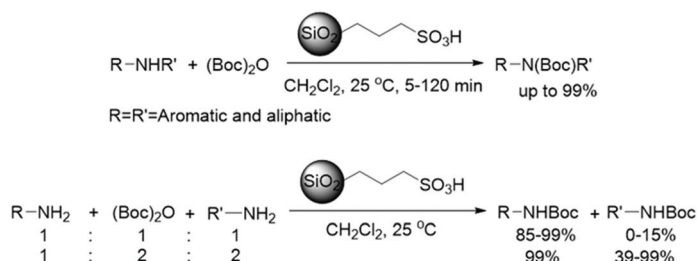
In 1993, our group investigated the catalytic impact of alumina on geminal arylaldehyde diacetates to afford the corresponding aldehydes. The results indicated the selective deacetylation of arylaldehyde diacetates that occurs under mild conditions using inexpensive aluminum oxide (Scheme 108).¹⁹⁷

Cleavage of semicarbazones and phenylhydrazones toward the corresponding ketones using ammonium persulfate on clay using microwave or ultrasonic irradiation was reported by Varma's group. Compared with ultrasonic irradiation, the use of microwaves afforded better yields (65–85%) in less time (Scheme 109).¹⁹⁸

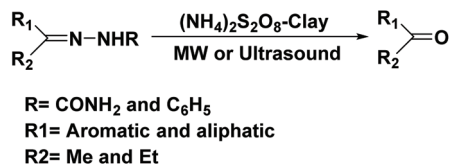
In a continuation of the ongoing program to develop benign and expeditious methods for organic transformation, Varma and his associates achieved the regeneration of ketones from thioketones using clay-supported nitrate salt (clayfen or clayan) as a catalytic system (Scheme 110).¹⁹⁹ The results show that the thioketones are rapidly converted into their parent



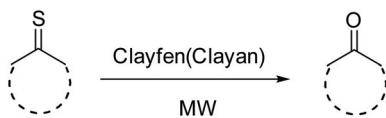
Scheme 108 Deprotection of benzaldehyde diacetates on neutral alumina.



Scheme 106 Selective Boc protection using a mixture of amines using sulfonic-acid-functionalized silica.



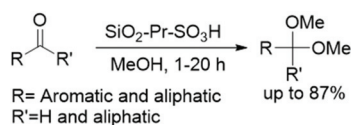
Scheme 109 Cleavage of semicarbazones and phenylhydrazones with ammonium persulfate-clay using microwave or ultrasonic irradiation.



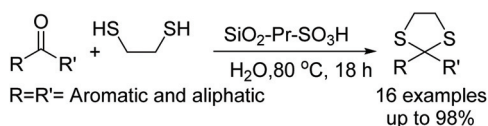
Scheme 110 Solvent-free transformation of thioketones to ketones by clayfen or clayan and microwave irradiation.

ketones by using clayfen or clayan upon microwave thermolysis under solvent-free conditions.

An acetalization reaction is one of the popular methods for the protection of carbonyl functional groups which can generally be performed using acidic media such as HClO₄-SiO₂ and SiO₂-Pr-SO₃H with excess methanol to prepare dimethyl acetals in good to high yields. Similarly, cyclic acetals, dioxolanes, can be easily prepared from the reaction of carbonyls with ethylene glycol in the presence of an acid catalyst, namely SiO₂-Pr-SO₃H. Condensation of carbonyl compounds with



Scheme 111 Aldehyde protection method *via* acetalization by SiO₂-Pr-SO₃H.



Scheme 112 SiO₂-Pr-SO₃H-catalyzed chemoselective thioacetalization of carbonyl compounds.

thiols is a common and popular process for the preparation of thioacetals as a protected form of carbonyl group (Scheme 111).¹⁹⁴

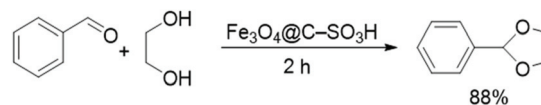
Dithioacetalization of a variety of carbonyl compounds using SiO₂-Pr-SO₃H in water has been developed but the aromatic and sterically hindered carbonyl compounds failed in refluxing water even after several hours (Scheme 112).²⁰⁰

A one-pot and high-yielding protocol for the synthesis of *N*-sulfonylimines has been developed that occurs rapidly by microwave thermolysis of aldehydes and sulfonamides under solvent-free conditions in the presence of benign reagents, calcium carbonate and montmorillonite K 10 clay.²⁰¹ Due to its shorter reaction time, simple reaction procedure and the formation of cleaner products without further purification, this method provides a better alternative to the existing routes (Scheme 113).

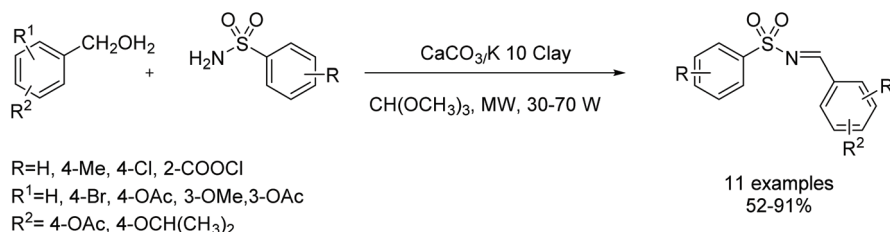
A simple and novel route for preparing a solid acid catalyst has been developed *via* grafting sulfonic groups on the surface of Fe₃O₄@C core-shell magnetic NPs (Fe₃O₄@C-SO₃H MNPs); the catalyst exhibited high catalytic activity and efficiency in condensation reactions between benzaldehyde and ethylene glycol with a conversion rate of 88.3% under mild conditions (Scheme 114).²⁰²

Four different sulfonic acids grafted onto silica-coated magnetic NP (SiMNP) supports have been prepared as hybrid organic/inorganic sulfonic acid catalysts and were evaluated in the deprotection reaction of benzaldehyde dimethylacetal in terms of activity and recyclability; they exhibited better activities than other commercially available sulfonic acid catalysts, such as Amberlyst A-15 and Nafion. Catalysts SBA1 and SBA4 showed enhanced activity when supported on 65-Angstrom mesoporous SBA-15 *versus* the nonporous SiMNPs (Scheme 115).²⁰³

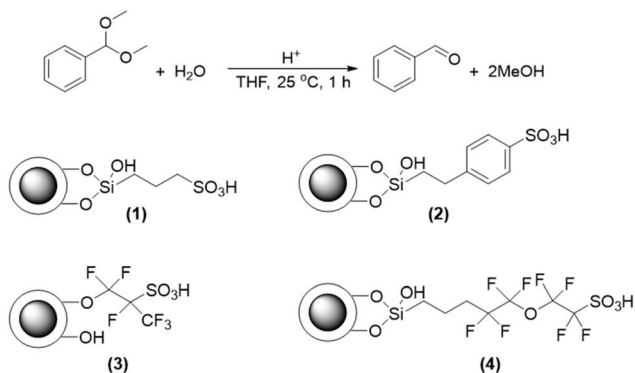
A gentle, efficient and green protocol for the deprotection and protection of various alcohols has been reported using recyclable MCM-41-SO₃H under solvent-free, ball-milling and ambient temperature conditions (Scheme 116). Similarly, de-



Scheme 114 Thioacetalization of carbonyl compounds using Fe₃O₄@C-SO₃H.



Scheme 113 Microwave-assisted synthesis of *N*-sulfonyl imines from aryl aldehyde acetals or arylaldehydes.



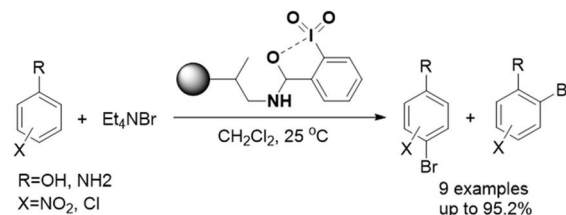
Scheme 115 Different hybrid organic/inorganic sulfonic acid catalysts for deprotection reactions of benzaldehyde dimethylacetal.

protection of trityl ethers was performed in the presence of MCM-41-SO₃H (20 mg) at room temperature for 10–90 min with 100% yield.²⁰⁴

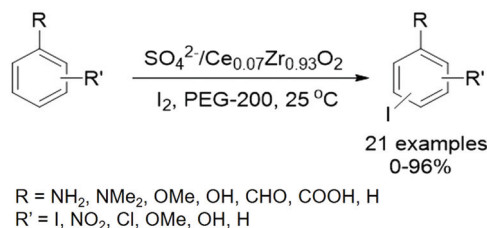
Halogenation of activated arenes

A mild and simple method was unexpectedly found for the bromination of activated aromatic compounds using a polymer-supported IBX reagent (IBX amide resin) and tetraethylammonium bromide (TEAB) where the oxidation of the bromide ion to the tribromide ion as an active brominating agent occurred using IBX amide resin, an efficient and stable alternative to the rather hazardous and cumbersome classical bromination methods (Scheme 117).²⁰⁵

Similarly, the selective mono-iodination of aromatic compounds has been developed using reusable sulphated ceria-zirconia (SO₄²⁻/Ce_{0.07}Zr_{0.93}O₂) and molecular iodine in PEG-200 under mild conditions. The protocol provides a synthesis of aryl iodides with the selective introduction of iodine at the para/ortho position in monosubstituted arenes. During the exploration of selectively, the iodination reaction was carried out with different iodine sources, wherein poor regioselectivity was observed with ICl, and the iodination products of aniline and molecular iodine gave better yield and selectivity under similar experimental conditions. The results indicated that sulphated ceria-zirconia, in view of the maximum number of acid sites (4.23 mmol g⁻¹), appears to be the best choice for the synthesis of aryl iodides in high yield (Scheme 118).²⁰⁶



Scheme 117 Bromination of activated arenes catalyzed through IBX amide resin.



Scheme 118 Iodination of various arenes with I₂ using the SO₄²⁻/Ce_{0.07}Zr_{0.93}O₂ synthesis of furfural from xylose.

Synthesis of furfural from xylose

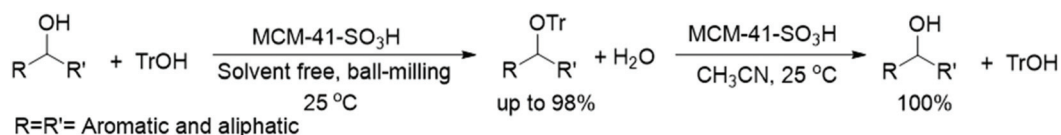
A sulfonated-polymer-impregnated carbon composite (P-C-SO₃H) was prepared by the pyrolysis of a polymer matrix impregnated with glucose followed by its sulfonation and was applied as an efficient and selective solid acid catalyst for the dehydration of xylose to furfural. Apparently, the P-C-SO₃H appears to be superior to the sulfonated carbon catalyst (C-SO₃H) and afforded almost quantitative conversion of xylose with the selective synthesis of furfural due to the greater sulfonic acid density in P-C-SO₃H as compared with in C-SO₃H (Scheme 119).²⁰⁷

Acetylation of anisole

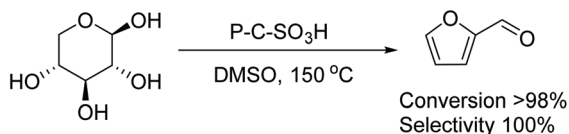
Acetylation of anisole in the presence of various catalysts has been discussed in several reports^{208–210} including large-pore zeolites, although conversion rapidly decreased because of the deactivation of zeolites in this reaction; SiO₂-Pr-SO₃H was used in an acetylation reaction of anisole with acetic anhydride with 100% conversion (Scheme 120).²¹¹

Aerobic oxidation of styrene

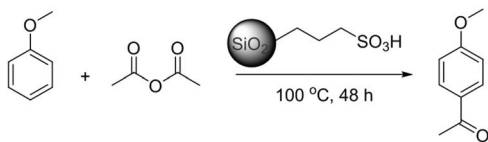
Sulphur-doped graphene as a metal-free carbo-catalyst has been used for the aerobic oxidation of styrenes. The pyrolysis



Scheme 116 Protection and deprotection reaction of alcohols catalyzed by MCM-41-SO₃H.



Scheme 119 P-C-SO₃H-catalyzed selective synthesis of furfural from xylose.



Scheme 120 Acetylation of anisole by using SiO₂-Pr-SO₃H.

of λ -carrageenan at 1000 °C and its subsequent exfoliation led to a S-doped graphene [(S)G] with two types of sulfur atoms on the (S)G, namely sulfide and sulfoxide, respectively. (S)G promoted the aerobic oxidation of styrene derivatives to their corresponding benzaldehydes accompanied by lesser amounts of styrene oxide while the reduced graphene oxide exhibited negligible activity. Using XPS analysis, the existence of two types of sulfur atom on the structure of (S)G was observed, namely, sulfide and sulfoxide, respectively, whereas TEM clearly indicated the typical layered structure expected for G-based materials. The (S)G catalyst could be reused two times

with no significant changes in conversion and selectivity (Scheme 121).²¹²

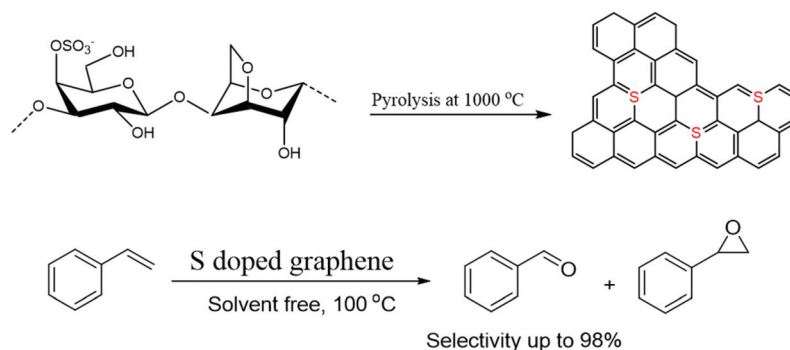
Oxidation of primary alcohols to carboxylic acids

Metal-free oxidations of primary/secondary alcohols with molecular O₂ to the corresponding carbonyl compounds and acids have been studied using mesoporous carbon nitride (MCN) as a catalyst. In the oxidation of aromatic alcohols with molecular oxygen and CO₂, a promotional effect was observed that showed conversions of between 34–63% with O₂ whereas in the co-presence of CO₂ augmented conversions (54–91%) with higher selectivity for acids were observed; initial activation of CO₂ *via* the formation of surface carbamate presumably occurred (Scheme 122).⁹⁸

Ritter reaction (amide functional group preparation)

The Ritter reaction is one of the most important methods for the synthesis of amide functional groups that are crucial moieties in natural products and drugs.

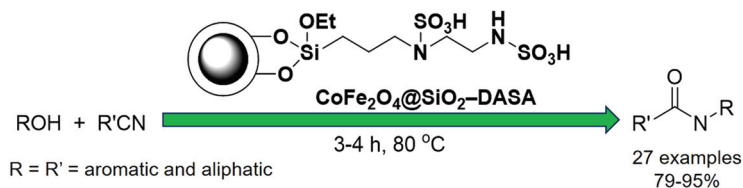
Over the years, researchers have applied sulfonated solid catalysts (CoFe₂O₄ NP-immobilized diamine-*N*-sulfamic acid (CoFe₂O₄@SiO₂-DASA), magnetite-sulfonic acid (Nanocat-Fe-



Scheme 121 Application of S-doped graphene for the oxidation of styrene.



Scheme 122 Oxidation of primary alcohols to carboxylic acids using MCN.



Scheme 123 Ritter reaction catalyzed with magnetic silica catalyst.

OSO₃H)) to prepare amide functional groups *via* a Ritter reaction with good recycling options using an external magnetic field (Scheme 123).²¹³

N-Formylation of amines

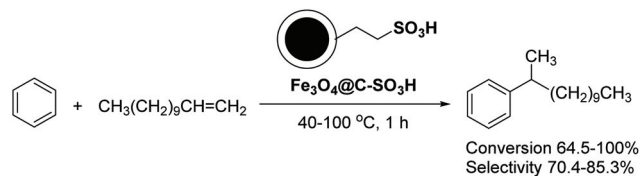
Heydari and coworkers prepared magnetic sulfonic acid supported on hydroxyapatite-encapsulated-g-Fe₂O₃ nanocrystallites and applied it as a Brønsted acid catalyst for the *N*-formylation of amines; the protocol was excellent for the catalytic conversion of aromatic, aliphatic, cyclic and linear amines to formamides. Recovery by simple decantation using an external magnet, enhanced the product purity with promising economic and environmental benefits being some of the salient features of this magnetic catalytic system (Scheme 124).²¹⁴

Alkylation of benzene

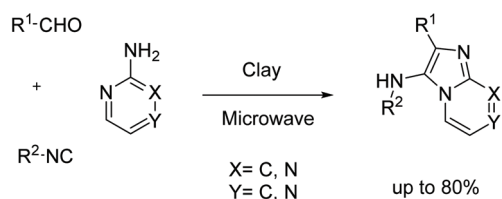
Similarly, a magnetic catalyst based on sulfonic-acid-supported carbon has been synthesized through the hydrothermal carbonization of glucose with magnetic cores and sulfonation with hydroxyethyl sulfonic acid. The core-shell-structured catalyst had a high specific surface with easily accessible acid sites on the shell for the reactants; high activity for the hydrophobic alkylation of benzene with 1-dodecene with complete conversion was shown. The abundant hydrophilic groups and the hydrogen donor functionalities such as carbonyl groups and hydroxyl groups effectively prevented the double bond migration, which resulted in high selectivity for the 2- or 3-dedecenylbenzene (Scheme 125).¹²⁷



Scheme 124 γ -Fe₂O₃@HAp-SO₃H for the synthesis of formamides.



Scheme 125 Alkylation of benzene and dodecene by using Fe₃O₄@C-SO₃H.



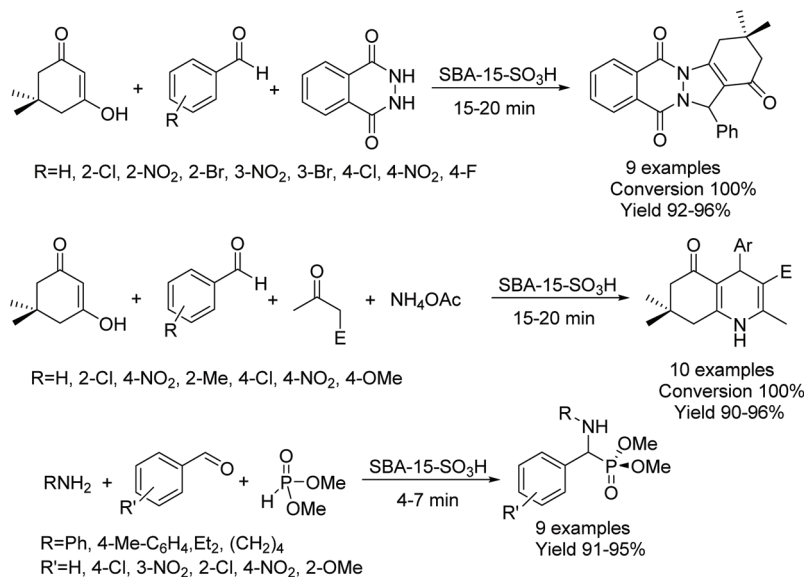
Scheme 126 Solvent-free synthesis of imidazo[1,2-*a*]annulated pyridines, pyrazines and pyrimidines using micro-wave irradiation by using clay.

Multicomponent reactions

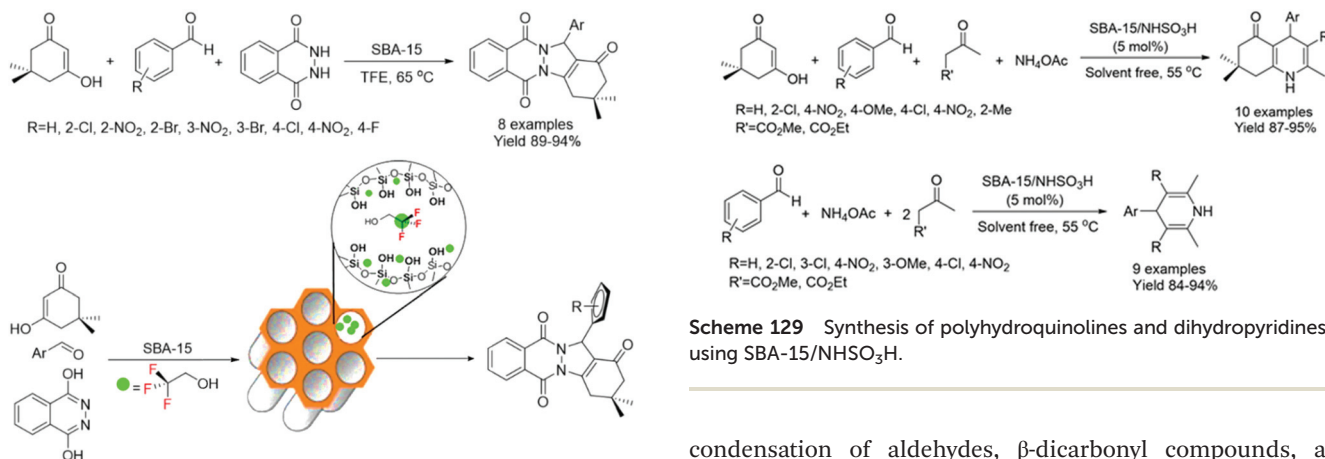
Varma and colleagues reported one-pot condensation of aldehydes to the corresponding 2-aminopyridine, pyrazine or pyrimidine and isocyanides in the presence of inexpensive, recyclable, economical and eco-friendly clay that provides a rapid and solventless method for the synthesis of multisubstituted imidazo[1,2-*a*]pyridines, imidazo[1,2-*a*]pyrazines and imidazo[1,2-*a*]pyrimidines (Scheme 126).²¹⁵

In order to develop the design of a metal-free catalyst to attain greener transformations with minimal by-products or waste generation and also to reduce the reaction time, the use of SBA-15/SO₃H was put forth using ultrasonic irradiation for the synthesis of indazolophthalazinetriones, polyhydroquinolines and α -aminophosphonates (Scheme 127); for indazolophthalazinetriones in 15–20 min in the presence of 6 mol% of SBA-15/SO₃H, 100% conversion with a 92–96% yield, for polyhydroquinoline derivatives using 4 mol% of SBA-15/SO₃H in 15–20 min, 100% conversion with a 96–90% yield, and for aminophosphonates in 5–7 min, a 97–91% yield was achieved.²¹⁶

An efficient and metal-free protocol without the need for SBA-15 activation or modification was developed using an additive compound (2,2,2-trifluoroethanol (TFE)) to synthesize greener indazolophthalazine derivatives from three com-



Scheme 127 One-pot synthesis of indazolophthalazinetriones, polyhydroquinolines and α -aminophosphonates catalyzed with SBA-15/SO₃H.



Scheme 128 SBA-15/TFE as a catalyst for the synthesis of indazolophthalazinetriones. Reproduced from ref. 217 with permission of Elsevier, copyright 2014.

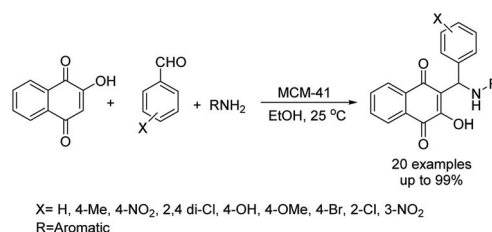
ponents, phthalic hydrazide, dimedon, and aromatic aldehydes (Scheme 128). The reaction was performed at 65 °C and for various derivatives using SBA-15/TFE (SBA-15 (0.02 g), TFE (4 mL)), excellent yields (89–94%) were obtained in 2–3 h; SBA-15/TFE was recycled and reused at least seven times without any significant decrease in activity.²¹⁷

A covalently bonded ionic liquid-type sulfamic acid on SBA-15 (SBA-15/NHSO₃H) was reported as a green and reusable catalyst for the efficient synthesis of polyhydroquinolines by a four-component reaction using dimedone, benzaldehyde, NH₄OAc, and methyl acetylacetonate under solvent-free and mild conditions. For all the desired products, a yield of 87–95% was achieved in 4–5 h at 55 °C. In addition, SBA-15/NHSO₃H has been applied as an efficient catalyst for the rapid synthesis of dihydropyridines by a three-component, one-pot

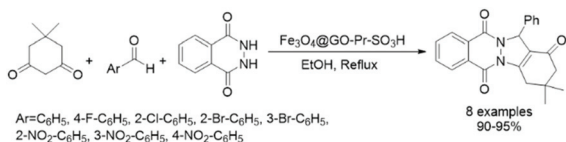
Scheme 129 Synthesis of polyhydroquinolines and dihydropyridines by using SBA-15/NHSO₃H.

condensation of aldehydes, β -dicarbonyl compounds, and ammonium acetate in excellent yields (84–94%) under 55 °C and solvent-free conditions (Scheme 129).²¹⁸

MCM-41 as a simple, efficient, and green heterogeneous catalyst is reported for the synthesis of 2-hydroxy-1,4-naphthoquinone derivatives *via* a one-pot procedure; the best performance for MCM-41 (5 mg) was obtained in EtOH at ambient temperature with a yield of 90–99% for the synthesis of 2-hydroxy(aryl(arylaminomethyl) naphthalene-1,4-diones (Scheme 130).²¹⁹



Scheme 130 Synthesis of naphthoquinones catalyzed by nanoporous MCM-41.



Scheme 131 One-pot synthesis of indazolophthalazinetriones using Fe₃O₄@GO-Pr-SO₃H.

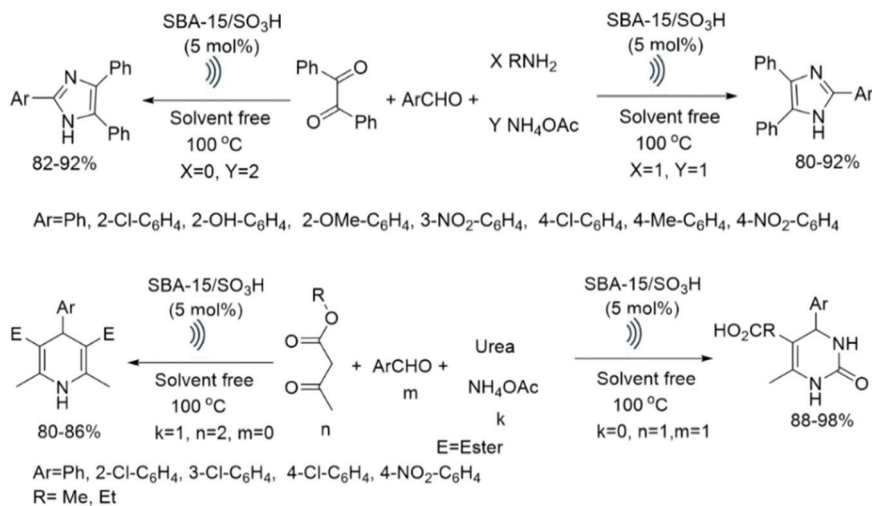
The reaction of dimedone, benzaldehyde, and phthalhydrazide has been used for the one-pot synthesis of indazolophthalazinetriones (Scheme 131) where the reactions were performed by deploying Fe₃O₄@GO-SO₃H in EtOH within a short time period; yields above 90% were achieved for all desired products and the catalyst showed acceptable performance, even after 11 cycles while maintaining its efficiency.²²⁰

A simple, efficient, ultrasound-mediated, and metal-free procedure using SBA-15/SO₃H catalyst as an ultra-fast combined bifunctional method was reported for the synthesis of heterocyclic compounds such as imidazoles, dihydropyrimidinones (DHPMs) and dihydropyridines (DHPs) based on multi-component coupling in high yield and in short times under mild condition reactions (Scheme 132). A variety of imidazole derivatives were obtained in 80–92% yields using ultrasonic waves and 5 mol% of catalyst, in 8 min under solvent-free con-

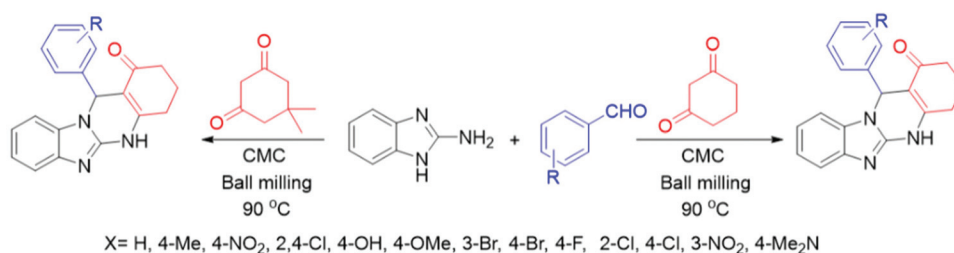
ditions at 100 °C. For DHPM derivatives using 10 mol% of the catalyst, a yield of 98–88% and for DHPs a yield of 82–96% was observed. The results of this study showed that the induction of ultrasound into SBA-SO₃H increases the catalytic efficiency *via* superior mass transfer without the need for anchoring, enclosing or embedding an additional hydrophobic group or ionic liquid.²²¹

The synthesis of quinazolinone derivatives was accomplished *via* three-component condensation of 2-aminobenzimidazole, dimedone or 1,3-cyclohexanedione, and various aldehydes using carboxymethyl cellulose (CMC) as an efficient and environmentally friendly catalyst (Scheme 133). High yields (89–70%) were obtained for all the derivatives using CMC in a ball mill at 90 °C; recovery and reuse of CMC during 6 cycles did not show any significant decrease in catalyst activity.²²²

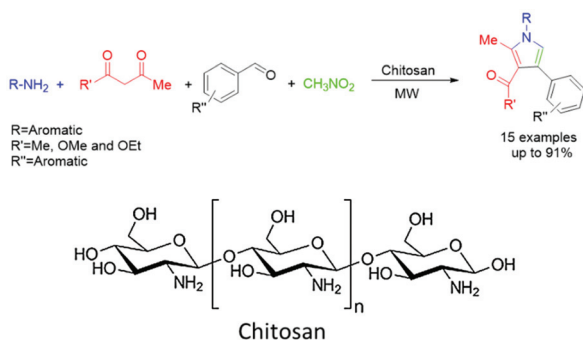
In another study, chitosan was introduced as an organo-catalyst in a green and environmentally benign synthesis of pyrroles using a multi-component protocol exploiting aldehydes, amines, 1,3-dicarbonyl compounds, and nitromethane (Scheme 134). Examination of the reaction under reflux and microwave (MW) conditions showed that the use of microwaves delivered better yields in less time; reaction times could be significantly decreased using MW irradiation where yields of 76–91% were observed for all products in 4–7 min.²²³



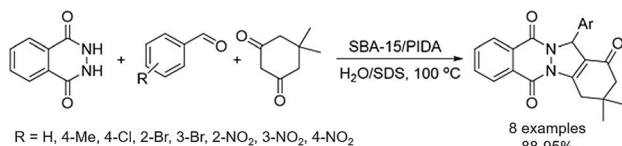
Scheme 132 SBA-SO₃H-catalyzed multicomponent syntheses under ultrasound irradiation.



Scheme 133 Synthesis of quinazolinones using CMC.



Scheme 134 Synthesis of various substituted pyrroles catalyzed by chitosan.



Scheme 135 Synthesis of indazolophthalazinetrione derivatives catalyzed by SBA-15/PIDA.

Rostamnia *et al.* studied the role of the distribution of amino acid-like *N*-propyliminodiacetic acid (PIDA) in correspondingly functionalized SBA-15 phases in the catalysis of a three-component reaction of dimedone, aldehydes, and phthalhydrazide for the synthesis of indazolophthalazinetrione (Scheme 135). Under the optimized conditions, 20 mg of SBA-15/PIDA and 1.1 mmol of various aldehydes, 1 mmol

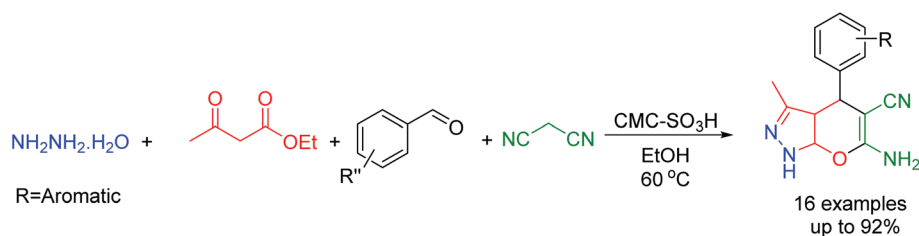
dimedone, and 1 mmol phthalhydrazide at 100 °C for 20 min in the presence of H₂O/SDS delivered indazolophthalazinetriones in 85–95% isolated yields. SBA-15/PIDA showed good recovery and reusability, which according to *ab initio* calculations has been attributed to the strong covalent bond between PIDA and SBA-15.²²⁴

In 2019, Naimi-Jamal and co-workers applied a simple, mild, and green reaction for the one-pot synthesis of various biologically important pyranopyrazoles using multicomponent reactions of different aldehydes, malononitrile, ethyl acetoacetate, and hydrazine hydrate in the presence of CMC-SO₃H (Scheme 136); high yields (78–92%) were obtained for different derivatives using 30 mg of catalyst at 60 °C for 35–70 min.²²⁵

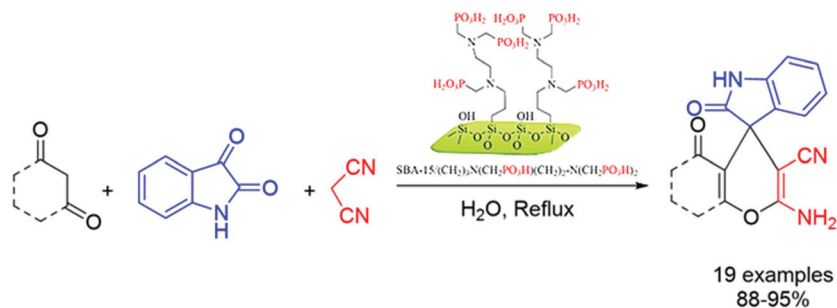
Zolfigol and co-workers have examined the three-component synthesis of spiroopyrans by using isatine, malononitrile and dimedone in the presence of SBA-15/(CH₂)₃N(CH₂PO₃H₂)-(CH₂)₂-N(CH₂PO₃H₂)₂; excellent yields (88–95%) were obtained in water under reflux conditions (Scheme 137).²²⁶

In 2019, the same group reported the synthesis of new pyrimido[4,5-*b*]quinolones and pyrido[2,3-*d*]pyrimidines *via* anomeric-based oxidation using SBA-15/PrN(CH₂PO₃H₂)₂ as a novel and heterogeneous catalyst containing phosphorous acid groups (Scheme 138). Deploying 0.01 gr of the catalyst, the three-component reaction of aldehyde, malononitrile, or dimedone and 6-amino-1,3-dimethylpyrimidine-2,4(1*H*,3*H*)-dione could be achieved under solvent-free conditions at 100 °C in 5–60 min; corresponding products were obtained in moderate to excellent yields (75–95%).²²⁷

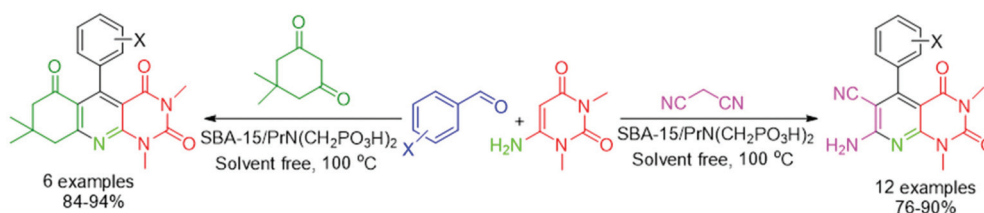
Recently, the use of -SO₃H bonded graphite carbon nitride (g-C₃N₄/NHSO₃H) has been reported as a green and cost-



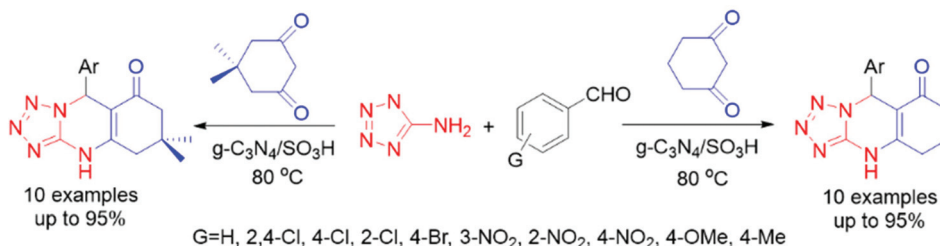
Scheme 136 One-pot four-component synthesis of pyranopyrazole derivatives using SCMC.



Scheme 137 Synthesis of spiroopyrans using SBA-15/PrN(CH₂PO₃H₂) Et-N(CH₂PO₃H₂)₂.



Scheme 138 Synthesis of pyridopyrimidines and pyrimidoquinolones using SBA-15/PrN(CH₂PO₃H)₂.



Scheme 139 Synthesis of tetrazoloquinazolines catalyzed by g-C₃N₄/NHSO₃H.

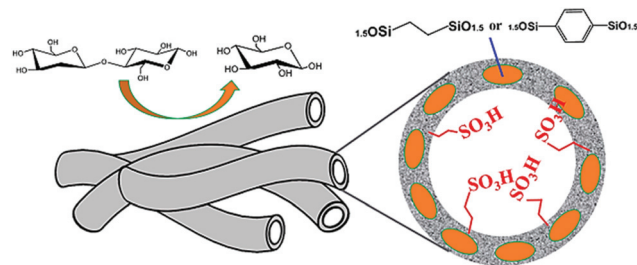
effective heterogeneous acid catalyst for the regioselective three-component (3-CRs) synthesis of tetrazoloquinazoline derivatives under mild conditions (Scheme 139); various aromatic aldehydes and dimedone and 1,3-cyclohexanedione ketones in the presence of 2-aminotetrazole afforded excellent yields (87–95%) of products in *i*-PrOH at 80 °C. The catalyst, after 8 steps of recovery and reuse, displayed no significant reduction in catalytic power.²²⁸

Synthesis of 2,4,5-triarylimidazoles derivatives in high yields (75–96%) has been examined through a one-pot three-component reaction between ammonium acetate, aldehyde derivatives, and benzyl under mild conditions (Scheme 140) in the presence of Fe₃O₄@Alg@CPTMS@Arg in refluxing EtOH for 15–45 min.²²⁹

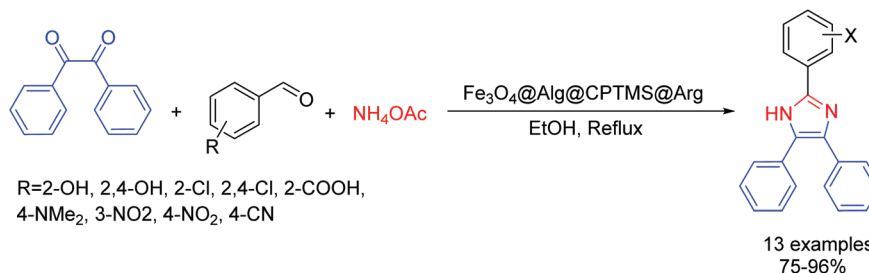
Hydrolysis of cellobiose

A sulfonic organosilica nanotube-based acid catalyst was reported for the hydrolysis of cellobiose wherein six types of acid catalyst (SO₃H_{0.1}-Et-SNT, SO₃H_{0.2}-Et-SNT, SO₃H_{0.3}-Et-SNT, SO₃H_{0.1}-Ph-SNT, SO₃H_{0.2}-Ph-SNT, SO₃H_{0.3}-Ph-SNT) were inves-

tigated. Among them, SO₃H_{0.3}-Ph-SNT catalyst showed excellent performance in the hydrolysis of cellobiose with the highest conversion of 92% and glucose selectivity of 96% within 2 h at 150 °C. Furthermore, SO₃H_{0.3}-Ph-SNT could be recovered and reused for at least 6 runs with 66% conversion and a glucose selectivity of 92% (Scheme 141).²³⁰



Scheme 141 Hydrolysis of cellobiose catalyzed by sulfonic organosilica nanotubes. Reproduced from ref. 230 with permission of MDPI, copyright 2017.



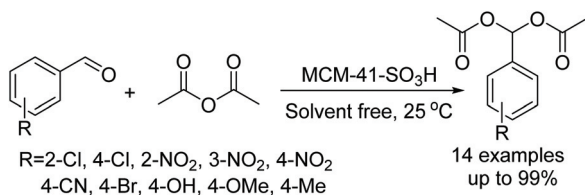
Scheme 140 Synthesis of 2,4,5-triaryl-1*H*-imidazoles catalyzed by Fe₃O₄@Alg@CPTMS@Arg.

Synthesis of acylals from aldehydes

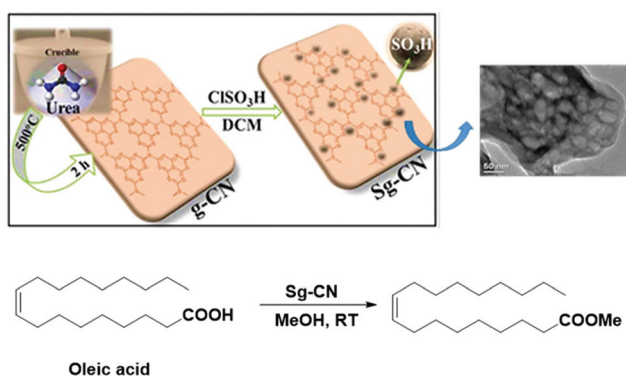
MCM-41-SO₃H-catalyzed high-yielding reactions of various aldehydes with acetic anhydride provided acylals under solvent-free conditions at ambient temperature in a short reaction time; the desired products were synthesized in the presence of 0.01 gr of MCM-41-SO₃H with high yield (up to 99%) in 3–180 min. This protocol tolerates acid-sensitive and unsaturated substrates such as cinnamaldehyde that polymerize under homogeneous acidic conditions (Scheme 142).²³¹

Biodiesel synthesis

The valorization of biomass to green fuel and energy is the key driving force for the Earth's inhabitants, especially vegetable oils containing fatty acids which can be converted into biodiesel. The key purpose to become more viable is the development of efficient, inexpensive and sustainable catalysts. In this



Scheme 142 MCM-41-SO₃H-catalyzed acetylation of aldehydes with acetic anhydride.



Scheme 143 Synthesis of Sg-CN for selective esterification reactions. Reproduced from ref. 232 with permission of Scientific Reports, copyright 2016.

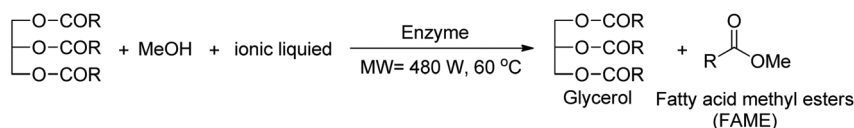
context, graphitic carbon nitride-based catalysts (g-C₃N₄) are suitable for upgrading of lignocellulosic biomass, yielding green production as biofuels. In recent years, many research groups have developed several catalysts based on g-C₃N₄ and applied them in biomass valorization.⁷³ Synthesis of biodiesel investigated by Varma's group used graphitic carbon nitride (g-C₃N₄) as a solid support to efficiently promote the esterification reactions. They reported sulfonated graphitic carbon nitride (Sg-CN) *via* simple sulfonation of g-C₃N₄ and then applied it in the efficient synthesis of biodiesel. Sulfonic acid anchored on g-C₃N₄ affords polar and strongly acidic sites, which display unprecedented reactivity and selectivity in esterification reactions at room temperature as well as resulting products without any purification (Scheme 143).²³²

Yu *et al.* have reported a synergistic effect of microwave irradiation and ionic liquids for Novozym 435-catalyzed biodiesel production of fatty acid methyl ester (FAME) with soybean oil and methanol through transesterification (Scheme 144).²³³ Under the optimum conditions including MW = 480 W, an [EMIM][PF₆]/oil volume ratio of 2 : 1, a methanol/oil molar ratio of 6 : 1, a 6% amount of Novozym 435 based on soybean oil weight, and water activity of 0.33 at 60 °C, a 92% yield of FAME could be attained in 6 h.

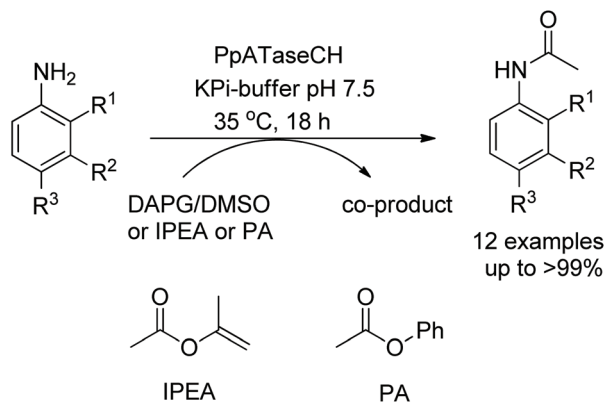
Turner *et al.* reported engineered TeSADH with a >10 000-fold switch from NADPH towards NADH as a biocatalytic hydrogen-borrowing system that employs catalytic amounts of NAD⁺, ammonia and an amine dehydrogenase (AmdH) for the conversion of various racemic alcohols into chiral amines.²³⁴ The utilization of TeSADH W110A/G198D biocatalyst in cascade reactions using aromatic and aliphatic alcohols gives corresponding amines in 11–90% yields with enantioselectivity up to 99%.

Poelarens and co-workers described the asymmetric 4-OT-catalyzed Michael-type addition of acetaldehyde to a series of mono-substituted β-nitrostyrene derivatives yielding enantio-enriched (*R*)- or (*S*)-γ-nitroaldehydes. The enzymatically obtained (*R*)-γ-nitroaldehydes and (*S*)-γ-nitroaldehydes had good to excellent ee values (between 82% and 97%) in the presence of NaH₂PO₄ buffer (pH 5.5) in EtOH and DMSO, showing that 4-OT is highly stereoselective during the catalytic proceedings. Michael addition of acetaldehyde to *trans*-2-hydroxy-β-nitrostyrene and then cyclization results in the synthesis of the 4-(nitromethyl)-chroman-2-ol.²³⁵

Acyltransferase from *Pseudomonas protegens* by using promiscuous *N*-acetylation activity towards a broad spectrum of aniline derivatives was reported by Kroutil *et al.*²³⁶ The reaction was performed using KPi buffer under pH 7.5 in the presence of PPATaseCH and acetyl donors (IPEA, DAPG4 and PA).

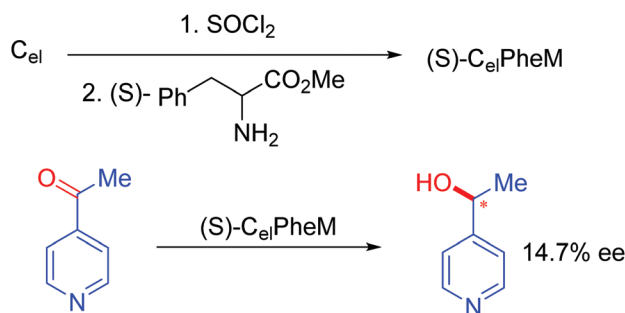


Scheme 144 Enzymatic FAME production using ILs under MW irradiation.



Scheme 145 Biocatalytic *N*-acetylation of anilines.

After the formation of amides in aqueous buffer and by identifying phenyl acetyl (PA) as the suitable acetyl donor, products with 99% conversion were obtained (Scheme 145). Conversion yields of less than 1% were observed for aniline derivatives having an OH and NO₂ group in the para or ortho position.



Scheme 146 Asymmetric electrochemical reduction of 4-acetylpyridine using a modified graphite electrode.

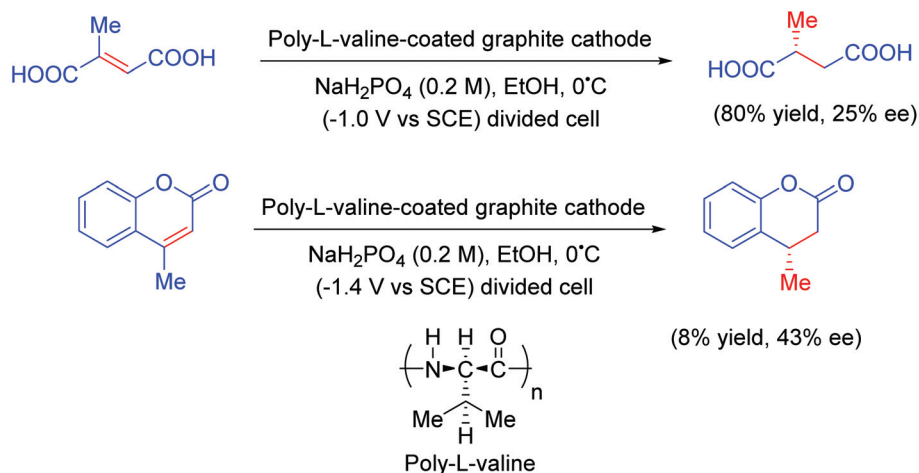
Organic electrochemistry

An attractive approach to sustainable synthesis is the utilization of electrochemical means, which can obviate the need for stoichiometric redox oxidation reactants and thus reduce the associated waste generation.^{237–240} Electrochemical synthesis endowed with sustainability and environmentally friendly attributes has been broadly applied to constructing a variety of chemical bonds,^{237,241–245} the first example of electrode modification being reported by Miller's group in 1975, *via* covalent binding.²⁴⁶ Air-oxidized graphite electrodes were modified by treatment with thionyl chloride followed by derivatization with (*S*)-(-)-phenylalanine methyl ester. The modified electrode [(*S*)-C_{el}PheM] was applied as a cathode for the electrochemical reduction of 4-acetylpyridines. The formation of the corresponding alcohols with an 14.7% optical yield confirmed that the modified electrodes served as chiral inductors (Scheme 146).

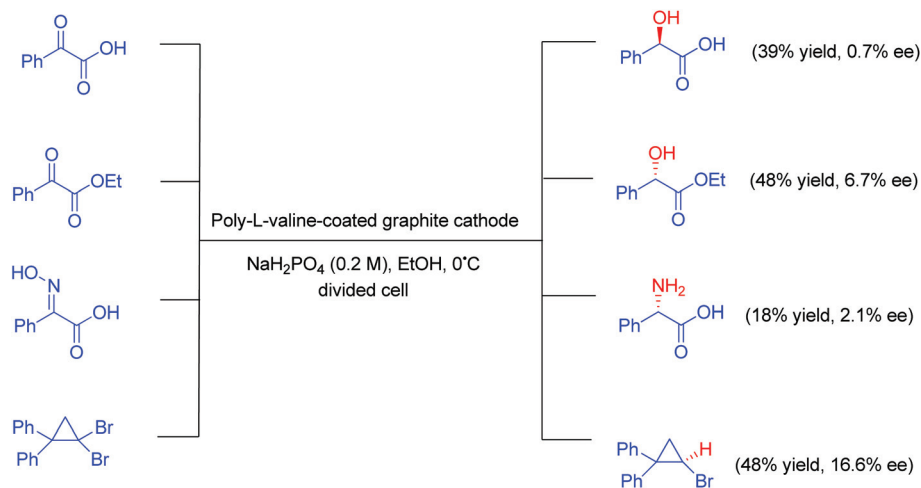
In 1983, Nonaka *et al.* reported a poly-L-valine-coated graphite cathode for asymmetric electrochemical reductions.²⁴⁷ They carried out an asymmetric reduction *via* the conversion of prochiral activated olefins to the corresponding products with optical yields of 25% and 43%, respectively (Scheme 147).

In another study, the same modified electrode was applied for the asymmetric reduction of prochiral carbonyl, oximes and gem-dibromo compounds (Scheme 148);²⁴⁸ the highest optical yield (16.6%) was obtained for bromo-cyclopropanes. According to the authors, the observed lower asymmetric yields might be due to the transmission of larger amounts of charge to facilitate the product isolation.

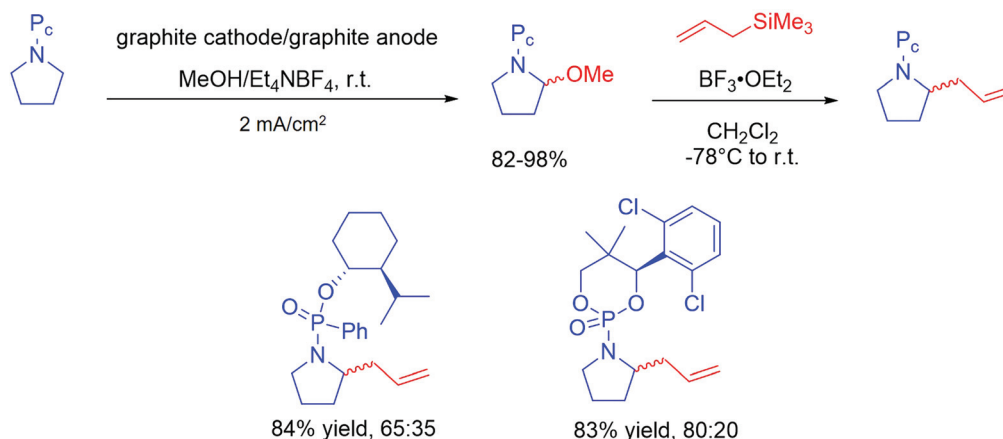
Martens and his group investigated the effect of chiral phosphorus esters as chiral auxiliaries in the α -alkylation of secondary amines *via* anodic oxidation. The methoxylation of *N*-protected chiral pyrrolidines in an undivided cell is depicted in Scheme 149;²⁴⁹ nucleophilic substitution of the corresponding product with allyltrimethylsilane in the presence of a Lewis acid resulted in α -alkylated products.



Scheme 147 Asymmetric electrochemical reduction of prochiral activated olefins *via* a poly-L-valine-coated graphite cathode.



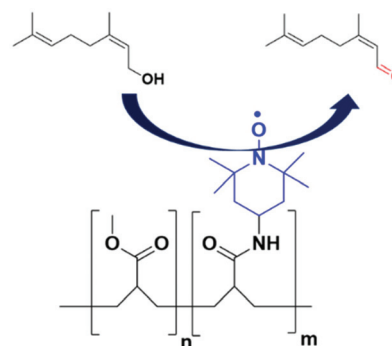
Scheme 148 Asymmetric reduction of prochiral carbonyl, oximes and gem-dibromo compounds using a poly-L-valine-coated graphite cathode.



Scheme 149 Effect of phosphorus-derived chiral auxiliaries on electrochemical diastereoselective α -alkylation of pyrrolidine-phosphorus esters.

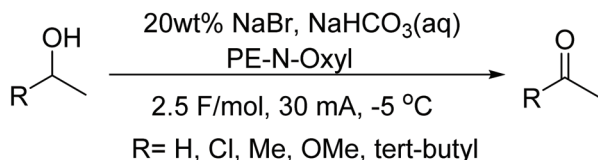
In 1988 and 1990, the Osa and Babbitt groups reported the immobilization of 4-NH₂-TEMPO on poly (acrylic acid) by an amide bond with a pair of reagents, *N,N*'-dicyclohexylcarbodiimide (DCC) in dimethylformamide (DMF), and then cast-coated onto a carbon electrode.^{250,251} While using a modified electrode for nerol oxidation, their studies revealed that the methylation of free carboxylic acid functional groups increased the stability of the electrode, and the methylated electrode realized more than 1560 TON for nerol oxidation compared with 500 TON for non-methylation electrodes (Scheme 150).

In another method, Tanaka *et al.* reported the use of bromide as an electrochemically regenerable mediator in combination with supported TEMPO catalysts for electrochemical alcohol oxidation.²⁵² Various primary and secondary alcohols were oxidized up to 91% in the presence of aminoxyl catalysts supported by SiO₂ or polymer particles under alkaline conditions buffered with NaHCO₃ and 20% NaBr (Scheme 151).

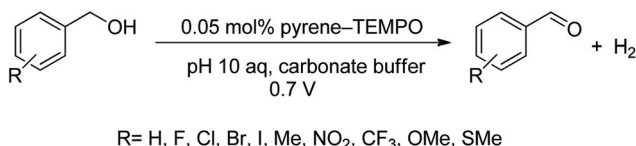


Scheme 150 The modified TEMPO-PAA electrode and its competence in the oxidation of nerol.

Pyrene-tethered TEMPO catalyst for electrochemical alcohol oxidation has been described by Das and Stahl.²⁵³ The reaction was performed using 0.05 mol% of pyrene-TEMPO under alka-



Scheme 151 N-Oxyl/bromide-salt-mediated electrooxidation of alcohols.



Scheme 152 Electrochemical alcohol oxidation with a pyrene-TEMPO.

line conditions (0.2 m NaHCO₃/Na₂CO₃ (1:1)) in water: acetonitrile solvent (99:1) and the higher yields of 74–97% were obtained for the desired aromatic carbonyl derivatives (Scheme 152).

Conclusions and outlooks

Over the past decades, synthetic organic chemists have considered the use of metal-free catalysts to develop new laboratory methods and to reinforce the use of efficient green protocols for performing organic reactions in line with green chemistry principles. Although heterogeneous and homogeneous metal-transfer-based catalysts are still significant in organic synthesis processes, it appears that the use of metal-free (with the exception of abundant iron) or organocatalysts can be beneficial for many catalytic reactions from an environmental and economic point of view. A review of the literature points to the fact that these emerging catalysts have an interesting domain for heterogeneity which can lead to a comprehensive greener path for the development of organic syntheses on an industrial scale, especially for commercial applications. Accordingly, as described in this review, there is tremendous interest in the development of efficient and environmentally friendly non-metallic catalysts with the potential for recyclability, as well as quick and easy preparative protocols comprising abundant graphitic carbon nitrides, mesoporous materials, graphene, magnetic nanoparticles, polymers, *etc.* It appears that the path for greener synthetic organic procedures requires purposeful steps towards achieving a comprehensive protocol based on green chemistry principles on a commercial scale. Given the importance of this field, many researchers are increasingly contributing to the design of sustainable and green protocols based on heterogeneous metal-free catalysts to perform organic reactions for the chemical industry, especially *via* electrochemical means. The extension of these findings in exploiting the use of alternative energy input systems such as ultrasound and microwave irradiation operations in conjunction with intensifi-

cation processes, namely continuous flow systems, bodes well for the future.

Conflicts of interest

The authors declare no competing financial interest.

Acknowledgements

This research was supported by the National Research Foundation of Korea (NRF) funded by the Ministry of Science and ICT (2020M2D8A206983011). Furthermore, financial support from the Basic Science Research Program (2017R1A2B3009135) through the National Research Foundation of Korea is appreciated.

References

- R. S. Varma, *ACS Sustainable Chem. Eng.*, 2019, **7**, 6458–6470.
- R. S. Varma, *Green Chem.*, 1999, **1**, 43–55.
- R. S. Varma, *ACS Sustainable Chem. Eng.*, 2016, **4**, 5866–5878.
- R. S. Varma, *Green Chem.*, 2014, **16**, 2027–2041.
- R. Mohammadinejad, S. Karimi, S. Irvani and R. S. Varma, *Green Chem.*, 2016, **18**, 20–52.
- R. Mohammadi, H. Alamgholiloo, B. Gholipour, S. Rostamnia, S. Khaksar, M. Farajzadeh and M. Shokouhimehr, *J. Photochem. Photobiol., A*, 2020, **402**, 112786.
- M. B. Gawande, V. D. B. Bonifacio, R. Luque, P. S. Branco and R. S. Varma, *ChemSusChem*, 2014, **7**, 24–44.
- S. Rostamnia, *RSC Adv.*, 2015, **5**, 97044–97065.
- S. Rostamnia, B. Gholipour, X. Liu, Y. Wang and H. Arandiyani, *J. Colloid Interface Sci.*, 2018, **511**, 447–455.
- E. Doustkhah, S. Rostamnia, B. Gholipour, B. Zeynizadeh, A. Baghban and R. Luque, *Mol. Catal.*, 2017, **434**, 7–15.
- S. Rostamnia, E. Doustkhah, R. Bulgar and B. Zeynizadeh, *Microporous Mesoporous Mater.*, 2016, **225**, 272–279.
- S. Rostamnia and E. Doustkhah, *RSC Adv.*, 2014, **4**, 28238–28248.
- M. B. Gawande, V. D. B. Bonifácio, R. Luque, P. S. Branco and R. S. Varma, *Chem. Soc. Rev.*, 2013, **42**, 5522–5551.
- S. E. Hooshmand, R. Afshari, D. J. Ramón, R. S. Varma, E. R. Engel and J. L. Scott, *Green Chem.*, 2020, **22**, 3659–3667.
- G. Chatel and R. S. Varma, *Green Chem.*, 2019, **21**, 6043–6050.
- R. S. Varma, *Green Chem.*, 2008, **10**, 1129–1130.
- R. Ballini, *Eco-friendly synthesis of fine chemicals*, Royal Society of Chemistry, 2009, vol. 3.
- R. A. Sheldon, *Green Chem.*, 2007, **9**, 1273–1283.
- R. A. Sheldon, *Chem. Commun.*, 2008, 3352–3365.

- 20 S. Rostamnia, B. Zeynizadeh, E. Doustkhah, A. Baghban and K. O. Aghbash, *Catal. Commun.*, 2015, **68**, 77–83.
- 21 S. Rostamnia, N. Nouruzi, H. Xin and R. Luque, *Catal. Sci. Technol.*, 2015, **5**, 199–205.
- 22 S. Rostamnia, B. Gholipour and H. Golchin Hosseini, *Process Saf. Environ. Prot.*, 2016, **100**, 74–79.
- 23 A. Modak, P. Bhanja, S. Dutta, B. Chowdhury and A. Bhaumik, *Green Chem.*, 2020, **22**, 4002–4033.
- 24 J. He, L. Chen, S. Liu, K. Song, S. Yang and A. Riisager, *Green Chem.*, 2020, **22**, 6714–6747.
- 25 Z. Guo, B. Liu, Q. Zhang, W. Deng, Y. Wang and Y. Yang, *Chem. Soc. Rev.*, 2014, **43**, 3480–3524.
- 26 E. Doustkhah, S. Rostamnia, N. Tsunoji, J. Henzie, T. Takei, Y. Yamauchi and Y. Ide, *Chem. Commun.*, 2018, **54**, 4402–4405.
- 27 M.-H. Sun, S.-Z. Huang, L.-H. Chen, Y. Li, X.-Y. Yang, Z.-Y. Yuan and B.-L. Su, *Chem. Soc. Rev.*, 2016, **45**, 3479–3563.
- 28 A. Ahadi, H. Alamgholiloo, S. Rostamnia, X. Liu, M. Shokouhimehr, D. A. Alonso and R. Luque, *ChemCatChem*, 2019, **11**, 4803–4809.
- 29 F. De Clippel, M. Dusselier, S. Van De Vyver, L. Peng, P. A. Jacobs and B. F. Sels, *Green Chem.*, 2013, **15**, 1398–1430.
- 30 H. B. Gray, *Nat. Chem.*, 2009, **1**, 7.
- 31 R. A. Sheldon, *Chem. Soc. Rev.*, 2012, **41**, 1437–1451.
- 32 R. B. N. Baig and R. S. Varma, *Chem. Commun.*, 2012, **48**, 5853–5855.
- 33 R. B. N. Baig and R. S. Varma, *Chem. Soc. Rev.*, 2012, **41**, 1559–1584.
- 34 E. Doustkhah, S. Rostamnia, M. Imura, Y. Ide, S. Mohammadi, C. J. T. Hyland, J. You, N. Tsunoji, B. Zeynizadeh and Y. Yamauchi, *RSC Adv.*, 2017, **7**, 56306–56310.
- 35 J. C. Colmenares, R. S. Varma and V. Nair, *Chem. Soc. Rev.*, 2017, **46**, 6675–6686.
- 36 V. Polshettiwar and R. S. Varma, *Green Chem.*, 2010, **12**, 743–754.
- 37 S. B. Kalidindi and B. R. Jagirdar, *ChemSusChem*, 2012, **5**, 65–75.
- 38 M. Nasrollahzadeh, N. Motahharifar, F. Ghorbannezhad, N. S. S. Bidgoli, T. Baran and R. S. Varma, *Mol. Catal.*, 2020, **480**, 110645.
- 39 M. Nasrollahzadeh, M. Sajjadi, M. Shokouhimehr and R. S. Varma, *Coord. Chem. Rev.*, 2019, **397**, 54–75.
- 40 M. Nasrollahzadeh, N. Shafiei, M. Maham, Z. Issaabadi, Z. Nezafat and R. S. Varma, *Mol. Catal.*, 2020, **494**, 111129.
- 41 M. B. Gawande, A. K. Rathi, J. Tucek, K. Safarova, N. Bundaleski, O. M. N. D. Teodoro, L. Kvitek, R. S. Varma and R. Zboril, *Green Chem.*, 2014, **16**, 4137–4143.
- 42 M. B. Gawande, V. D. B. Bonifácio, R. S. Varma, I. D. Nogueira, N. Bundaleski, C. A. A. Ghumman, O. M. N. D. Teodoro and P. S. Branco, *Green Chem.*, 2013, **15**, 1226–1231.
- 43 R. K. Sharma, S. Dutta, S. Sharma, R. Zboril, R. S. Varma and M. B. Gawande, *Green Chem.*, 2016, **18**, 3184–3209.
- 44 S. Sá, M. B. Gawande, A. Velhinho, J. P. Veiga, N. Bundaleski, J. Trigueiro, A. Tolstogousov, O. M. N. D. Teodoro, R. Zboril and R. S. Varma, *Green Chem.*, 2014, **16**, 3494–3500.
- 45 T. Cheng, D. Zhang, H. Li and G. Liu, *Green Chem.*, 2014, **16**, 3401–3427.
- 46 S. Rostamnia, H. Xin and N. Nouruzi, *Microporous Mesoporous Mater.*, 2013, **179**, 99–103.
- 47 S. Rostamnia, A. Hassankhani, H. G. Hossieni, B. Gholipour and H. Xin, *J. Mol. Catal. A: Chem.*, 2014, **395**, 463–469.
- 48 S. Rostamnia and E. Doustkhah, *Nanochem. Res.*, 2016, **1**, 19–32.
- 49 M. J. Gaunt, C. C. C. Johansson, A. McNally and N. T. Vo, *Drug Discovery Today*, 2007, **12**, 8–27.
- 50 G. Yang, Y. Ma and J. Xu, *J. Am. Chem. Soc.*, 2004, **126**, 10542–10543.
- 51 D. Chen, Y. Wang and J. Klankermayer, *Angew. Chem., Int. Ed.*, 2010, **49**, 9475–9478.
- 52 A. S. K. Hashmi, *Angew. Chem., Int. Ed.*, 2000, **39**, 3590–3593.
- 53 H. Huang, X. Ji, W. Wu and H. Jiang, *Chem. Soc. Rev.*, 2015, **44**, 1155–1171.
- 54 T. Jiang, H. Zhang, Y. Ding, S. Zou, R. Chang and H. Huang, *Chem. Soc. Rev.*, 2020, **49**, 1487–1516.
- 55 I. Nakamura and Y. Yamamoto, *Chem. Rev.*, 2004, **104**, 2127–2198.
- 56 I. Nakamura and Y. Yamamoto, *Adv. Synth. Catal.*, 2002, **344**, 111–129.
- 57 F. Pan and Z.-J. Shi, *ACS Catal.*, 2014, **4**, 280–288.
- 58 C. Sambigioglio, D. Schönbauer, R. Blicke, T. Dao-Huy, G. Pototschnig, P. Schaaf, T. Wiesinger, M. F. Zia, J. Wencel-Delord and T. Basset, *Chem. Soc. Rev.*, 2018, **47**, 6603–6743.
- 59 Z. Shi, C. Zhang, C. Tang and N. Jiao, *Chem. Soc. Rev.*, 2012, **41**, 3381–3430.
- 60 R. Skoda-Földes and L. Kollár, *Chem. Rev.*, 2003, **103**, 4095–4130.
- 61 J. Tsuji, *Innov. Org. Synth.*, 2000, p. 14.
- 62 G. W. Parshall, *J. Mol. Catal.*, 1978, **4**, 243–270.
- 63 A. Mortreux and F. Petit, *Industrial applications of homogeneous catalysis*, Springer Science & Business Media, 1987, vol. 10.
- 64 L. Lloyd, *Handbook of industrial catalysts*, Springer Science & Business Media, 2011.
- 65 E. P. Kündig, in *Transition Metal Arene π -Complexes in Organic Synthesis and Catalysis*, Springer, 2004, pp. 3–20.
- 66 J. Falbe and H. Bahrmann, *J. Chem. Educ.*, 1984, **61**, 961.
- 67 B. Cornils and W. A. Herrmann, *J. Catal.*, 2003, **216**, 23–31.
- 68 G. P. Chiusoli and P. M. Maitlis, *Metal-catalysis in Industrial Organic Processes*, The Royal Society of Chemistry, 2008.
- 69 L. Brandsma, S. F. Vasilevsky and H. D. Verkruijse, *Application of transition metal catalysts in organic synthesis*, Springer Science & Business Media, 2012.

- 70 H.-U. Blaser, A. Indolese and A. Schnyder, *Curr. Sci.*, 2000, 1336–1344.
- 71 C. L. Sun and Z. J. Shi, *Chem. Rev.*, 2014, **114**, 9219–9280.
- 72 I. Atodiresei, C. Vila and M. Rueping, *ACS Catal.*, 2015, **5**, 1972–1985.
- 73 P. G. Bulger, *9.10 Industrial Applications of Organocatalysis*, Elsevier Ltd, 2012, vol. 9.
- 74 H. Srour, *Recent Advances in Organocatalysis*, 2016.
- 75 F. Xu, *Sustain. Catal. Challenges Pract. Pharm. Fine Chem. Ind.*, 2013, pp. 317–337.
- 76 A. Rajendran, M. Rajendiran, Z. F. Yang, H. X. Fan, T. Y. Cui, Y. G. Zhang and W. Y. Li, *Chem. Rec.*, 2020, **20**, 513–540.
- 77 D. S. Su, J. Zhang, B. Frank, A. Thomas, X. Wang, J. Paraknowitsch and R. Schlögl, *ChemSusChem*, 2010, **3**, 169–180.
- 78 P. Zhang, Y. Wang, J. Yao, C. Wang, C. Yan, M. Antonietti and H. Li, *Adv. Synth. Catal.*, 2011, **353**, 1447–1451.
- 79 Z. Wei, M. Liu, Z. Zhang, W. Yao, H. Tan and Y. Zhu, *Energy Environ. Sci.*, 2018, **11**, 2581–2589.
- 80 W. J. Ong, L. L. Tan, Y. H. Ng, S. T. Yong and S. P. Chai, *Chem. Rev.*, 2016, **116**, 7159–7329.
- 81 G. Nabi, N. Malik, M. B. Tahir, W. Raza, M. Rizwan, M. Maraj, A. Siddiqua, R. Ahmed and M. Tanveer, *Physica B: Condens. Matter*, 2021, **602**, 412556.
- 82 N. F. F. Moreira, M. J. Sampaio, A. R. Ribeiro, C. G. Silva, J. L. Faria and A. M. T. Silva, *Appl. Catal., B*, 2019, **248**, 184–192.
- 83 X. H. Li, J. S. Chen, X. Wang, J. Sun and M. Antonietti, *J. Am. Chem. Soc.*, 2011, **133**, 8074–8077.
- 84 M. Ismael, *J. Alloys Compd.*, 2020, **846**, 156446.
- 85 Y. Gong, M. Li, H. Li and Y. Wang, *Green Chem.*, 2015, **17**, 715–736.
- 86 X. Dai, Y. Zhu, X. Xu and J. Weng, *Youji Huaxue*, 2017, **37**, 577–585.
- 87 Q. Cao, B. Kumru, M. Antonietti and B. V. K. J. Schmidt, *Mater. Horiz.*, 2020, **7**, 762–786.
- 88 C. Parmeggiani and F. Cardona, *Green Chem.*, 2012, **14**, 547–564.
- 89 W. J. Chung, D. K. Kim and Y. S. Lee, *Tetrahedron Lett.*, 2003, **44**, 9251–9254.
- 90 W. J. Chung, D. K. Kim and Y. S. Lee, *Synlett*, 2005, 2175–2178.
- 91 H. S. Jang, Y. H. Kim, Y. O. Kim, S. M. Lee, J. W. Kim, W. J. Chung and Y. S. Lee, *J. Ind. Eng. Chem.*, 2014, **20**, 29–36.
- 92 G. Pozzi, M. Cavazzini, S. Quici, M. Benaglia and G. Dell'Anna, *Org. Lett.*, 2004, **6**, 441–443.
- 93 C. I. Herreras, T. Y. Zhang and C. J. Li, *Tetrahedron Lett.*, 2006, **47**, 13–17.
- 94 B. Karimi, A. Biglari, J. H. Clark and V. Budarin, *Angew. Chem., Int. Ed.*, 2007, **46**, 7210–7213.
- 95 A. Schätz, R. N. Grass, W. J. Stark and O. Reiser, *Chem. – Eur. J.*, 2008, **14**, 8262–8266.
- 96 F. Su, S. C. Mathew, G. Lipner, X. Fu, M. Antonietti, S. Blechert and X. Wang, *J. Am. Chem. Soc.*, 2010, **132**, 16299–16301.
- 97 Z. Zheng and X. Zhou, *Chin. J. Chem.*, 2012, **30**, 1683–1686.
- 98 M. B. Ansari, H. Jin and S. E. Park, *Catal. Sci. Technol.*, 2013, **3**, 1261–1266.
- 99 D. R. Dreyer, H. P. Jia and C. W. Bielawski, *Angew. Chem., Int. Ed.*, 2010, **49**, 6813–6816.
- 100 B. Karimi and E. Badreh, *Org. Biomol. Chem.*, 2011, **9**, 4194–4198.
- 101 L. Di and Z. Hua, *Adv. Synth. Catal.*, 2011, **353**, 1253–1259.
- 102 B. Karimi and E. Farhangi, *Chem. – Eur. J.*, 2011, **17**, 6056–6060.
- 103 J. Long, X. Xie, J. Xu, Q. Gu, L. Chen and X. Wang, *ACS Catal.*, 2012, **2**, 622–631.
- 104 B. Karimi, S. Vahdati and H. Vali, *RSC Adv.*, 2016, **6**, 63717–63723.
- 105 W. Zhang, A. Bariotaki, I. Smonou and F. Hollmann, *Green Chem.*, 2017, **19**, 2096–2100.
- 106 Y. Chen, J. Zhang and X. Wang, *Chem. Sci.*, 2013, **4**, 3244–3248.
- 107 K. Saito, K. Hirose, T. Okayasu, H. Nishide and M. T. W. Hearn, *RSC Adv.*, 2013, **3**, 9752–9756.
- 108 Y. H. Kim, H. S. Jang, Y. O. Kim, S. D. Ahn, S. Yeo, S. M. Lee and Y. S. Lee, *Synlett*, 2013, **24**, 2282–2286.
- 109 L. Zhang, D. Liu, J. Guan, X. Chen, X. Guo, F. Zhao, T. Hou and X. Mu, *Mater. Res. Bull.*, 2014, **59**, 84–92.
- 110 H. Watanabe, S. Asano, S. I. Fujita, H. Yoshida and M. Arai, *ACS Catal.*, 2015, **5**, 2886–2894.
- 111 M. A. Patel, F. Luo, M. R. Khoshi, E. Rabie, Q. Zhang, C. R. Flach, R. Mendelsohn, E. Garfunkel, M. Szostak and H. He, *ACS Nano*, 2016, **10**, 2305–2315.
- 112 M. Bellardita, E. I. García-López, G. Marci, I. Krivtsov, J. R. García and L. Palmisano, *Appl. Catal., B*, 2018, **220**, 222–233.
- 113 X. Zhang, X. Fu, Y. Zhang, Y. Zhu and J. Yang, *Catal. Lett.*, 2016, **146**, 945–950.
- 114 J. Payormhorm, X. B. Li, T. Maschmeyer, N. Laosiripojana and S. Chuangchote, *Mater. Sci. Forum*, 2017, **890 MSF**, 248–251.
- 115 Y. Nabae, M. Mikuni, N. Takusari, T. Hayakawa and M. A. Kakimoto, *High Perform. Polym.*, 2017, **29**, 646–650.
- 116 G. E. Dwulet and D. L. Gin, *Chem. Commun.*, 2018, **54**, 12053–12056.
- 117 H. K. Kadam and S. G. Tilve, *RSC Adv.*, 2015, **5**, 83391–83407.
- 118 H. H. Byung, H. S. Dae and Y. C. Sung, *Tetrahedron Lett.*, 1985, **26**, 6233–6234.
- 119 B. Li and Z. Xu, *J. Am. Chem. Soc.*, 2009, **131**, 16380–16382.
- 120 X. Kong, Z. Sun, M. Chen and Q. Chen, *Energy Environ. Sci.*, 2013, **6**, 3260–3266.
- 121 J. Liu, X. Yan, L. Wang, L. Kong and P. Jian, *J. Colloid Interface Sci.*, 2017, **497**, 102–107.
- 122 Z. Wang, R. Su, D. Wang, J. Shi, J. X. Wang, Y. Pu and J. F. Chen, *Ind. Eng. Chem. Res.*, 2017, **56**, 13610–13617.
- 123 Y. Suzuki, M. Matsushima and M. Kodomari, *Chem. Lett.*, 1998, **27**, 319–320.

- 124 M. Kodomari, Y. Suzuki and K. Yoshida, *Chem. Commun.*, 1997, 1567–1568.
- 125 F. Goettmann, A. Fischer, M. Antonietti and A. Thomas, *Chem. Commun.*, 2006, 4530–4532.
- 126 G. A. Sereda, V. B. Rajpara and R. L. Slaba, *Tetrahedron*, 2007, **63**, 8351–8357.
- 127 X. Liang, *Chem. Eng. J.*, 2015, **264**, 251–257.
- 128 X. Zhang, Y. Zhao and Q. Yang, *J. Catal.*, 2014, **320**, 180–188.
- 129 Q. Yang, W. Wang, Y. Zhao, J. Zhu, Y. Zhu and L. Wang, *RSC Adv.*, 2015, **5**, 54978–54984.
- 130 B. Garrigues, C. Laporte, R. Laurent, A. Laporterie and J. Dubac, *Liebigs Ann.*, 1996, 739–741.
- 131 B. Garrigues, R. Laurent, C. Laporte, A. Laporterie and J. Dubac, *Liebigs Ann.*, 1996, **11**, 743–744.
- 132 M. F. R. Pereira, J. J. M. Orfão and J. L. Figueiredo, *Appl. Catal., A*, 2000, **196**, 43–54.
- 133 M. F. R. Pereira, J. J. M. Orfão and J. L. Figueiredo, *Appl. Catal., A*, 2001, **218**, 307–318.
- 134 J. Zhang, D. Su, A. Zhang, D. Wang, R. Schlögl and C. Hébert, *Angew. Chem., Int. Ed.*, 2007, **46**, 7319–7323.
- 135 J. Zhang, X. Liu, R. Blume, A. Zhang, R. Schlögl and D. S. Su, *Science*, 2008, **322**, 73–77.
- 136 B. Frank, J. Zhang, R. Blume, R. Schlögl and D. S. Su, *Angew. Chem., Int. Ed.*, 2009, **48**, 6913–6917.
- 137 B. Frank, M. Morassutto, R. Schomäcker, R. Schlögl and D. S. Su, *ChemCatChem*, 2010, **2**, 644–648.
- 138 B. H. Min, M. B. Ansari, Y. H. Mo and S. E. Park, *Catal. Today*, 2013, **204**, 156–163.
- 139 Y. Kubota, H. Ikeya, Y. Sugi, T. Yamada and T. Tatsumi, *J. Mol. Catal. A: Chem.*, 2006, **249**, 181–190.
- 140 B. Movassagh, L. Tahershamsi and A. Mobaraki, *Tetrahedron Lett.*, 2015, **56**, 1851–1854.
- 141 G. Demicheli, R. Maggi, A. Mazzacani, P. Righi, G. Sartori and F. Bigi, *Tetrahedron Lett.*, 2001, **42**, 2401–2403.
- 142 T. M. Suzuki, M. Yamamoto, K. Fukumoto, Y. Akimoto and K. Yano, *J. Catal.*, 2007, **251**, 249–257.
- 143 T. M. Suzuki, T. Nakamura, K. Fukumoto, M. Yamamoto, Y. Akimoto and K. Yano, *J. Mol. Catal. A: Chem.*, 2008, **280**, 224–232.
- 144 K. Motokura, M. Tada and Y. Iwasawa, *Angew. Chem., Int. Ed.*, 2008, **47**, 9230–9235.
- 145 W. Zhang, S. Wang, J. Ji, Y. Li, G. Zhang, F. Zhang and X. Fan, *Nanoscale*, 2013, **5**, 6030–6033.
- 146 K. R. Kloetstra and H. Van Bekkum, *J. Chem. Soc., Chem. Commun.*, 1995, 1005–1006.
- 147 N. Kan-Nari, S. Okamura, S. I. Fujita, J. I. Ozaki and M. Arai, *Adv. Synth. Catal.*, 2010, **352**, 1476–1484.
- 148 F. Su, M. Antonietti and X. Wang, *Catal. Sci. Technol.*, 2012, **2**, 1005–1009.
- 149 N. Lashgari, G. M. Ziarani, A. Badiei and P. Gholamzadeh, *Eur. J. Chem.*, 2012, **3**, 310–313.
- 150 F. Nemati, M. M. Heravi and R. Saeedi Rad, *Chin. J. Catal.*, 2012, **33**, 1825–1831.
- 151 A. R. Kiasat and J. Davarpanah, *J. Mol. Catal. A: Chem.*, 2013, **373**, 46–54.
- 152 P. Li, C. Y. Cao, H. Liu, Y. Yu and W. G. Song, *J. Mater. Chem. A*, 2013, **1**, 12804–12810.
- 153 L. Zhang, H. Wang, Z. Qin, J. Wang and W. Fan, *RSC Adv.*, 2015, **5**, 22838–22846.
- 154 B. Singh, K. R. Mote, C. S. Gopinath, P. K. Madhu and V. Polshettiwar, *Angew. Chem., Int. Ed.*, 2015, **54**, 5985–5989.
- 155 G. Tuci, L. Luconi, A. Rossin, E. Berretti, H. Ba, M. Innocenti, D. Yakhvarov, S. Caporali, C. Pham-Huu and G. Giambastiani, *ACS Appl. Mater. Interfaces*, 2016, **8**, 30099–30106.
- 156 P. Sharma and Y. Sasson, *RSC Adv.*, 2017, **7**, 25589–25596.
- 157 A. Ghorbani-Choghmarani, Z. Heidarneshad, B. Tahmasbi and G. Azadi, *J. Iran. Chem. Soc.*, 2018, **15**, 2281–2293.
- 158 P. Sharma, D. K. Patel, S. Kancharlapalli, S. Magdassi and Y. Sasson, *ACS Sustainable Chem. Eng.*, 2020, **8**, 2350–2360.
- 159 S. W. Jun, M. Shokouhimehr, D. J. Lee, Y. Jang, J. Park and T. Hyeon, *Chem. Commun.*, 2013, **49**, 7821–7823.
- 160 B. Basu, S. Kundu and D. Sengupta, *RSC Adv.*, 2013, **3**, 22130–22134.
- 161 P. Kowalski, K. Mitka, K. Ossowska and Z. Kolarska, *Tetrahedron*, 2005, **61**, 1933–1953.
- 162 M. C. Carreão, *Chem. Rev.*, 1995, **95**, 1717–1760.
- 163 I. Fernández and N. Khair, *Chem. Rev.*, 2003, **103**, 3651–3705.
- 164 A. Shaabani and A. H. Rezayan, *Catal. Commun.*, 2007, **8**, 1112–1116.
- 165 K. Bahrami, M. M. Khodaei and P. Fattahpour, *Catal. Sci. Technol.*, 2011, **1**, 389–393.
- 166 D. R. Dreyer, H. P. Jia, A. D. Todd, J. Geng and C. W. Bielawski, *Org. Biomol. Chem.*, 2011, **9**, 7292–7295.
- 167 P. Zhang, Y. Wang, H. Li and M. Antonietti, *Green Chem.*, 2012, **14**, 1904–1908.
- 168 H. M. Shen, W. J. Zhou, H. K. Wu, W. Bin Yu, N. Ai, H. B. Ji, H. X. Shi and Y. Bin She, *Tetrahedron Lett.*, 2015, **56**, 4494–4498.
- 169 E. Doustkhah and S. Rostamnia, *Mater. Chem. Phys.*, 2016, **177**, 229–235.
- 170 G. Abdi, A. Alizadeh and M. M. Khodaei, *Mater. Chem. Phys.*, 2017, **201**, 323–330.
- 171 X. Chen, K. Deng, P. Zhou and Z. Zhang, *ChemSusChem*, 2018, **11**, 2444–2452.
- 172 F. Goettmann, A. Fischer, M. Antonietti and A. Thomas, *New J. Chem.*, 2007, **31**, 1455–1460.
- 173 X. H. Li, X. Wang and M. Antonietti, *ACS Catal.*, 2012, **2**, 2082–2086.
- 174 P. Tang, Y. Gao, J. Yang, W. Li, H. Zhao and D. Ma, *Chin. J. Catal.*, 2014, **35**, 922–928.
- 175 C. Ricca, F. Labat, N. Russo, C. Adamo and E. Sicilia, *J. Phys. Chem. C*, 2014, **118**, 12275–12284.
- 176 Y. Wang, H. Li, J. Yao, X. Wang and M. Antonietti, *Chem. Sci.*, 2011, **2**, 446–450.
- 177 A. Dhakshinamoorthy, A. Primo, P. Concepcion, M. Alvaro and H. Garcia, *Chem. – Eur. J.*, 2013, **19**, 7547–7554.

- 178 C. Anand, S. V. Priya, G. Lawrence, G. P. Mane, D. S. Dhawale, K. S. Prasad, V. V. Balasubramanian, M. A. Wahab and A. Vinu, *Catal. Today*, 2013, **204**, 164–169.
- 179 S.-I. Fujita, K. Yamada, A. Katagiri, H. Watanabe, H. Yoshida and M. Arai, *Appl. Catal., A*, 2014, **488**, 171–175.
- 180 S. Rostamnia and E. Doustkhah, *J. Mol. Catal. A: Chem.*, 2016, **411**, 317–324.
- 181 J. C. Manayil, C. V. M. Inocencio, A. F. Lee and K. Wilson, *Green Chem.*, 2016, **18**, 1387–1394.
- 182 A. Mobaraki, B. Movassagh and B. Karimi, *Appl. Catal., A*, 2014, **472**, 123–133.
- 183 A. Kara and B. Erdem, *J. Mol. Catal. A: Chem.*, 2011, **349**, 42–47.
- 184 A. K. Purohit, A. Kumar, V. Singh, R. Goud D, R. Jain and D. K. Dubey, *Tetrahedron Lett.*, 2014, **55**, 6844–6846.
- 185 R. Radhakrishnan, D. M. Do, S. Jaenicke, Y. Sasson and G. K. Chuah, *ACS Catal.*, 2011, **1**, 1631–1636.
- 186 X. Zhang, M. Wang, Y. Wang, C. Zhang, Z. Zhang, F. Wang and J. Xu, *Chin. J. Catal.*, 2014, **35**, 703–708.
- 187 H. J. Yoon, J. W. Choi, H. S. Jang, J. K. Cho, J. W. Byun, W. J. Chung, S. M. Lee and Y. S. Lee, *Synlett*, 2011, 165–168.
- 188 R. S. Varma, K. P. Naicker, D. Kumar, R. Dahiya and P. J. Liesen, *J. Microw. Power Electromagn. Energy*, 1999, **34**, 113–123.
- 189 N. Oger, Y. F. Lin, E. Le Grogne, F. Rataboul and F. X. Felpin, *Green Chem.*, 2016, **18**, 1531–1537.
- 190 R. S. Varma, M. Varma and A. K. Chatterjee, *J. Chem. Soc., Perkin Trans. 1*, 1993, 999–1000.
- 191 R. S. Varma, A. K. Chatterjee and M. Varma, *Tetrahedron Lett.*, 1993, **34**, 4603–4606.
- 192 R. S. Varma, J. B. Lamture and M. Varma, *Tetrahedron Lett.*, 1993, **34**, 3029–3032.
- 193 D. Zareyee and B. Karimi, *Tetrahedron Lett.*, 2007, **48**, 1277–1280.
- 194 K. Shimizu, E. Hayashi, T. Hatamachi, T. Kodama and Y. Kitayama, *Tetrahedron Lett.*, 2004, **45**, 5135–5138.
- 195 B. Das, K. Venkateswarlu, M. Krishnaiah and H. Holla, *Tetrahedron Lett.*, 2006, **47**, 7551–7556.
- 196 M. B. Gawande, V. Polshettiwar, R. S. Varma and R. V. Jayaram, *Tetrahedron Lett.*, 2007, **48**, 8170–8173.
- 197 R. S. Varma, A. K. Chatterjee and M. Varma, *Tetrahedron Lett.*, 1993, **34**, 3207–3210.
- 198 R. S. Varma and H. M. Meshram, *Tetrahedron Lett.*, 1997, **38**, 7973–7976.
- 199 R. S. Varma and D. Kumar, *Synth. Commun.*, 1999, **29**, 1333–1340.
- 200 B. Karimi and M. Khalkhali, *J. Mol. Catal. A: Chem.*, 2007, **271**, 75–79.
- 201 A. Vass, J. Dudas and R. S. Varma, *Tetrahedron Lett.*, 1999, **40**, 4951–4954.
- 202 F. C. Zheng, Q. W. Chen, L. Hu, N. Yan and X. K. Kong, *Dalton Trans.*, 2014, **43**, 1220–1227.
- 203 C. S. Gill, B. A. Price and C. W. Jones, *J. Catal.*, 2007, **251**, 145–152.
- 204 Z. Gholamzadeh, M. R. Naimi-Jamal and A. Maleki, *C. R. Chim.*, 2014, **17**, 994–1001.
- 205 D. K. Kim, W. J. Chung and Y. S. Lee, *Synlett*, 2005, 279–282.
- 206 S. S. Kahandal, S. R. Kale, M. B. Gawande, R. Zboril, R. S. Varma and R. V. Jayaram, *RSC Adv.*, 2014, **4**, 6267–6274.
- 207 P. K. Khatri, N. Karanwal, S. Kaul and S. L. Jain, *Tetrahedron Lett.*, 2015, **56**, 1203–1206.
- 208 K. Chandra, T. K. Roy, J. N. Naoum, C. Gilon, R. B. Gerber and A. Friedler, *Org. Biomol. Chem.*, 2014, **12**, 1879–1884.
- 209 D. Lim and A. J. Fairbanks, *Chem. Sci.*, 2017, **8**, 1896–1900.
- 210 N. J. Venkatesha, Y. S. Bhat and B. S. J. Prakash, *RSC Adv.*, 2016, **6**, 45819–45828.
- 211 S. Shylesh, S. Sharma, S. P. Mirajkar and A. P. Singh, *J. Mol. Catal. A: Chem.*, 2004, **212**, 219–228.
- 212 A. Dhakshinamoorthy, M. Latorre-Sanchez, A. M. Asiri, A. Primo and H. Garcia, *Catal. Commun.*, 2015, **65**, 10–13.
- 213 X. N. Zhao, H. C. Hu, F. J. Zhang and Z. H. Zhang, *Appl. Catal., A*, 2014, **482**, 258–265.
- 214 L. Ma'mani, M. Sheykhani, A. Heydari, M. Faraji and Y. Yamini, *Appl. Catal., A*, 2010, **377**, 64–69.
- 215 R. S. Varma and D. Kumar, *Tetrahedron Lett.*, 1999, **40**, 7665–7669.
- 216 S. Rostamnia, H. Xin, X. Liu and K. Lamei, *J. Mol. Catal. A: Chem.*, 2013, **374–375**, 85–93.
- 217 S. Rostamnia and E. Doustkhah, *Tetrahedron Lett.*, 2014, **55**, 2508–2512.
- 218 S. Rostamnia and A. Hassankhani, *Synlett*, 2014, **25**, 2753–2756.
- 219 S. Shaabani, M. R. Naimi-Jamal and A. Maleki, *Dyes Pigm.*, 2015, **122**, 46–49.
- 220 E. Doustkhah and S. Rostamnia, *J. Colloid Interface Sci.*, 2016, **478**, 280–287.
- 221 E. Doustkhah, S. Rostamnia and A. Hassankhani, *J. Porous Mater.*, 2016, **23**, 549–556.
- 222 M. Karimi and M. R. Naimi-Jamal, *J. Saudi Chem. Soc.*, 2019, **23**, 182–187.
- 223 M. Hassani, M. R. Naimi-Jamal and L. Panahi, *ChemistrySelect*, 2018, **3**, 666–672.
- 224 E. Doustkhah, A. Baghban, M. H. N. Assadi, R. Luque and S. Rostamnia, *Catal. Lett.*, 2019, **149**, 591–600.
- 225 E. Ali, M. R. Naimi-Jamal and R. Ghahramanzadeh, *ChemistrySelect*, 2019, **4**, 9033–9039.
- 226 M. Zarei, M. A. Zolfigol, A. R. Moosavi-Zare, E. Noroozizadeh and S. Rostamnia, *ChemistrySelect*, 2018, **3**, 12144–12149.
- 227 F. Jalili, M. Zarei, M. A. Zolfigol, S. Rostamnia and A. R. Moosavi-Zare, *Microporous Mesoporous Mater.*, 2020, **294**, 109865.
- 228 A. Hassankhani, B. Gholipour and S. Rostamnia, *Polyhedron*, 2020, **175**, 114217.

- 229 S. Amirnejat, A. Nosrati, S. Javanshir and M. R. Naimi-Jamal, *Int. J. Biol. Macromol.*, 2020, **152**, 834–845.
- 230 J. Sun, X. Liu, X. Zhu, H. Wang, S. Rostamnia and J. Han, *Catalysts*, 2017, **7**, 1–11.
- 231 H. Tourani, M. R. Naimi-Jamal, M. G. Dekamin and M. Amirnejad, *C. R. Chim.*, 2012, **15**, 1072–1076.
- 232 R. B. N. Baig, S. Verma, M. N. Nadagouda and R. S. Varma, *Sci. Rep.*, 2016, **6**, 1–6.
- 233 D. Yu, C. Wang, Y. Yin, A. Zhang, G. Gao and X. Fang, *Green Chem.*, 2011, **13**, 1869–1875.
- 234 M. P. Thompson and N. J. Turner, *ChemCatChem*, 2017, **9**, 3833–3836.
- 235 Y. Miao, P. G. Tepper, E. M. Geertsema and G. J. Poelarends, *Eur. J. Org. Chem.*, 2016, **2016**, 5350–5354.
- 236 A. Źądło-Dobrowolska, N. G. Schmidt and W. Kroutil, *Chem. Commun.*, 2018, **54**, 3387–3390.
- 237 B. A. Frontana-Urbe, R. D. Little, J. G. Ibanez, A. Palma and R. Vasquez-Medrano, *Green Chem.*, 2010, **12**, 2099–2119.
- 238 E. J. Horn, B. R. Rosen and P. S. Baran, *ACS Cent. Sci.*, 2016, **2**, 302–308.
- 239 M. D. Kärkäs, *Chem. Soc. Rev.*, 2018, **47**, 5786–5865.
- 240 S. Möhle, M. Zirbes, E. Rodrigo, T. Gieshoff, A. Wiebe and S. R. Waldvogel, *Angew. Chem., Int. Ed.*, 2018, **57**, 6018–6041.
- 241 R. Francke and R. D. Little, *Chem. Soc. Rev.*, 2014, **43**, 2492–2521.
- 242 R. Hayashi, A. Shimizu and J. Yoshida, *J. Am. Chem. Soc.*, 2016, **138**, 8400–8403.
- 243 Y. N. Ogibin, M. N. Elinson and G. I. Nikishin, *Russ. Chem. Rev.*, 2009, **78**, 89.
- 244 J. Yoshida, K. Kataoka, R. Horcajada and A. Nagaki, *Chem. Rev.*, 2008, **108**, 2265–2299.
- 245 L. Zhu, P. Xiong, Z. Mao, Y. Wang, X. Yan, X. Lu and H. Xu, *Angew. Chem.*, 2016, **128**, 2266–2269.
- 246 B. F. Watkins, J. R. Behling, E. Kariv and L. L. Miller, *J. Am. Chem. Soc.*, 1975, **97**, 3549–3550.
- 247 S. Abe, T. Nonaka and T. Fuchigami, *J. Am. Chem. Soc.*, 1983, **105**, 3630–3632.
- 248 S. Abe, T. Fuchigami and T. Nonaka, *Chem. Lett.*, 1983, **12**, 1033–1036.
- 249 E. Siernecki, S. Turcaud, T. Martens and J. Royer, *Synthesis*, 2006, 3199–3208.
- 250 T. Osa, U. Akiba, I. Segawa and J. M. Bobbitt, *Chem. Lett.*, 1988, **17**, 1423–1426.
- 251 T. Osa, Y. Kashiwagi, K. Mukai, A. Ohsawa and J. M. Bobbitt, *Chem. Lett.*, 1990, **19**, 75–78.
- 252 H. Tanaka, J. Kubota, S. J. Itogawa, T. Ido, M. Kuroboshi, K. Shimamura and T. Uchida, *Synlett*, 2003, 951–954.
- 253 A. Das and S. S. Stahl, *Angew. Chem., Int. Ed.*, 2017, **56**, 8892–8897.